

1 **CCSP Synthesis and Assessment Product 1.2**
2 **Past Climate Variability and Change in the Arctic and at High**
3 **Latitudes**

4
5 **Chapter 4 — Temperature and Precipitation History of the Arctic**

6
7 **Chapter Lead Authors:**

8 **Gifford H. Miller**, University of Colorado, Boulder, CO

9 **Julie Brigham-Grette**, University of Massachusetts, Amherst , MA

10 **Contributing Authors:**

11 Lesleigh Anderson, U.S.Geological Survey, Denver, CO

12 Henning Bauch, GEOMAR, University of Kiel, DE

13 Mary Anne Douglas, University of Alberta, Edmonton, Alberta, CA

14 Mary E. Edwards, University of Southampton, UK

15 Scott Elias, Royal Holloway, University of London, UK

16 Bruce Finney, University of Alaska, Fairbanks, AK

17 Svend Funder, University of Copenhagen, DK

18 Timothy Herbert, Brown University, Providence, RI

19 Larry Hinzman, University of Alaska, Fairbanks, AK

20 Darrell Kaufman, Northern Arizona University, Flagstaff, AZ

21 Glen MacDonald, University of California, Los Angeles, CA

22 Alan Robock, Rutgers University, Rutgers, NJ

SAP1.2 DRAFT 5 Agency Cleared

- 23 Mark Serreze, University of Colorado, Boulder, CO
- 24 John Smol, Queen's University, Kingston, Ontario, CA
- 25 Robert Spielhagen, GEOMAR, University of Kiel, DE
- 26 Alexander P. Wolfe, University of Alberta, Edmonton, Alberta, CA
- 27 Eric Wolff, British Antarctic Survey, Cambridge, UK
- 28

28 **ABSTRACT**

29

30 The Arctic has undergone dramatic changes in temperature and precipitation
31 during the Cenozoic Era, the past 65 million years (Ma) of Earth history. Arctic summer
32 surface air temperature changes during this interval exceeded global average temperature
33 changes. Sufficient data are available for the past 4 Ma of Earth history to evaluate the
34 difference between Arctic and global or hemispheric temperatures during times when the
35 mean climate was both warmer and colder than the past century. This evaluation
36 supports the concept of **Arctic amplification**. (Strong positive feedbacks—processes that
37 amplify the effects of a change in the controls on global temperature—produce larger
38 changes in temperature in the Arctic than elsewhere). Warm times in the past, those
39 periods when the Arctic was at least 1 °C warmer than the average 20th Century
40 temperature in either summer or winter season, help to constrain scenarios for future
41 warming in the Arctic. Although past warm times are rarely ideal **analogues** of future
42 warming because the **boundary conditions** (such as continental positions and
43 topography) during past times of exceptional warmth may have differed from those of the
44 present. Nevertheless, many times of peak global warmth in the past are also times of
45 increased atmospheric greenhouse gases, and paleoclimate records help to define the
46 climate sensitivity of the planet to changes in both greenhouse gases and solar insolation,
47 and to quantify Arctic amplification.

48 At the start of the Cenozoic, 65 Ma ago, the planet was ice free; there was no sea
49 ice in the Arctic Ocean, nor was there a Greenland or an Antarctic ice sheet.

50 Atmospheric CO₂ levels were ca. 4 times those of the pre-industrial world (Berner and

51 Kothavala, 2001). General cooling through the Cenozoic is attributed mainly to a slow
52 drawdown of greenhouse gases in the atmosphere through the weathering of silicic rocks
53 that exceeded the release of stored carbon through volcanism and reprocessing (Berner and
54 Kothavala, 2001). Over the past 65 Ma, atmospheric CO₂ has decreased about 1200
55 ppmv, or on average 1 ppmv for every 50 ka. This is much more gradual than the rate of
56 atmospheric CO₂ increase over the past 150 years of about 100 ppmv due to fossil fuel
57 combustion.

58 As the Arctic cooled, high-elevation mountain glaciers formed as did seasonal sea
59 ice in the Arctic Ocean, but a detailed record of changes in the Arctic is available only for
60 the last few million years. A global warm period that affected both seasons in the middle
61 Pliocene, about 3.5 Ma, is well represented in the Arctic; at that time extensive deciduous
62 forests occupied lands that now support only polar desert and **tundra**. Global oceanic and
63 atmospheric circulation was substantially different between 3 and 2.5 Ma ago than
64 subsequently. The development of the first continental ice sheets over North America
65 and Eurasia led to changes in the circulation of both the atmosphere and oceans. The
66 onset of continental glaciation is most clearly defined by the first appearance of rock
67 fragments in sediment cores from the central Atlantic Ocean about 2.6 Ma ago. These
68 rock fragments, often referred to as ice-rafted detritus (IRD) is too heavy to have blown
69 or been washed into the central Atlantic, and must have been delivered by large icebergs
70 emminating from continental ice sheets. The first appearance of IRD marks the onset of
71 the Quaternary Period (2.6–0 Ma), generally equated with “ice-age” time, even though a
72 small fraction (about 10%) of the time the ice sheets were very likely to have been as
73 small as or smaller than their present size. From about 2.7 to about 0.8 Ma, the ice sheets

74 came and went about every 41 thousand years (ka), the same timing as cycles in the tilt of
75 Earth's axis. Ice sheets grew when Earth's tilt was at a minimum, resulting in less
76 seasonality (cooler summers, warmer winters), and they melted when tilt was at a
77 maximum and seasonality was at its greatest (warmer summers and cooler winters). For
78 the past 600 ka, ice sheets have grown larger and ice-age times have been longer, lasting
79 about 100 ka; those icy intervals have been separated by brief warm periods
80 (interglaciations), when sea level was close to present (ice volumes were close to
81 present). The duration of interglaciations ranges from about 10 ka to perhaps 40 ka. The
82 cause of the shift from 41 ka to 100 ka glacial cycles is still being debated. Most
83 explanations center on the continued gradual planetary cooling that may have produced
84 larger ice sheets that were more resistant to melting, or with removal of soft sedimentary
85 cover over bedrock in glaciated regions that, once removed, increased the frictional
86 coupling of the ice sheet to its bed, resulting in steeper ice-sheet profiles and thicker ice
87 sheets, again more resistant to melting (e.g. Clark & Pollard, 1998, Raymo et al., 2006,
88 Huybers, 2007, Bintanja et al., 2008).

89 The relatively warm planetary state during which human civilization developed is
90 the most recent of the warm interglaciations, the Holocene (about 11.5–0 ka). During the
91 penultimate warm interval, about 130–120 ka, solar energy in summer in the northern
92 high latitudes was greater than at any time in the current warm interval. As a
93 consequence, the Arctic summer was about 5°C warmer than at present and almost all
94 glaciers melted completely except for the *Greenland Ice Sheet*, and even it was reduced
95 in size substantially from its present extent. With the increased ice melt, sea level was
96 about 5 meters higher than present, with the extra melt coming from both Greenland and

97 Antarctica as well as small glaciers (Overpeck et al., 2006; Meier et al., 2007). Although
98 sea ice is difficult to reconstruct, the evidence suggests that the central Arctic Ocean
99 retained some permanent ice cover or was periodically ice free, even though the flow of
100 warm Atlantic water into the Arctic Ocean was very likely to have been greater than
101 during the present warm interval.

102 The last glacial maximum peaked about 20 ka when mean annual temperatures
103 over parts of the Arctic were as much as 20°C lower than at present. Ice recession was
104 well underway by 16 ka, and most of the Northern Hemisphere ice sheets had melted by
105 7 ka ago. Solar energy due to Earth's proximity to the Sun in summer rose in the Arctic
106 steadily from 20 ka ago to a maximum (10% higher than at present) about 11 ka ago and
107 has been decreasing since then, as the precession of the equinoxes has tilted the Northern
108 Hemisphere farther from the Sun in summer. The extra energy received in early Holocene
109 summers warmed summers throughout the Arctic about 1°–3°C above 20th century
110 averages, enough to completely melt many small glaciers throughout the Arctic (although
111 the *Greenland Ice Sheet* was only slightly smaller than present). Summer sea ice limits
112 were substantially smaller than their 20th century average, and the flow of Atlantic water
113 into the Arctic Ocean was substantially greater. As summer solar energy decreased in the
114 second half of the Holocene, glaciers re-established or advanced, sea ice extended, and
115 the flow of warm Atlantic water into the Arctic Ocean diminished. Late Holocene cooling
116 reached its nadir during the Little Ice Age (about 1250–1850 AD), when most Arctic
117 glaciers reached their maximum Holocene extent. During the warming of the past century
118 and a half, glaciers have receded throughout the Arctic, terrestrial ecosystems have
119 advanced northward, and perennial Arctic Ocean sea ice has diminished.

120 Paleoclimate reconstructions of Arctic temperatures, compared with global
121 temperature changes during four key intervals in the past 4 Ma, allow a quantitative
122 estimate of Arctic amplification. These data suggest that Arctic temperature change is
123 three to four times as large as the global average temperature change during both warm
124 and cold intervals. If global warming forecasts are correct, this relation indicates that
125 Arctic temperatures are likely to increase dramatically in the next century.

126

127 **4.1 Introduction**

128

129 Recent instrumental records show that during the last few decades, surface air
130 temperatures throughout much of the far north have risen more rapidly than temperatures
131 in lower latitudes and usually about twice as fast (Delworth and Knutson, 2000; Knutson
132 et al., 2006). The remarkable reduction in Arctic Ocean summer sea ice in 2007 (Figure
133 4.1) has outpaced the most recent predictions from available climate models (Stroeve et
134 al., 2008), but it is in concert with widespread reductions in glacier length, increased
135 borehole temperatures, increased coastal erosion, changes in vegetation and wildlife
136 habitats, the northward migration of marine life, and degradation of permafrost. On the
137 basis of the past century's trend of increasing greenhouse gases, climate models forecast
138 continuing warming into the foreseeable future (Figure 4.2) and a continuing
139 amplification in the Arctic of global changes (Serreze and Francis, 2006). As outlined by
140 the Arctic Climate Impact Assessment (ACIA, 2005), the sensitivity of the Arctic to
141 changed forcing is due to strong positive feedbacks in the Arctic climate system (see
142 Chapter 3.3). These feedbacks strongly amplify changes to the climate of the Arctic and

143 also affect the global climate system.

144

145 FIGURE 4.1 NEAR HERE

146 FIGURE 4.2 NEAR HERE

147

148 Because strong Arctic feedbacks act on climate changes caused by either nature or by
149 humans, natural variability and human-caused changes are large in the Arctic, and separating
150 them requires understanding and characterization of its natural variability. The short time
151 interval for which instrumental data are available in the Arctic is not sufficient to characterize
152 that natural variability, so a paleoclimatic perspective is required.

153 This chapter focuses primarily on the history of temperature and precipitation in
154 the Arctic. These topics are important in their own right, and they also set the stage for
155 understanding the histories of the *Greenland Ice Sheet* and the Arctic Ocean sea ice,
156 which are described in Chapters 6 (History of the Greenland Ice Sheet) and 7 (Sea Ice
157 History). Because of the great interest in rates of change, and because of some technical
158 details in extracting rate of change from the broad history of temperature or precipitation,
159 careful consideration of rates of change is deferred to Chapter 5 (past rates of Arctic
160 climate change).

161 Before providing the history of temperature and precipitation in the Arctic, this
162 chapter supplements the discussion in Chapter 3 (paleoclimate concepts) on forcings,
163 feedbacks, and proxies by providing additional information on those aspects particularly
164 relevant to the histories of temperature and precipitation in the Arctic. The climate history
165 of the past 65 Ma is then summarized; it focuses on temperature and precipitation

166 changes that span the full range of the Arctic's natural climate variability and response
167 under different forcings. The authors place special emphasis on relevant intervals in the
168 past with a mean climate state warmer than the 20th Century average. Where possible,
169 causes of these changes are discussed. From these summaries, it is possible to estimate
170 the magnitude of polar amplification and to characterize how the Arctic system responds
171 to global warm times.

172

173 **4.2 Feedbacks Influencing Arctic Temperature and Precipitation**

174

175 The most commonly used measure of the climate is the mean surface air
176 temperature (Figure 4.3), which is influenced by climate forcings and climate feedbacks.
177 As discussed with references in Chapter 3.2, important forcings during the past several
178 millennia have been changes in the distribution of solar radiation that resulted from
179 features of Earth's orbit; volcanism; and changes in atmospheric greenhouse-gas
180 concentrations. On longer time scales (tens of millions of years), the long-term increase
181 in the solar constant (a 30% increase in the past 4600 Ma) was important, and the
182 redistribution of continental landmasses caused by plate motions also affected the
183 planetary energy balance.

184

185

FIGURE 4.3 NEAR HERE

186

187 How much the temperature changes in response to a forcing of a given magnitude
188 (or in response to the net magnitude of a set of forcings in combination) depends on the

189 sum of all of the feedbacks. Feedbacks can act in days or less or endure for millions of
190 years. The focus here is on faster feedbacks. For example, a warming may have many
191 causes (such as brighter Sun, higher concentration of greenhouse gases in the atmosphere,
192 less blocking of the Sun by volcanoes). Whatever the cause, warmer air moving over the
193 ocean tends to entrain more water vapor, which itself is a greenhouse gas, so more water
194 vapor in the atmosphere leads to a further rise in global mean surface temperature
195 (Pierrehumbert et al., 2007). The discussion below focuses on those feedbacks that are
196 especially linked to the Arctic. Several processes linked to ice-age cycling are included
197 here, because of the dominant role of northern land in supporting ice-sheet growth,
198 although ice-age processes (like some of the other processes discussed below) clearly
199 extend well beyond the Arctic.

200

201 **4.2.1 Ice-albedo feedback**

202 Ice and snow present highly reflective surfaces. The albedo of a surface is defined
203 as the reflectivity of that surface to the wavelengths of solar radiation. Fresh ice and snow
204 have the highest albedo of any widespread surfaces on the planet (Figure 4.4), so it is
205 apparent that changes in the seasonal and areal distribution of snow and ice will exert
206 strong influences on the planetary energy balance (Peixoto and Oort, 1992). Open ocean,
207 on the other hand, has a low albedo; it absorbs almost all solar energy when the Sun angle
208 is high. Changes in albedo are most important in the Arctic summer, when solar radiation
209 is at a maximum, whereas changes in the winter albedo have little influence on the energy
210 balance because little solar radiation reaches the surface then. In general, warming

211 reduces ice and snow whereas cooling allows them to extend, so the changes in ice and
212 snow act as positive feedbacks to amplify climate changes (e.g., Lemke et al., 2007).

213

214 FIGURE 4.4 NEAR HERE

215

216 5.2.2 Ice-insulation feedback

217 In addition to its effects on albedo, sea ice also causes a positive insulation
218 feedback, primarily in the wintertime. Ice effectively blocks heat transfer between
219 relatively warm ocean (at or above the freezing point of seawater) and cold atmosphere
220 (which, in the Arctic winter, averages -40°C (Chapman and Walsh, 2007). If sea ice is
221 thinned by warming, then the ocean heats the overlying atmosphere in winter months,
222 amplifying that warming.

223 Feedbacks involving snow insulation of the ground are also important, through
224 their effects on vegetation and on permafrost temperature and its influence on storage or
225 release of greenhouse gases, as described in the next subsections (e.g., Ling and Zhang,
226 2007).

227

228 4.2.3 Vegetation feedbacks

229 A related terrestrial feedback involves changing vegetation. A warming climate
230 can cause **tundra** to give way to shrub vegetation. However, the shrub vegetation has a
231 lower albedo than **tundra**, and the shrubs thus cause further warming (Figure 4.5)
232 (Chapin et al., 2005; Goetz et al., 2007). Interactions involving the **boreal** forest and
233 deciduous forest can also be important. When, as a result of warming, deciduous forest

234 replaces evergreen **boreal** forest, then winter surface albedo increases—an example of a
235 negative feedback to the warming climate.(Bonan et al., 1992; Rivers and Lynch, 2004).

236

237

FIGURE 4.5 NEAR HERE

238

239 **4.2.4 Permafrost feedbacks**

240 Additional but poorly understood feedbacks in the Arctic involve changes in the
241 extent of permafrost and how changes in cloud cover interact both with permafrost and
242 with the release of carbon dioxide and methane from the land surface. Feedbacks between
243 permafrost and climate became widely recognized only in recent decades (building on the
244 works of Kvenvolden, 1988; 1993; MacDonald, 1990, and Haeberli et al., 1993. As
245 permafrost thaws under a warmer summer climate (Figure 4.6), it is likely to release
246 more greenhouse gases such as CO₂ and methane from the decomposition of organic
247 matter previously sequestered in permafrost and in widespread Arctic **yedoma** deposits
248 (e.g., Vörösmarty, 2001; Thomas et al., 2002, Smith et al., 2004, Archer, 2007; Walter et
249 al., 2007). Because CO₂ and methane are greenhouse gases, atmospheric temperature is
250 likely to increase in turn, a positive feedback. Walter et al. (2007) suggest that methane
251 bubbling from the thawing of newly formed **thermokarst** lakes across parts of the Arctic
252 during deglaciation could account for as much as 33–87% of the increase in atmospheric
253 methane measured in ice cores. Such a release would have contributed a strong and rapid
254 positive feedback to warming during the last deglaciation, and it likely continues today
255 (Walter et al., 2006).

256

257

258

FIGURE 4.6 NEAR HERE

259

260

261 **4.2.5 Freshwater balance feedbacks and thermohaline circulation**

262 The Arctic Ocean is almost completely surrounded by continents (Figure 4.7).

263 Because precipitation is low over the ice-covered ocean (Serreze et al., 2006), the
264 freshwater input to the Arctic Ocean largely derives from the runoff from large rivers in
265 Eurasia and North America and by the inflow of relatively low-salinity Pacific water
266 through the *Bering Strait*. The *Yenisey*, *Ob*, and *Lena* are among the nine largest rivers on
267 Earth, and there are several other large rivers, such as the *Mackenzie*, that feed into the
268 Arctic Ocean (see Vörösmarty et al., 2008). The freshwater discharged by these rivers
269 dilutes the saltiness of ocean surface waters, maintaining low salinities on the broad,
270 shallow, and seasonally ice-free seas bordering the Arctic Ocean. The largest of these
271 border the Eurasian continent, where they serve as the dominant area in the Arctic Ocean
272 in which sea ice is produced (for some fundamentals on Arctic sea ice, see Barry et al.,
273 1993). Sea ice forms along the Eurasian margin and then drifts toward *Fram Strait*;
274 transit time is 2–3 years in the current regime. In the *Amerasian* part of the Arctic Ocean,
275 the clockwise-rotating Beaufort Gyre is the dominant ice-drift feature (see Figure 8.1).

276 Surface currents transport low-salinity surface water (its upper 50 m) and sea ice
277 (freshwater) out of the Arctic Ocean (e.g., Schlosser et al., 2000). Surface waters are
278 primarily exported from the Arctic Ocean to the northern North Atlantic (*Nordic Seas*)
279 through western *Fram Strait*, after which they follow the east coast of Greenland and exit

280 the *Nordic Seas* into the North Atlantic through *Denmark Strait*. A smaller volume of
281 surface water flows out through the inter-island channels of the *Canadian Arctic*
282 *Archipelago*, and it eventually reaches the North Atlantic through the *Labrador Sea*. The
283 low-saline outflow from the Arctic Ocean is compensated by a relatively warm inflow of
284 saline Atlantic water through eastern *Fram Strait*. Despite its warmth, Atlantic water has
285 sufficiently high salt content that its density is higher than the low-salinity surface waters.
286 The inflowing relatively dense Atlantic water is forced to sink beneath the colder, but
287 fresher, surface water upon entering the Arctic Ocean. North of *Svalbard*, Atlantic water
288 spreads as a boundary current into the Arctic Basin and forms the Atlantic Water Layer
289 (Morison et al., 2000). The strong vertical gradients of salinity and temperature in the
290 Arctic Ocean produce a relatively stable stratification. However, recent observations have
291 shown that in some areas in the *Eurasian* part of the *Arctic Ocean*, the warm Atlantic
292 layer mixes with the surface mixed layer (Rudels et al., 1996; Steele and Boyd, 1998;
293 Schauer et al., 2002), thereby limiting sea ice formation and promoting vertical heat
294 transfer to the Arctic atmosphere in winter. In recent decades circum-Arctic glaciers and
295 ice sheets have been losing mass (more snow and ice melting in summer than
296 accumulates as snow in winter) (Dowdeswell et al., 1997; Rignot and Thomas, 2002;
297 Meier et al., 2007), and since the 1930s river runoff to the Arctic Ocean has been
298 increasing (Peterson et al., 2002). Recent studies suggest that changes in river runoff
299 strongly influence the stability of Arctic Ocean stratification (Steele and Boyd, 1998;
300 Martinson and Steele, 2001; Björk et al., 2002; Boyd et al., 2002; McLaughlin et al.,
301 2002; Schlosser et al., 2002).

302 In the North Atlantic, primarily in the *Nordic Seas* and the *Labrador Sea*,

303 wintertime cooling of the relatively warm and salty waters increases its density. The
304 denser waters then sink and flow southward to participate in the global thermohaline
305 circulation (“thermo” for temperature and “haline” for salt, the two components that
306 determine density. This circulation system also is referred to as the meridional
307 overturning circulation (MOC). Although the two terms are sometimes used
308 interchangeably, the MOC is confined to the Atlantic Ocean where the phenomenon is
309 quantified by using tracers that show surface waters sinking in the Nordic and Labrador
310 seas. The thermohaline circulation refers to a conceptual model of vertical ocean
311 circulation that encompasses the global ocean and is driven by the fact that colder and/or
312 saltier water sinks because it is denser than warmer or less salty water.

313 Continuing surface inflow from the south, which replaces the water sinking in the
314 *Nordic and Labrador seas* (MOC), promotes persistent open water rather than sea ice in
315 these regions. In turn, this lack of sea ice promotes notably warmer conditions, especially
316 in wintertime, over and near the North Atlantic and extending downwind across Europe
317 and beyond (Seager et al., 2002). Salt rejected from sea ice growing nearby very likely
318 contributes to the density of the adjacent sea water and to its sinking.

319 If the surface waters are made sufficiently less salty by an increase in freshwater
320 from runoff of melting ice or from direct precipitation, then the rate of sinking of those
321 surface waters will diminish or stop (e.g., Broecker et al., 1985). Results of numerical
322 models indicate that if freshwater runoff into the Arctic Ocean and the North Atlantic
323 increases as surface waters warm in the northern high latitudes, then the thermohaline
324 circulation in the North Atlantic will weaken, with consequences for marine ecosystems
325 and energy transport (e.g., Rahmstorf, 1996, 2002; Marotzke, 2000; Schmittner, 2005).

326 Reducing the rate of North Atlantic thermohaline circulation likely has global as
327 well as regional effects (e.g., Obata, 2007). Oceanic overturning is an important
328 mechanism for transferring atmospheric CO₂ to the deep ocean. Reducing the rate of deep
329 convection in the ocean would allow a higher proportion of **anthropogenic** CO₂ to
330 remain in the atmosphere. Similarly, a slowdown in thermohaline circulation would
331 reduce the turnover of nutrients from the deep ocean, with potential consequences across
332 the Pacific Ocean.

333

334 **4.2.6 Feedbacks during glacial-interglacial cycles**

335 The polar ice sheets currently cover ca. 14 km², whereas at their Quaternary
336 maxima, as recently as 20 ka ago, they covered approximately twice that area, including
337 the modern sites of New York and Chicago. The growth and decay of the Quaternary ice
338 sheets were paced by the orbital variations often called Milankovitch forcings (e.g.,
339 Imbrie et al., 1993) described in Chapter 3 (paleoclimate concepts). There is little doubt
340 that the orbital forcings drove this glacial-interglacial cycling, but a remarkably rich and
341 varied literature debates the detailed mechanisms (see, e.g., Roe, 1999).

342 The generally accepted explanation of the glacial-interglacial cycling is that ice
343 sheets grew when limited summer sunshine at high northern latitudes allowed survival of
344 accumulated snow, and ice sheets shrank when abundant summer sunshine in the north
345 melted the ice. The north is more important than the south because the Antarctic has
346 remained ice covered during this cycling of the last million years and more, and there is
347 no other high-latitude land in the south on which ice sheets could grow.

348 The increased reflectivity produced by expanded ice contributed to cooling. This
349 effect is the ice-albedo feedback as described above, but with slower response controlled
350 by the flow of the great ice sheets. Atmospheric dust was more abundant in the ice ages
351 than in the intervening warm interglacials, and that additional ice-age dust contributed to
352 cooling by blocking sunlight. The changes in Earth's orbit and ice-sheet growth led to
353 complex changes in the ocean-atmosphere system that shifted carbon dioxide from the air
354 to the ocean and reduced the atmospheric greenhouse effect. The carbon-dioxide changes
355 lagged behind the orbital forcing, and thus carbon dioxide was clearly a feedback, but the
356 large global cooling of the ice ages has been successfully explained only if the reduced
357 greenhouse effect is included (Jansen et al., 2007). By analogy, overspending a credit
358 card induces debt, which is made larger by interest payments on that debt. The interest
359 payments clearly lag the debt in time and did not cause the debt, but they contribute to the
360 size of the debt, and the debt cannot be explained quantitatively unless the interest
361 payments are included.

362 Abrupt climate changes have been associated with the ice-age cycles. The most
363 prominent and best known of these are linked to jumps in the wintertime extent of sea ice
364 in the North Atlantic, which in turn were linked to changes in the large-scale circulation
365 of the ocean (e.g., Alley, 2007), as described in the previous section. The associated
366 temperature changes were very large around the North Atlantic (as much as 10°C or
367 more) but much smaller in remote regions, and they were in the opposite direction in the
368 far south (northern cooling was accompanied by slight southern warming). Hence, the
369 globally averaged temperature changes were small and were probably linked primarily to
370 ice-albedo feedback and small changes in the strength of the greenhouse effect. As

371 reviewed by Alley (2007), the large ice-age ice sheets seem to have both triggered these
372 abrupt swings and created conditions under which triggering was easier. Although such
373 events remain possible, they are less likely without the large ice sheet on Canada.

374

375 **4.2.7 Arctic Amplification**

376 The positive feedbacks outlined above amplify the Arctic response to climate
377 forcings. The ice-albedo feedback is potentially strong in the Arctic because it hosts so
378 much snow and ice (see Serreze and Francis, 2006 for additional discussion); if
379 conditions are too warm for snow to form, no ice-albedo feedback can exist. Climate
380 models initialized from modern or similar conditions and forced in various ways are in
381 widespread agreement that global temperature trends are amplified in the Arctic and that
382 the largest changes are over the Arctic Ocean during the cold season (autumn through
383 spring) (e.g., Manabe and Stouffer, 1980; Holland and Bitz, 2003; Meehl et al., 2007).
384 Summer changes over the Arctic Ocean are relatively damped, although summer changes
385 over Arctic lands are likely to be substantial (Serreze and Francis, 2006). The strong
386 wintertime changes over the Arctic Ocean are linked to the insulating character of sea ice.

387 Think first of an unperturbed climate in balance on annual time scales. During
388 summer, solar energy melts the sea ice cover. As the ice cover melts, areas of open water
389 are exposed. The albedo of the open water is much lower than that of sea ice, so the open
390 water gains heat. Because much of the solar energy goes into melting ice and warming
391 the ocean, the surface air temperature does not rise much and, indeed, over the melting
392 ice it stays fairly close to the freezing point. Through autumn and winter, when little or
393 no solar energy is received, this ocean heat is released back to the atmosphere. Until sea

394 ice forms, heat stored in the ocean's surface waters is transferred to the atmosphere,
395 limiting the extreme cold Arctic air temperatures despite the lack of solar energy. The
396 formation of sea ice itself further releases heat back to the atmosphere. And once the sea
397 ice is formed, it insulates the atmosphere from the relatively warm ocean waters allow
398 much colder surface air temperatures to develop.

399 However, if the climate warms (regardless of the forcing) then the summer melt
400 season lengthens and intensifies, and more areas of low-albedo open water form in
401 summer and absorb solar radiation. As more heat is gained in the upper ocean, more heat
402 is released back to the atmosphere in autumn and winter; this additional heat is expressed
403 as a rise in air temperature. Furthermore, because the ocean now contains more heat, the
404 ice that forms in autumn and winter is thinner, and therefore less insulating than before.
405 This thinner ice melts more easily in summer and produces even more low-albedo open
406 water that absorbs solar radiation, meaning even larger releases of heat to the atmosphere
407 in autumn and even thinner ice the next spring, and so on. The process can also work in
408 reverse. An initial Arctic cooling melts less ice during the summer and creates less low-
409 albedo open water. If less summer heat is gained in the ocean, then less heat is released
410 back to the atmosphere in autumn and winter, and air temperatures fall further .

411 Although the albedo feedback over the ocean seems to dominate, an albedo
412 feedback over land is much more direct. Under a warming climate, snow melts earlier in
413 spring and thus low-albedo **tundra**, shrub, and forest cover is exposed earlier and fosters
414 further spring warming. Similarly, later autumn snow cover will foster further autumn
415 warming. More snow-free days produce a longer period of surface warming and imply
416 warmer summers. Again, the process can work in reverse: initial cooling leads to more

417 snow cover, fostering further cooling. Collectively, these processes result in stronger net
418 positive feedbacks to forced temperature change (regardless of forcing mechanism) than
419 is typical globally, thereby producing “**Arctic amplification**”.

420 During longer time intervals, an ice sheet such as the *Laurentide Ice Sheet* on
421 North America can grow, or an ice sheet such as that on Greenland can melt. This growth
422 or melting in turn influences albedo, freshwater fluxes to the ocean, broad patterns of
423 atmospheric circulation, greenhouse-gas storage or release in the ocean and on land, and
424 more.

425

426 **4.3 Proxies of Arctic Temperature and Precipitation**

427

428 Temperature and precipitation are especially important climate variables. Climate
429 change is typically driven by changes in key forcing factors, which are then amplified or
430 retarded by regional feedbacks that affect temperature and precipitation (section 5.2 and
431 4.2). Because feedbacks have strong regional variability, spatially variable responses to
432 hemispherically symmetric forcing are common throughout the Arctic (e.g., Kaufman et
433 al., 2004). Consequently, spatial patterns of temperature and precipitation must be
434 reconstructed regionally.

435 Reconstructing temperature and precipitation in pre-industrial times requires
436 reliable proxies (see section 4.3 for a general discussion of proxies) that can be used to
437 derive qualitative or, preferably, quantitative estimates of past climates. To capture the
438 expected spatial variability, proxy climate reconstructions must be spatially distributed
439 and span a wide range of geological time. In general, the use of several proxies to

440 reconstruct past climates provides the most robust evidence for past changes in
441 temperature and precipitation.

442

443 **4.3.1 Proxies for Reconstruction of Temperature**

444 **4.3.1a Vegetation/pollen records**

445 Estimates of past temperature from data that describe the distribution of
446 vegetation (primarily fossil pollen assemblages but also plant macrofossils such as fruits
447 and seeds) may be relative (warmer or colder) or quantitative (number of degrees of
448 change). Most information pertains to the growing season, because plants are dormant in
449 the winter and so are less influenced by climate than during the growing season (but see
450 below). For example, evidence of **boreal** forest vegetation (the presence of one or more
451 **boreal** tree species) would be more strongly associated with warmer growing seasons
452 than would evidence of treeless **tundra**—and the general position of northern treeline
453 today approximates the location of the July 10 °C isotherm.

454 Indicator species are species with well studied and relatively restricted modern
455 climatic ranges. The appearance of these species in the fossil record indicates that a
456 certain climate milestone was reached, such as exceeding a minimum summer
457 temperature threshold for successful growth or a winter minimum temperature of freezing
458 tolerance (Figure 4.8). This methodology was developed early in Scandinavia (Iversen,
459 1944); Matthews et al. (1990) used indicator species to constrain temperatures during the
460 last interglaciation in northwest Canada, and Ritchie et al. (1983) used indicator species
461 to highlight early Holocene warmth in northwest Canada. The technique has been used
462 extensively with fossil insect assemblages.

463

464

FIGURE 4.8 NEAR HERE

465

466 Methodologies for the numerical estimation of past temperatures from pollen
467 assemblages follow one of two approaches. The first is the inverse-modeling approach, in
468 which fossil data from one or more localities are used to provide temperature estimates
469 for those localities (this approach also underlies the relative estimates of temperature
470 described above). A modern “calibration set” of data (in this case, pollen assemblages) is
471 related by equations to observed modern temperature, and the functions thus obtained are
472 then applied to fossil data. This method has been developed and applied in Scandinavia
473 (e.g., Seppä et al., 2004). A variant of the inverse approach is **analogue** analysis, in
474 which a large modern dataset with assigned climate data forms the basis for comparison
475 with fossil spectra. Good matches are derived statistically, and the resulting set of
476 **analogues** provides an estimate of the past mean temperature and accompanying
477 uncertainty (Anderson et al., 1989; 1991).

478 Inverse modeling relies upon observed modern relationships. Some plant species
479 were more abundant in the past than they are today, and the fossil pollen spectra they
480 produced may have no recognizable modern counterpart—so-called “no-**analogue**”
481 assemblages. Outside the envelope of modern observations, fossil pollen spectra, which
482 are described in terms of pollen abundance, cannot be reliably related to past climate.
483 This problem led to the adoption of a second approach to estimating past temperature (or
484 other climate variable) called forward modeling. The pollen data are not used to develop
485 numerical values but are used to test a “hypothesis” about the status of past temperature

486 (a key ingredient of climate). The hypothesis may be a conceptual model of the status of
487 past climate, but typically it is represented by a climate-model simulation for a given time
488 in the past. The climate simulation drives a vegetation model that assigns vegetation
489 cover on the basis of bioclimatic rules (such as the winter minimums or required warmth
490 of summer growing temperatures mentioned above). The resultant map is compared with
491 a map of past vegetation developed from the fossil data. The philosophy of this approach
492 is described by Prentice and Webb (1998). Such data and models have been compared for
493 the Arctic by Kaplan et al. (2003) and Wohlfahrt et al. (2004). The great advantage of
494 this approach is that underlying the model simulation are hypothesized climatic
495 mechanisms; those mechanisms allow not only the description but also an explanation of
496 past climate changes.

497

498 **4.3.1b Dendroclimatology**

499 Seasonal differences in climate variables such as temperature and precipitation
500 throughout many parts of the world, including the high latitudes, are known to produce
501 annual rings that reflect distinct changes in the way trees grow and respond, year after
502 year, to variations in the weather (Fritts, 1976). Alternating light and dark bands
503 (couplets) of low-density early wood (spring and summer) and higher density late wood
504 (summer to late summer) have been used for decades to reproduce long time series of
505 regional climate change thought to directly influence the production of **meristematic**
506 **cells** in the trees' vascular cambium, just below the bark. Cambial activity in many parts
507 of the northern **boreal** forests can be short; late wood production very likely starts in late
508 June and annual-ring width is complete by early August (e.g., Esper and Schweingruber,

509 2004). Fundamental to the use of tree rings is the fact that the average width of a tree ring
510 couplet reflects some combination of environmental factors, largely temperature and
511 precipitation, but it can also reflect local climatic variables such as wind stress, humidity
512 and soil properties (see Bradley, 1999, for review). As a general guideline, growing
513 season conditions favorable for the production of wide annual rings tend to be
514 characterized by warmer than average summers with sufficient precipitation to maintain
515 adequate soil moisture. Narrow tree rings occur during unusually cold or dry growing
516 seasons.

517 The extraction of a climate signal from ring width and wood density
518 (dendroclimatology), relies on the identification and calibration of regional climate
519 factors and on the ability to distinguish local climate influences from regional noise (
520 Figure 4.9). How sites for tree sampling are selected is also important depending upon the
521 climatological signal of interest. Trees in marginal growth sites, perhaps on drier
522 substrates or near an ecological transition, are likely to be most sensitive to minor
523 changes in temperature stress or moisture stress. On the other hand, trees in less-marginal
524 sites likely reflect conditions of more widespread change. In the high latitudes, research
525 is commonly focused on trees at both the latitude and elevation limits of tree growth or of
526 the forest-**tundra** ecotone.

527

528

FIGURE 4.9 NEAR HERE

529

530 Pencil-sized increment cores or sanded trunk cross sections are routinely used for
531 stereomicroscopic examination and measurement (Figure 4.10). A number of tree

532 species are examined, most commonly varieties of the genera *Larix* (larch), *Pinus* (pine),
533 and *Picea* (spruce). Raw ring-width time series are typically generated at a resolution of
534 0.01 mm along one or more radii of the tree, and these data are normalized for changes in
535 ring width that reflect the natural increase in tree girth (a young tree produces wider
536 rings). Ring widths for a number of trees are then averaged to produce a master curve for
537 a particular site. The replication of many time series throughout a wide area at a
538 particular site permits extraction of a climate-related signal and the elimination of
539 anomalous ring biases caused by changes in competition or the ecology of any particular
540 tree. Abrupt growth that caused a large change in ring width (Figure 4.9) can only be
541 causally evaluated based on forest-site characteristics; that is, if the change isn't
542 replicated in nearby trees, it's probably not related to climate.

543

544

FIGURE 4.10 NEAR HERE

545

546 Dendroclimatology is statistically laborious, and a variety of approaches are used
547 by the science community. Ring widths or ring density must first be calibrated by a
548 response-function analysis in which tree growth and monthly climatic data are compared
549 for the instrumental period. Once this is done, then cross-dated tree ring series reaching
550 back millennia can be used as predictors of past change. Principal-components analysis,
551 along with some form of multiple regression analysis, is commonly used to identify key
552 variables. A comprehensive review of statistical treatments is beyond the scope of this
553 report, but summaries can be found in Fritts (1976), Briffa and Cook (1990), Bradley
554 (1999, his Chapter 10), and Luckman (2007).

555

556 **4.3.1c Marine isotopic records**

557 The oxygen isotope composition of the calcareous shells of planktic foraminifers
558 accurately records the oxygen isotope composition of ambient seawater, modulated by
559 the temperature at which the organisms built their shells (Epstein et al., 1953; Shackleton,
560 1967; Erez and Luz, 1982; Figure 4.11). (The term $\delta^{18}\text{O}$ refers to the proportion of the
561 heavy isotope, ^{18}O , relative to the lighter, more abundant isotope, ^{16}O .) However, the low
562 horizontal and vertical temperature variability found in Arctic Ocean surface waters (less
563 than -1°C) has little effect on the oxygen isotope composition of *N. pachyderma* (sin.)
564 (maximum 0.2‰, according to Shackleton, 1974). Because meteoric waters, discharged
565 into the ocean by precipitation and (indirectly) by river runoff, have considerably lower
566 $\delta^{18}\text{O}$ values than do ocean waters, a reasonable correlation can be interpreted between
567 salinity and the oxygen isotope composition of Arctic surface waters despite the
568 complications of seasonal sea ice (Bauch et al., 1995; LeGrande and Schmidt, 2006).
569 Accordingly, the spatial variability of surface-water salinity in the Arctic Ocean is
570 recorded today by the $\delta^{18}\text{O}$ of planktic foraminifers (Spielhagen and Erlenkeuser, 1994;
571 Bauch et al., 1997).

572

573

FIGURE 4.11 NEAR HERE

574

575 The $\delta^{18}\text{O}$ values of planktic foraminifers in cores of ancient sediment from the
576 deep Arctic Ocean vary considerably on millennial time scales (e.g., Aksu, 1985; Scott et
577 al., 1989; Stein et al., 1994; Nørgaard-Pedersen et al., 1998; 2003; 2007a,b; Polyak et al.,

578 2004; Spielhagen et al., 2004; 2005). The observed variability in foraminiferal $\delta^{18}\text{O}$
579 commonly exceeds the change in the isotopic composition of seawater that results merely
580 from storing, on glacial-interglacial time scales, isotopically light freshwater in glacial ice
581 sheets (about 1.0–1.2‰ $\delta^{18}\text{O}$) (Fairbanks, 1989; Adkins et al., 1997; Schrag et al. 2002).
582 Changes with time in freshwater balance of the near-surface waters, and in the
583 temperature of those waters, are both recorded in the $\delta^{18}\text{O}$ values of foraminifer shells.
584 Moreover, in cases where independent evidence of a regional warming of surface waters
585 is available (e.g., in the eastern Fram Strait during the last glacial maximum; Nørgaard-
586 Pedersen et al., 2003), this warming is thought to have been caused by a stronger influx
587 of saline Atlantic Water. Because salinity influences $\delta^{18}\text{O}$ of foraminifer shells from the
588 Arctic Ocean more than temperature does, it is difficult to reconstruct temperatures in the
589 past on the basis of systematic variations in calcite $\delta^{18}\text{O}$ in Arctic Ocean sediment cores.

590

591 **4.3.1d Lacustrine isotopic records**

592 Isotopic records preserved in lake sediment provide important paleoclimatic
593 information on landscape change and hydrology. Lakes are common in high-latitude
594 landscapes, and sediment deposited continuously provides uninterrupted, high-resolution
595 records of past climate (Figure 4.12).

596

597 **FIGURE 4.12 NEAR HERE**

598

599 Oxygen isotope ratios in precipitation reflect climate processes, especially
600 temperature (see 4.3.1e). The oxygen isotope ratios of shells and other materials in lakes

601 primarily reflect ratios of the lake water. The isotopic ratios in the lake water are
602 dominantly controlled by the isotopic ratios in precipitation—unless evaporation from the
603 lake is sufficiently rapid, compared with inflow of new water, to shift the isotopic ratios
604 towards heavier values by preferentially removing isotopically lighter water. Those lakes
605 that have streams entering and leaving (open lakes) have isotopic ratios that are generally
606 not affected much by evaporation, as do some lakes supplied only by water flow through
607 the ground (closed lakes). These lakes allow isotopic ratios of shells and other materials
608 in them to be used to reconstruct climate, especially temperature. However, some closed
609 lakes are affected notably by evaporation, in which case the isotopic ratios of the lake are
610 at least in part controlled by lake hydrology. Unless independent evidence of lake
611 hydrology is available, quantitative interpretation of $\delta^{18}\text{O}$ is difficult. Consequently, $\delta^{18}\text{O}$
612 is normally combined with additional climate proxies to constrain other variables and
613 strengthen interpretations. For example, in rare cases, ice core records that are located
614 near lakes can provide an oxygen isotope record for direct comparison (Fisher et al.,
615 2004; Anderson and Leng, 2004; Figure 4.13). Oxygen isotope ratios are relatively easy
616 to measure on carbonate shells or other carbonate materials. Greater difficulty, which
617 limits the accuracy (i.e., the time-resolution) of the records, is associated with analyses of
618 oxygen isotopes in silica from diatom shells (Leng and Marshall, 2004) and in organic
619 matter (Sauer et al., 2001; Anderson et al., 2001). Additional uncertainty arises with
620 organic matter because its site of origin is unknown: although some of it grew in the lake,
621 some was also washed in and is likely to have been stored on the landscape for an
622 indeterminate time previously.
623

624

FIGURE 4.13 NEAR HERE

625

626

4.3.1e Ice cores

627

628

629

630

631

632

633

634

635

636

637

638

639

FIGURE 4.14 NEAR HERE

640

641

642

643

644

645

646

The most common way to deduce temperature from ice cores (Figures 5.13 and 5.14) is through the isotopic content their water, i.e., the ratio of H_2^{18}O to H_2^{16}O , or of HDO to H_2O (where D is deuterium, ^2H). The ratios are expressed as $\delta^{18}\text{O}$ and δD respectively, relative to standard mean ocean water (SMOW). Pioneering studies (Dansgaard, 1964) showed how $\delta^{18}\text{O}$ is related to climatic variables in modern precipitation. At high latitudes both $\delta^{18}\text{O}$ and δD are generally, with some caveats, considered to represent the mean annual temperature at the core site, and the use of both measures together offers additional information about conditions at the source of the water vapor (e.g., Dansgaard et al., 1989). Recent work by Werner et al. (2000), however, demonstrates that changes in the seasonal cycle of precipitation over the ice sheets can affect measurements of ice-core temperature.

647 shown from spatial surveys (Johnsen et al., 1989) and, indeed, from modeling studies
648 using models enabled with water isotopes (e.g., Hoffmann et al., 1998; Mathieu et al.,
649 2002) that a good spatial relationship between temperature and water isotope ratio exists.

650 The relationship is

651

$$652 \quad \delta = aT + b$$

653 where T is mean annual surface temperature, and δ is annual mean $\delta^{18}\text{O}$ or δD value in
654 precipitation in the polar regions, and the slope, a , has values typically around 0.6 for
655 Greenland $\delta^{18}\text{O}$.

656

657 **FIGURE 4.15 NEAR HERE**

658

659 Temperature is not the only factor that can affect isotopic ratios. Changes in the
660 season when snow falls, in the source of the water vapor, and other things are potentially
661 important (Jouzel et al., 1997; Werner et al., 2000) (Figure 4.16). For this reason, it is
662 common whenever possible to calibrate the isotopic ratios using additional
663 paleothermometers. For short intervals, instrumental records of temperature can be
664 compared with isotopic ratios (e.g., Shuman et al., 1995). The few comparisons that have
665 been done (summarized in Jouzel et al., 1997) tend to show δ/T gradients that are slightly
666 lower than the spatial gradient. Accurate reconstructions of past temperature, but with
667 low time resolution, are obtained from the use of borehole thermometry. The center of the
668 *Greenland Ice Sheet* has not finished warming from the ice age, and the remaining cold
669 temperatures reveal how cold the ice age was (Cuffey et al., 1995; Johnsen et al., 1995).

670 Additional paleothermometers are available that use a thermal diffusion effect. In this
671 effect, gas isotopes are separated slightly when an abrupt temperature change at the
672 surface creates a temperature difference between the surface and the region a few tens of
673 meters down, where bubbles are pinched off from the interconnected pore spaces in old
674 snow (called firn). The size of the gas-isotope shift reveals the size of an abrupt warming,
675 and the number of years between the indicators of an abrupt change in the ice and in the
676 bubbles trapped in ice reveals the temperature before the abrupt change—if the snowfall
677 rate before the abrupt change is known (Severinghaus et al., 1998; Severinghaus and
678 Brook, 1999; Huber et al., 2006). These methods show that the value of the δ/T slope
679 produced by many of the large changes recorded in Greenland ice cores was considerably
680 less (typically by a factor of 2) than the spatial value, probably because of a relatively
681 larger reduction in winter snowfall in colder times (Cuffey et al., 1995; Werner et al.,
682 2000; Denton et al., 2005). The actual temperature changes were therefore larger than
683 would be predicted by the standard calibration.

684

FIGURE 4.16 NEAR HERE

686

687 In summary, water isotopes in polar precipitation are a reliable proxy for mean
688 annual air temperature, but for quantitative use, some means of calibrating them is
689 required. They may be calibrated either against instrumental data by using an alternative
690 estimate of temperature change, or through modeling, even for ice deposited during the
691 Holocene (Schmidt et al., 2007).

692

693 **4.3.1f Fossil assemblages and sea surface temperatures**

694 Different species live preferentially at different temperatures in the modern ocean.
695 Modern observations can be used to learn the preferences of species. An inherent
696 assumption is that species maintain their preferences through time. With that assumption,
697 the mathematical expression of these preferences plus the history of where the various
698 species lived in the past can then be used to interpret past temperatures (Imbrie and Kipp,
699 1971; CLIMAP, 1981). This line of reasoning is primarily applied to near-surface
700 (planktic) species, and especially to foraminifers, diatoms, and dinoflagellates. The
701 presence or absence and the relative abundance of species can be used. Such methods are
702 now commonly supported by sea-surface temperature estimates using emerging
703 biomarker techniques outlined below.

704

705 **4.3.1g Biogeochemistry**

706 Within the past decade, two new organic proxies have emerged that can be used
707 to reconstruct past ocean surface temperature. Both measurements are based on
708 quantifying the proportions of **biomarkers**—molecules produced by restricted groups of
709 organisms—preserved in sediments. In the case of the “ $U^{k'}_{37}$ index” (Brassell et al., 1986
710 ; Prahl et al., 1988), a few closely related species of coccolithophorid algae are entirely
711 responsible for producing the 37-carbon ketones (“alkenones”) used in the
712 paleotemperature index, whereas crenarcheota (archaea) produce the tetra-ether lipids that
713 make up the TEX_{86} index (Wuchter et al., 2004). Although the specific function that the
714 alkenones and glycerol dialkyl tetraethers serve for these organisms is unclear, the
715 relationship of the biomarker $U^{k'}_{37}$ index to temperature has been confirmed

716 experimentally in the laboratory (Prahl et al., 1988) and by extensive calibrations of
717 modern surface sediments to overlying surface ocean temperatures (Muller et al., 1998,
718 Conte et al., 2006, Wuchter et al., 2004).

719 Biomarker reconstructions have several advantages for reconstructing sea surface
720 conditions in the Arctic. First, in contrast to $\delta^{18}\text{O}$ analyses of marine carbonates (outlined
721 above), the confounding effects of salinity and ice volume do not compromise the utility
722 of **biomarkers** as paleotemperature proxies (a brief discussion of caveats in the use of
723 U^{k}_{37} is given below). Both the U^{k}_{37} and TEX_{86} proxies can be measured reproducibly to
724 high precision (analytical errors correspond to about 0.1°C for U^{k}_{37} and 0.5°C for
725 TEX_{86}), and sediment extractions and gas or liquid chromatographic detections can be
726 automated for high sampling rates. The abundances of **biomarkers** also provide insights
727 into the composition of past ecosystems, so that links between the physical oceanography
728 of the high latitudes and carbon cycling can be assessed. And lastly, organic **biomarkers**
729 can usually be recovered from Arctic sediments that do not preserve carbonate or
730 siliceous microfossils. It should be noted, however, that the harsh conditions of the
731 northern high latitudes mean that the organisms producing the alkenone and tetraethers
732 possibly were excluded at certain times and places; thus, continuous records cannot be
733 guaranteed.

734 The principal caveats in using **biomarkers** for paleotemperature reconstructions
735 come from ecological and evolutionary considerations. Alkenones are produced by algae
736 that are restricted to the region of abundant light (the photic zone), so paleotemperature
737 estimates based on them apply to this layer, which approximates the sea surface
738 temperature. In the vast majority of the ocean, the alkenone signal recorded by sediments

739 closely correlates with mean annual sea-surface temperature (Muller et al., 1998; Conte et
740 al., 2006; Figure 4.17). However, in the case of highly seasonal high-latitude oceans, the
741 temperatures inferred from the alkenone $U^{k'}_{37}$ index may better approximate summer
742 surface temperatures than mean annual sea-surface temperature. Furthermore, past
743 changes in the season of production could bias long-term time series of past temperatures
744 that are based on the $U^{k'}_{37}$ proxy. Depending on water column conditions, past production
745 could have been highly focused toward a short (summer?) or a more diffuse (late spring–
746 early fall?) productive season. A survey of modern surface sediments in the North
747 Atlantic (Rosell-Mele et al., 1995) shows that the seasonal bias in alkenone unsaturation
748 is not important except at high (greater than 65°N.) latitudes (Rosell-Mele et al., 1995). A
749 possible additional complication with the $U^{k'}_{37}$ proxy is that in the Nordic Seas an
750 additional alkenone (of the 37:4 type) is common, although it is rare or absent in most of
751 the world ocean including the Antarctic. The relatively fresh and cold waters of the
752 Nordic Seas likely affect alkenone production by the usual species, or the mixture of
753 species that produce alkenone. Regardless, this oddity suggests caution in applying the
754 otherwise robust global calibration of alkenone unsaturation to Nordic Sea surface
755 temperature (Rosell-Mele and Comes, 1999).

756

757

FIGURE 4.17 NEAR HERE

758

759 In contrast to the near-surface restriction of the algae producing the $U^{k'}_{37}$
760 proxy, the marine crenarcheota that produce the tetraether membrane lipids used in the
761 TEX_{86} index can range widely through the water column. In situ analyses of particles

762 suspended in the water column show that the tetraether lipids are most abundant in winter
763 and spring months in many ocean provinces (Wuchter et al., 2005) and are present in
764 large amounts below 100 m depth. However, it appears that the chemical basis for the
765 TEX₈₆ proxy is fixed by processes in the upper lighted (photic) zone, so that the
766 sedimentary signal originates near the sea surface (Wuchter et al., 2005), just as for the
767 U^k₃₇ proxy. No studies have yet been conducted to assess how high-latitude seasonality
768 affects the TEX₈₆ proxy.

769 As for many other proxies, use of these biomarker proxies is based on the
770 assumption that the modern relation between organic proxies and temperature was the
771 same in the past. The two modern (and genetically closely related) species producing the
772 alkenones in the U^k₃₇ proxy can be traced back in time in a continuous lineage to the
773 Eocene (about 50 Ma), and alkenone occurrences coincide with the fossil remains of the
774 ancestral lineage in the same sediments (Marlowe et al., 1984). One might suppose that
775 past evolutionary events in the broad group of algae that includes these species might
776 have produced or eliminated other species that generated these chemicals but with a
777 different relation to temperature. However, other such species would cause jumps in
778 climate reconstructions at times of evolutionary events in the group, and no such jumps
779 are observed. The TEX₈₆ proxy can be applied to marine sediments 70–100 million years
780 old. The working assumption is, therefore, that both organic proxies can be applied
781 accurately to sediments containing the appropriate chemicals.

782 Because these biomarker proxies depend on changes in relative abundance of
783 chemicals, it is important that natural processes after death of the producing organisms do
784 not preferentially break down one chemical and thus change the ratio. Fortunately, the

785 ratio appears to be stable (Prah1 et al., 1989; Grice et al., 1998, Teece et al., 1998;
786 Herbert, 2003; Schouten et al., 2004). An additional complication is that sediments can
787 be moved around by ocean currents, so that the material sampled at one place might have
788 been produced in another place under different climate conditions (Thomsen et al., 1998;
789 Ohkouchi et al., 2002). Ordinarily, lengthy transport of **biomarkers** into a depositional
790 site is rare and volumes are small compared with the supply from the productive ocean
791 above, so that the proxy indeed records local climate. However, at some times and places,
792 the Arctic has been comparatively unproductive, so that transport from other parts of the
793 ocean, or from land in the case of the TEX₈₆ proxy, likely was important (Weijers et al.,
794 2006).

795

796 **4.3.1h Biological proxies in lakes**

797 Lakes and ponds are common in most Arctic regions and provide useful records
798 of climate change (Smol and Cumming, 2000; Cohen, 2003; Schindler and Smol, 2006;
799 Smol 2008). Many different biological climate proxies are preserved in Arctic lake and
800 pond sediments (Pienitz et al., 2004). Diatom shells (Douglas et al., 2004) and remains of
801 non-biting midge flies (chironomid head capsules; Bennike et al., 2004) are among the
802 biological indicators most commonly used to reconstruct ancient Arctic climate (Figure
803 4.18). The approach generally used by those who study the history of lakes
804 (paleolimnologists) is first to identify useful species— those that grow only within a
805 distinct range of conditions. Then, the modern conditions preferred by these indicator
806 species are determined, as are the conditions beyond which these indicator species cannot
807 survive. (Typically used are surface sediment calibration sets or training sets to which are

808 applied statistical approaches such as canonical correspondence analysis and weighted
809 averaging regression and calibration; see Birks, 1998.) The resulting mathematical
810 relations (or transfer functions such as those used in marine records) are then used to
811 reconstruct the environmental variables of interest, on the basis of the distribution of
812 indicator assemblages preserved in dated sediment cores (Smol, 2008). Where well-
813 calibrated transfer functions are not available, such as for some parts of the Arctic, less-
814 precise climate reconstructions are commonly based on the known ecological and life-
815 history characteristics of the organisms.

816

817

FIGURE 4.18 NEAR HERE

818

819 Ideally, sedimentary characteristics would be linked directly to key climatic
820 variables such as temperature (e.g., Pienitz and Smol, 1993; Joynt and Wolfe, 2001;
821 Bigler and Hall, 2003; Bennike et al., 2004; Larocque and Hall, 2004; Woller et al. 2004,
822 Finney et al., 2004, other chapters in Pienitz et al., 2004; Barley et al., 2006; Weckström
823 et al., 2006;). However, lake sediments typically record conditions in the lake that are
824 only indirectly related to climate (Douglas and Smol, 1999). For example, lake
825 ecosystems are strongly influenced by the length of the ice-free versus the ice-covered
826 season, by the Sun-blocking effect of any snow cover on ice (Figure 4.19) (e.g., Smol,
827 1988; Douglas et al., 1994; Sorvari and Korhola, 1998; Douglas and Smol, 1999; Sorvari
828 et al., 2002; Rühland et al., 2003; Smol and Douglas, 2007a) and by the existence or
829 absence of a seasonal layer of warm water near the lake surface that remains separate
830 from colder waters beneath (Figure 4.20). Shells and other features in the lake sediment

831 record the species living in the lake and conditions under which they grew. These factors
832 rather directly reflect the ice and snow cover and lake stratification and only indirectly
833 reflect the atmospheric temperature and precipitation that control the lake conditions.

834

835 FIGURE 4.19 NEAR HERE

836 FIGURE 4.20 NEAR HERE

837

838 **4.3.1i Insect proxies.**

839 Insects are common and typically are preserved well in Arctic sediment. Because
840 many insect types live only within narrow ranges of temperature or other environmental
841 conditions, the remains of particular insects in old sediments provides useful information
842 on past climate.

843 Calibrating the observed insect data to climate involves extensive modern and
844 recent studies, together with careful statistical analyses. For example, fossil beetles are
845 typically related to temperature using what is known as the Mutual Climatic Range
846 method (Elias et al., 1999; Bray et al., 2006). This method quantitatively assesses the
847 relation between the modern geographical ranges of selected beetle species and modern
848 meteorological data. A “climate envelope” is determined, within which a species can
849 thrive. When used with paleodata, the method allows for the reconstruction of several
850 parameters such as mean temperatures of the warmest and coldest months of the year.

851

852 **4.3.1j Sand dunes** When plant roots anchor the soil, sand cannot blow around to
853 make dunes. In the modern Arctic, and especially in Alaska (Figure 4.21) and Russia,

854 sand dunes are forming and migrating in many places where dry, cold conditions restrict
855 vegetation. During the last glacial interval and at some other times, dunes formed in
856 places that now lack active dunes and indicate colder or drier conditions at those earlier
857 times (Carter, 1981; Oswald et al., 1999; Beget, 2001; Mann et al., 2002). Some wind-
858 blown mineral grains are deposited in lakes. The rate at which sand and silt are deposited
859 in lakes increases as nearby vegetation is removed by cooling or drying, so analysis of the
860 sand and silt in lake sediments provides additional information on the climate (e.g.,
861 Briner et al., 2006).

862

863

FIGURE 4.21 NEAR HERE

864

865 **4.3.2 Proxies for Reconstruction of Precipitation**

866 In the case of sand dunes described above, separating the effects of changing
867 temperature from those of changing precipitation is likely to be difficult, but additional
868 indicators such as insect fossils in lake sediments very likely help by constraining the
869 temperature. In general, precipitation is more difficult to estimate than is temperature, so
870 reconstructions of changes in precipitation in the past are less common, and typically less
871 quantitative, than are reconstructions of past temperature changes.

872

873 **4.3.2a Vegetation-derived precipitation estimates** Different plants live in wet
874 and dry places, so indications of past vegetation provide estimates of past wetness. Plants
875 do not respond primarily to rainfall but instead to moisture availability. Availability is
876 primarily controlled in most places by the difference between precipitation and

877 evaporation, although some soils carry water downward so efficiently that dryness occurs
878 even without much evaporation.

879 Much modern **tundra** vegetation grows where precipitation exceeds evaporation.
880 Plants such as *Sphagnum* (bog moss), cotton-grass (*Eriophorum*), and cloudberry (*Rubus*
881 *chamaemorus*) indicate moist growing conditions. In contrast, grasses dominate dry
882 **tundra** and polar semi-desert. Such differences are evident today (Oswald et al., 2003)
883 and can be reconstructed from pollen and larger plant materials (macrofossils) in
884 sediments. Some regions of Alaska and Siberia retain sand dunes that formed in the last
885 glacial maximum but are inactive today; typically, those regions are near areas that had
886 grasses then but now have plants requiring greater moisture (Colinvaux, 1964; Ager and
887 Brubaker, 1985; Lozhkin et al. 1993; Goetcheus and Birks 2001, Zazula et al., 2003).

888 In Arctic regions, deep snow cover very likely allows the persistence of shrubs
889 that would be killed if exposed during the harsh winter cold and wind. For example,
890 dwarf willow can survive if snow depths exceed 50 cm (Kaplan et al., 2003). Siberian
891 stone pine requires considerable winter snow to weigh down and bury its branches
892 (Lozhkin et al, 2007). The presence of these species therefore indicates certain minimum
893 levels of winter precipitation.

894 Moisture levels can also be estimated quantitatively from pollen assemblages by
895 means of formal techniques such as inverse and forward modeling, following techniques
896 also used to estimate past temperatures. Moisture-related transfer functions have been
897 developed, in Scandinavia for example (Seppä and Hammarlund, 2000). Kaplan et al.
898 (2003) compared pollen-derived vegetation with vegetation derived from model
899 simulations for the present and key times in the past. The pollen data indicated that model

900 simulations for the Last Glacial Maximum tended to be “too moist”—the simulations
901 generated shrub-dominated biomes whereas the pollen data indicated drier **tundra**
902 dominated by grass.

903

904 **4.3.2b Lake-level derived precipitation estimates** In addition to their other uses
905 in paleoclimatology as described above, lakes act as natural rain gauges. If precipitation
906 increases relative to evaporation, lakes tend to rise, so records of past lake levels provide
907 information about the availability of moisture.

908 Most of the water reaching a lake first soaked into the ground and flowed through
909 spaces as groundwater, before it either seeped directly into the lake or else came back to
910 the surface in a stream that flowed into the lake. Smaller amounts of water fall directly on
911 the lake or flow over the land surface to the lake without first soaking in (e.g.,
912 MacDonald et al., 2000b). Lakes lose water to streams (“overflow”), as outflow into
913 groundwater, and by evaporation. If water supply to a lake increases, the lake level will
914 rise and the lake will spread. This spread will increase water loss from the lake by
915 increasing the area for evaporation, by increasing the area through which groundwater is
916 leaving and the “push” (hydraulic head) causing that outflow, and perhaps by forming a
917 new outgoing stream or increasing the size of an existing stream. Thus, the level of a lake
918 adjusts in response to changes in the balance between precipitation and evaporation in the
919 region feeding water to the lake (the catchment). Because either an increase in
920 precipitation or a reduction in evaporation will cause a lake level to rise, an independent
921 estimate of either precipitation or evaporation is required before one can estimate the
922 other on the basis of a history of lake levels (Barber and Finney, 2000).

923 Former lake levels can be identified by deposits such as the fossil shoreline they
924 leave (Figure 4.22); sometimes these deposits are preserved under water and can be
925 recognized in sonar surveys or other data, and these deposits can usually be dated.
926 Furthermore, the sediments of the lake very likely retain a signature of lake-level
927 fluctuations: coarse-grained material generally lies near the shore and finer grained
928 materials offshore (Digerfeldt, 1988), and these too can be identified, sampled, and dated
929 (Abbott et al., 2000).

930

931

FIGURE 4.22 NEAR HERE

932

933 For a given lake, modern values of the major inputs and outputs can be obtained
934 empirically, and a model can then be constructed that simulates lake-level changes in
935 response to changing precipitation and evaporation. Allowable pairs of precipitation and
936 evaporation can then be estimated for any past lake level. Particularly in cases where
937 precipitation is the primary control of water depth, it is possible to model lake level
938 responses to past changes in precipitation (e.g., Vassiljev, 1998; Vassiljev et al., 1998).
939 For two lakes in interior Alaska, this technique suggested that precipitation now was as
940 much as 50% lower than at the time of the Last Glacial Maximum (about 20 ka) (Barber
941 and Finney, 2000).

942

943

944

945

Biological groups living within lakes also leave fossil assemblages that can be
interpreted in terms of lake level by comparing them with modern assemblages. In all
cases, factors other than water depth (e.g., conductivity and salinity) likely influence the
assemblages (MacDonald et al., 2000b), but these factors are themselves likely to be

946 indirectly related to water depth. Aquatic plants, which are represented by pollen and
947 macrofossils, tend to dominate from nearshore to moderate depths, and shifts in the
948 abundance of pollen or seeds in one of more sediment profiles can indicate relative water-
949 level changes (Hannon and Gaillard, 1997; Edwards et al., 2000). Diatom and chironomid
950 (midge) assemblages may also be related quantitatively to lake depth by means of inverse
951 modeling and the transfer functions used to reconstruct past lake levels (Korhola et al.,
952 2000; Ilyashuk et al., 2005).

953 The great variety of lakes, and the corresponding range of sedimentary indicators,
954 requires that field scientists be broadly knowledgeable in selecting which lakes to study
955 and which techniques to use in reconstructions. For some important case studies, see
956 Hannon and Gaillard, 1997; Abbott et al., (2000), Edwards et al., (2000), Korhola et al.,
957 2000; Pienitz et al., (2000), Anderson et al., (2005), and Ilyashuk et al., 2005).

958

959 **4.3.2c Precipitation estimates from ice cores.** Ice cores provide a direct way of
960 recording the net accumulation rate at sites with permanent ice. The initial thickness of an
961 annual layer in an ice core (after mathematically accounting for the amount of air trapped
962 in the ice) is the annual accumulation. Most ice cores are drilled in cold regions that
963 produce little meltwater or runoff. Furthermore, sublimation or condensation and snow
964 drift generally account for little accumulation, so that accumulation is not too different
965 from the precipitation (e.g., Box et al., 2006). The thickness of layers deeper in the core
966 must be corrected for the thinning produced as the ice sheet spreads and thins under its
967 own weight, but for most samples this correction can be made with much accuracy by
968 using simple ice flow models (e.g., Alley et al., 1993; Cuffey and Clow, 1997).

969 The annual-layer thickness can be recorded using any component that varies
970 regularly with a defined seasonal cycle. Suitable components include visible layering
971 (e.g. Figure 4.14a), which responds to changes in snow density or impurities (Alley et
972 al., 1997), the seasonal cycle of water isotopes (Vinther et al., 2006), and seasonal cycles
973 in different chemical species (e.g. Rasmussen et al., 2006). Using more than one
974 component gives extra security to the combined output of counted years and layer
975 thicknesses.

976 Although the correction for strain (layer thinning) increases the uncertainty in
977 estimates of absolute precipitation rate deeper in ice cores, estimates of changes in
978 relative accumulation rate along an ice core can be considered reliable (e.g., Kapsner et
979 al., 1995). Because the accumulation rate combines with the temperature to control the
980 rate at which snow is transformed to ice, and because the isotopic composition of the
981 trapped air (Sowers et al., 1989) and the number of trapped bubbles in a sample (Spencer
982 et al., 2006) record the results of that transformation, then accumulation rates can also be
983 estimated from measurements of these parameters plus independent estimation of past
984 temperature using techniques described above.

985

986 **4.4 Arctic Climate over the past 65 Ma**

987

988 During the past 65 Ma (the Cenozoic), the Arctic has experienced a greater
989 change in temperature, vegetation, and ocean surface characteristics than has any other
990 Northern Hemisphere latitudinal band (e.g., Sewall and Sloan, 2001; Bice et al., 2006;
991 and see results presented below). Those times when the Arctic was unusually warm offer

992 insights into the feedbacks within the Arctic system that can amplify changes imposed
993 from outside the Arctic regions. Evidence from which the Cenozoic history of climate in
994 the Arctic is reconstructed is presented below, focussing especially on warm times as
995 identified by climate and environmental proxies outlined in section 5.3.

996

997 **4.4.1 Early Cenozoic and Pliocene Warm Times**

998 Records of the $\delta^{18}\text{O}$ composition of bottom-dwelling foraminifers from the global
999 ocean document a long-term cooling of the deep sea during the past 70 Ma (Figure 4.8;
1000 Zachos et al., 2001) and the development of large Northern Hemisphere continental ice
1001 sheets at 2.6–2.9 Ma (Duk-Rodkin et al., 2004). As discussed below and in Chapter 5
1002 (past rates of Arctic climate change), Arctic climate history is broadly consistent with the
1003 global data reported by Zachos et al. (2001): general cooling and increase in ice was
1004 punctuated by short-lived and longer lived reversals, by variations in cooling rate, and by
1005 additional features related to growth and shrinkage of ice once the ice was well
1006 established. A detailed Arctic Ocean record that is equivalent to the global results of
1007 Zachos et al. (2001) is not yet available, and because the Arctic Ocean is geographically
1008 somewhat isolated from the world ocean (e.g., Jakobsson and MacNab, 2006), the
1009 possibility exists that some differences would be found. Emerging paleoclimate
1010 reconstructions from the Arctic Ocean derived from recently recovered sediment cores on
1011 the *Lomonosov Ridge* (Backman et al., 2006; Moran et al., 2006) shed new light on the
1012 Cenozoic evolution of the Arctic Basin, but the data have yet to be fully integrated with
1013 the evidence from terrestrial records or with the sketchy records from elsewhere in the
1014 Arctic Ocean (see Chapter 7, Arctic sea ice).

1015 Data clearly show warm Arctic conditions during the Cretaceous and early
1016 Cenozoic. For example, late Cretaceous (70 Ma) Arctic Ocean temperatures of 15°C
1017 (compared to near-freezing temperatures today) are indicated by TEX₈₆-based estimates
1018 (Jenkyns et al., 2004). The same indicator shows that peak Arctic Ocean temperatures
1019 near the North Pole rose from about 18°C to more than 23°C during the short-lived
1020 Paleocene-Eocene thermal maximum about 55 Ma (Figure 4.23) (Moran et al., 2006;
1021 also see Sluijs et al., 2006; 2008). This rise was synchronous with warming on nearby
1022 land from a previous temperature of about 17°C to peak temperature during the event of
1023 about 25°C (Weijers et al., 2007). By about 50 Ma, Arctic Ocean temperatures were
1024 about 10°C and relatively fresh surface waters were dominated by aquatic ferns
1025 (Brinkhuis et al., 2006). Restricted connections to the world ocean allowed the fern-
1026 dominated interval to persist for about 800,000 years; return of more-vigorous
1027 interchange between the Arctic and North Atlantic oceans was accompanied by a
1028 warming in the central Arctic Ocean of about 3°C (Brinkhuis et al., 2006). On Arctic
1029 lands during the Eocene (55–34 Ma), forests of *Metasequoia* dominated a landscape
1030 characterized by organic-rich floodplains and wetlands quite different from the modern
1031 **tundra** (McKenna, 1980; Francis, 1988; Williams et al., 2003).

1032

1033

FIGURE 4.23 NEAR HERE

1034

1035 Terrestrial evidence shows that warm conditions persisted into the early Miocene
1036 (23–16 Ma), when the central *Canadian Arctic Islands* were covered in mixed conifer-
1037 hardwood forests similar to those of southern Maritime Canada and New England today

1038 (Whitlock and Dawson, 1990). *Metasequoia* was still present although less abundant than
1039 in the Eocene. Still younger, deposits known as the Beaufort Formation and tentatively
1040 dated to about 8–3 Ma (and thus within Miocene to Pliocene times) record an extensive
1041 riverside forest of pine, birch, and spruce, which lived throughout the *Canadian Arctic*
1042 *Archipelago* before geologic processes formed many of the channels that now divide the
1043 islands.

1044 The relatively warm climates of the earlier Cenozoic altered to the colder times of
1045 the Quaternary Ice Age, which was marked by cyclic growth and shrinkage of extensive
1046 land ice, during the Pliocene (5–1.8 Ma). Climate changed although continental
1047 configurations remained similar to those of the present, and most Pliocene plant and
1048 animal species were similar to those that remain today. A well-documented warm period
1049 in the middle Pliocene (about 3 Ma), just before the planet transitioned into the
1050 Quaternary ice age, supported forests that covered large regions near the Arctic Ocean
1051 that are currently polar deserts. Fossils of *Arctica islandica* (a marine bivalve that does
1052 not live near seasonal sea ice) in marine deposits as young as 3.2 Ma on Meighen Island
1053 at 80°N., likely record the peak Pliocene mean warmth of the ocean (Fyles et al., 1991).
1054 As compared with recent conditions, warmer conditions then are widely indicated
1055 (Dowsett et al., 1994). At a site on *Ellesmere Island*, application of a novel technique for
1056 paleoclimatic reconstruction based on ring-width and isotopic measurements of wood
1057 suggests mean-annual temperatures 14°C warmer than recently (Ballantyne et al., 2006).
1058 Additional data from records of beetles and plants indicate mid-Pliocene conditions as
1059 much as 10°C warmer than recently for mean summer conditions, and even larger
1060 wintertime warming to a maximum of 15°C or more (Elias and Matthews, 2002).

1061 Much attention has been focused on learning the causes of the slow, bumpy slide
1062 from Cretaceous hothouse temperatures to the recent ice age. As discussed below,
1063 changes in greenhouse-gas concentrations appear to have played the dominant role, and
1064 linked changes in continental positions, in sea level, and in oceanic circulation also
1065 contributed.

1066 Based on general circulation models of climate, Barron et al. (1993) found that
1067 continental position had little effect on temperature difference between Cretaceous and
1068 modern temperatures (also see Poulsen et al., 1999 and references therein). Years later,
1069 Donnadieu et al. (2006), using more sophisticated climate modeling, found that
1070 continental motions and their effects on atmospheric and oceanic circulation modified
1071 global average temperature by almost 4°C from Early to Late Cretaceous; this result does
1072 not compare directly with modern conditions, but it does suggest that continental motions
1073 can notably affect climate. However, despite much effort, modeling does not indicate that
1074 the motion of continents by itself can explain either the long-term cooling trend from the
1075 Cretaceous to the ice age or the “wiggles” within that cooling.

1076 The direct paleoclimatic data provide one interesting perspective on the role of
1077 oceanic circulation in the warmth of the later Eocene. When the Arctic Ocean was filled
1078 with water ferns living in “brackish” water (less salty than normal marine water) in an
1079 ocean that was ice-free or nearly so, the oceanic currents reaching the near-surface Arctic
1080 Ocean must have been greatly weakened relative to today for the fresh water to persist.
1081 Thus, heat transport by oceanic currents cannot explain the Arctic-Ocean warmth of that
1082 time. The resumption of stronger currents and normal salinity was accompanied by a

1083 warming of about 3°C (Brinkhuis et al., 2006), important but not dominant in the
1084 temperature difference between then and now.

1085 As discussed in section 4.2.4, the atmospheric CO₂ concentration has changed
1086 during tens of millions of years in response to many processes, and especially to those
1087 processes linked to plate tectonics and perhaps also to biological evolution. Many lines of
1088 proxy evidence (see Royer, 2006) show that atmospheric CO₂ was higher in the warm
1089 Cretaceous than it was recently, and that it subsequently fell in parallel with the cooling (
1090 Figure 4.24). Furthermore, models find that the changing CO₂ concentration is sufficient
1091 to explain much of the cooling (e.g., Bice et al., 2006; Donnadieu et al., 2006).

1092

1093 FIGURE 4.24 NEAR HERE

1094

1095 A persistent difficulty is that models driven by changes in greenhouse gases
1096 (mostly CO₂) tend to underestimate Arctic warmth (e.g., Sloan and Barron, 1992). Many
1097 possible explanations have been offered for this situation: underestimation of CO₂ levels
1098 (Shellito et al., 2003; Bice et al., 2006); an enhanced greenhouse effect from polar
1099 stratospheric clouds during warm times (Sloan and Pollard, 1998; Kirk-Davidoff et al.,
1100 2002); changed planetary obliquity (Sewall and Sloan, 2004); reduced biological
1101 productivity that provided fewer cloud-condensation nuclei and thus fewer reflective
1102 clouds (Kump and Pollard, 2008); and greater heat transport by tropical cyclones (Korty
1103 et al., 2008). Several of these mechanisms use feedbacks not normally represented in
1104 climate models and that serve to amplify warming in the Arctic. Consideration of the
1105 literature cited above and of additional materials points to some combination of stronger

1106 greenhouse-gas forcing (see Alley, 2003 for a review) and to stronger long-term
1107 feedbacks than typically are included in models, rather than to large change in Earth's
1108 orbit, although that cannot be excluded.

1109 It is thought that greenhouse gases were the primary control on Arctic temperature
1110 changes because the warmth of the Paleocene-Eocene Thermal Maximum took place in
1111 the absence of any ice—and therefore the absence of any ice-albedo or snow-albedo
1112 feedbacks. As described above (see Sluijs et al., 2008 for an extensively referenced
1113 summary of the event together with new data pertaining to the Arctic), this thermal
1114 maximum was achieved by a rapid (within a few centuries or less), widespread warming
1115 coincident with a large increase in atmospheric greenhouse-gas concentrations from a
1116 biological source (whether from sea-floor methane, living biomass, soils, or other sources
1117 remains debated). Following the thermal maximum, the anomalous warmth decayed more
1118 slowly and the extra greenhouse gases dissipated for tens of thousands of years, to
1119 roughly 100,000 years ago. The event in the Arctic seems to have been positioned within
1120 a longer interval of restricted oceanic circulation into the Arctic Ocean (Sluijs et al.,
1121 2008), and it was too fast for any notable effect of plate tectonics or evolving life. The
1122 reconstructed CO₂ change thus is strongly implicated in the warming (e.g., Zachos et al.,
1123 2008).

1124 Taken very broadly, the Arctic changes parallel the global ones during the
1125 Cenozoic, except that changes in the Arctic were larger than globally averaged ones (e.g.,
1126 Sluijs et al., 2008). The global changes parallel changing atmospheric carbon-dioxide
1127 concentrations, and changing CO₂ is the likely cause of most of the temperature change
1128 (e.g., Royer, 2006; Royer et al., 2007).

1129 The well-documented warmth of the Pliocene is not fully explained. This interval
1130 is recent enough that continental positions were substantially the same as today. As
1131 reviewed by Jansen et al. (2007), many reconstructions show notable Arctic warmth but
1132 little low-latitude change; however, recent work suggests the possibility of low-latitude
1133 warmth as well (Haywood et al., 2005). Reconstructions of Pliocene atmospheric CO₂
1134 concentration (reviewed by Royer, 2006) generally agree with each other within the
1135 considerable uncertainties, but they allow values above, similar to, or even below the
1136 typical levels just before major human influence. Data remain equivocal on whether the
1137 ocean transported more heat during Pliocene warmth (reviewed by Jansen et al., 2007).
1138 The high-latitude warmth thus is likely to have originated primarily from changes in
1139 greenhouse-gas concentrations in the atmosphere, or from changes in oceanic or
1140 atmospheric circulation, or from some combination, perhaps with a slight possibility that
1141 other processes also contributed.

1142

1143 **4.4.2 The Early Quaternary: Ice-Age Warm Times**

1144 A major reorganization of the climate system occurred between 3.0 and 2.5 Ma.
1145 As a result, the first continental ice sheets developed in the North American and Eurasian
1146 Arctic and marked the onset of the Quaternary Ice Ages (Raymo, 1994). For the first 1.5–
1147 2.0 Ma, ice age cycles appeared at a 41 ka interval, and the climate oscillated between
1148 glacial and interglacial states (Figure 4.25). A prominent but apparently short-lived
1149 interglacial (warm interval) about 2.4 Ma is recorded especially well in the *Kap*
1150 *København* Formation, a 100-m-thick sequence of estuarine sediments that covered an
1151 extensive lowland area near the northern tip of Greenland (Funder et al., 2001).

1152

1153

FIGURE 4.25 NEAR HERE

1154

1155

1156

1157

1158

1159

1160

1161

1162

1163

1164

1165

1166

1167

1168

1169

1170

FIGURE 4.26 NEAR HERE

1171

1172

1173

1174

The rich and well-preserved fossil fauna and flora in the *Kap København* Formation (Figure 4.26) record warming from cold conditions into an interglacial and then subsequent cooling during 10,000–20,000 years. During the peak warmth, forest trees reached the Arctic Ocean coast, 1000 kilometers (km) north of the northernmost trees today. Based on this warmth, Funder et al. (2001) suggested that the *Greenland Ice Sheet* must have been reduced to local ice caps in mountain areas (Figure 4.26a) (see Chapter 5, Greenland Ice Sheet). Although finely resolved time records are not available throughout the Arctic Ocean at that time, by analogy with present faunas along the Russian coast, the coastal zone would have been ice-free for 2 to 3 months in summer. Today this coast of Greenland experiences year-round sea ice, and models of diminishing sea ice in a warming world generally indicate long-term persistence of summertime sea ice off these shores (e.g., Holland et al., 2006). Thus, the reduced sea ice off northern Greenland during deposition of the *Kap København* Formation suggests a widespread warm time in which Arctic sea ice was much diminished.

1175 deposition of the Kap København were not caused by notably greater solar insolation,
1176 owing to the relative repeatability of the Milankovitch variations during millions of years
1177 (e.g., Berger et al., 1992). As discussed above, uncertainties in estimation of atmospheric
1178 CO₂ concentration, ocean heat transport, and perhaps other factors at the time of the *Kap*
1179 *København* Formation are sufficiently large to preclude strong conclusions about the
1180 causes of the unusual warmth.

1181 Potentially correlative records of warm interglacial conditions are found in
1182 deposits on coastal plains along the northern and western shores of Alaska. High sea
1183 levels during interglaciations repeatedly flooded the *Bering Strait*, and they rapidly
1184 modified the configuration of the coastlines, altered regional continentality (isolation
1185 from the moderating influence of the sea), and reinvigorated the exchange of water
1186 masses between the North Pacific, Arctic, and North Atlantic oceans. Since the first
1187 submergence of the *Bering Strait* about 5.5–5 Ma (Marincovich and Gladenkov, 2001),
1188 this marine gateway has allowed relatively warm Pacific water from as far south as
1189 northern Japan to reach as far north as the *Beaufort Sea* (Brigham-Grette and Carter,
1190 1992). The *Gubik Formation* of northern *Alaska* records at least three warm high sea
1191 stands in the early Quaternary (Figure 4.27). During the Colvillian transgression, about
1192 2.7 Ma, the *Alaskan Coastal Plain* supported open **boreal** forest or spruce-birch
1193 woodland with scattered pine and rare fir and hemlock (Nelson and Carter, 1991). Warm
1194 marine conditions are confirmed by the general character of the ostracode fauna, which
1195 includes *Pterygocythereis vannieuwenhuisei* (Brouwers, 1987), an extinct species of a
1196 genus whose modern northern limit is the *Norwegian Sea* and which, in the northwestern
1197 Atlantic Ocean, is not found north of the southern cold-temperate zone (Brouwers, 1987).

1198 Despite the high sea level and relative warmth indicated by the Colvillian transgression,
1199 erratics (rocks not of local origin) in Colvillian deposits southwest of *Barrow*, Alaska,
1200 indicate that glaciers then terminated in the Arctic Ocean and produced icebergs large
1201 enough to reach northwest Alaska at that time.

1202

1203 FIGURE 4.27 NEAR HERE

1204

1205 Subsequently, the Bigbendian transgression (about 2.5 Ma) was also warm, as
1206 indicated by rich molluscan faunas such as the gastropod *Littorina squalida* and the
1207 bivalve *Clinocardium californiense* (Carter et al., 1986). The modern northern limit of
1208 both of these mollusk species is well to the south (Norton Sound, Alaska). The presence
1209 of sea otter bones suggests that the limit of seasonal ice on the *Beaufort Sea* was
1210 restricted during the Bigbendian interval to positions north of the Colville River and thus
1211 well north of typical 20th-century positions (Carter et al., 1986); modern sea otters cannot
1212 tolerate severe seasonal sea-ice conditions (Schneider and Faro, 1975).

1213 The youngest of these early Quaternary events of high sea level is the
1214 Fishcreekian transgression (about 2.1–2.4 Ma), suggested to be the same age as the *Kap*
1215 *Kobenhavn* Formation on Greenland (Brigham-Grette and Carter, 1992). However, age
1216 control is not complete, and Brigham (1985) and Goodfriend et al. (1996) suggested that
1217 the Fishcreekian could be as young as 1.4 Ma. This deposit contains several mollusk
1218 species that currently are found only to the south. Moreover, sea otter remains and the
1219 intertidal gastropod *Littorina squalida* at Fish Creek suggest that perennial sea ice was
1220 absent or severely restricted during the Fishcreekian transgression (Carter et al., 1986).

1221 Correlative deposits rich in mollusk species that currently live only well to the south are
1222 reported from the coastal plain at *Nome, Alaska* (Kaufman and Brigham-Grette, 1993).

1223 The available data clearly indicate episodes of relatively warm conditions that
1224 correlate with high sea levels and reduced sea ice in the early Quaternary. The high sea
1225 levels suggest melting of land ice (see Chapter 67, Greenland Ice Sheet). Thus the
1226 correlation of warmth with diminished ice on land and at sea (see Chapter 7, Arctic sea
1227 ice)—indicated by recent instrumental observations, model results, and data from other
1228 time intervals—is also found for this time interval. Improved time resolution of histories
1229 of forcing and response will be required to assess the causes of the changes, but estimates
1230 of forcings indicate that they were relatively moderate and thus that the strong **Arctic**
1231 **amplification** of climate change was active in these early Quaternary events.

1232

1233 **4.4.3 The Mid-Pleistocene Transition: 41 ka and 100 ka worlds**

1234 Since the late Pliocene, the cyclical waxing and waning of continental ice sheets
1235 have dominated global climate variability. The variations in sunshine caused by features
1236 of Earth's orbit have been very important in these ice-sheet changes, as described in
1237 Chapter 3 (paleoclimate concepts).

1238 After the onset of glaciation in North America about 2.7 Ma (Raymo, 1994), ice
1239 grew and shrank as Earth's obliquity (tilt) varied in its 41 ka cycle. But between 1.2 and
1240 0.7 Ma, the variations in ice volume became larger and slower, and an approximately
1241 100-ka period has dominated especially during the last 700 ka or so (Figure 4.25).

1242 Although Earth's eccentricity varies with an approximately 100-ka period, this variation
1243 does not cause as much change in sunshine in the key regions of ice growth as did the

1244 faster cycles, so the reasons for the dominant 100-ka period in ice volume remain
1245 obscure. Roe and Allen (1999) assessed six different explanations of this behavior and
1246 found that all fit the data rather well. The record is still too short to allow the data to
1247 demonstrate the superiority of any one model.

1248 Models for the 100-ka variability commonly assign a major role to the ice sheets
1249 themselves and especially to the *Laurentide Ice Sheet* on North America, which
1250 dominated the total global change in ice volume (e.g., Marchant and Denton, 1996). For
1251 example, Marshall and Clark (2002) modeled the growth and shrinkage of the Laurentide
1252 Ice Sheet and found that during growth the ice was frozen to the bed beneath and unable
1253 to move rapidly. After many tens of thousands of years, ice had thickened sufficiently
1254 that it trapped Earth's heat and thawed the bed, which allowed faster flow. Faster flow of
1255 the ice sheet lowered the upper surface, which allowed warming and melting (see Chapter
1256 6, Greenland Ice Sheet). Behavior such as that described could cause the main variations
1257 of ice volume to be slower than the main variations in sunshine caused by Earth's orbital
1258 features, and the slow-flowing ice might partly ignore the faster variations in sunshine
1259 until the shift to faster flow allowed a faster response. Note that this explanation remains
1260 a hypothesis, and other possibilities exist. Alternative hypotheses require interactions in
1261 the Southern Ocean between the ocean and sea ice and between the ocean and the
1262 atmosphere (Gildor et al., 2002). For example, Toggweiler (2008) suggested that because
1263 of the close connection between the southern westerly winds and meridional overturning
1264 circulation in the Southern Ocean, shifts in wind fields very likely control the exchange
1265 of CO₂ between the ocean and the atmosphere. Carbon models support the notion that
1266 weathering and the burial of carbonate can be perturbed in ways that alter deep ocean

1267 carbon storage and that result in 100 ka CO₂ cycles (Toggweiler, 2008). Others have
1268 suggested that 100 ka cycles and CO₂ might be controlled by variability in obliquity
1269 cycles (i.e., two or three 41 ka cycles (Huybers, 2006) or by variable precession cycles
1270 (altering the 19 ka and 23 ka cycles (Raymo, 1997)). Ruddimann (2006) recently
1271 furthered these ideas but suggested that since 900 ka, CO₂-amplified ice growth
1272 continued at the 41 ka intervals but that polar cooling dampened ice ablation. His CO₂-
1273 feedback hypothesis suggests a mechanism that combines the control of 100 ka cycles
1274 with precession cycles (19 ka and 23 ka) and with tilt cycles (41 ka). The cause of the
1275 switch in the length of climate cycles from about 41 ka to about 100 k.y, known as the
1276 mid-Pleistocene transition, also remains obscure. This transition is of particular interest
1277 because it does not seem to have been caused by any major change in Earth's orbital
1278 behavior, and so the transition likely reflects a fundamental threshold within the climate
1279 system.

1280 The mid-Pleistocene transition is very likely to be at least in part related to the
1281 continuation of the gradual global cooling that began in the early Cenozoic, as described
1282 above (Raymo et al., 1997; 2006; Ruddiman, 2003). If, for example, the 100-ka cycle
1283 requires that the *Laurentide Ice Sheet* grow sufficiently large and thick to trap enough of
1284 Earth's internal heat that thaws the ice-sheet bed (Marshall and Clark, 2002), then long-
1285 term cooling may have reached the threshold at which the ice sheet became large enough.

1286 However, such a cooling model does not explain the key observation (Clark et al.,
1287 2006) that the ice sheets of the last 700 ka configured a larger volume (Clark et al., 2006)
1288 into a smaller area (Boellstorff, 1978; Balco et al., 2005a,b) than was true of earlier ice
1289 sheets. Clark and Pollard (1998) used this observation to argue that the early *Laurentide*

1290 *Ice Sheet* must have been substantially lower in elevation than in the late Pleistocene,
1291 possibly by as much as 1 km. Clark and Pollard (1998) suggested that the tens of millions
1292 of warm years back to the Cretaceous and earlier had produced thick soils and broken-up
1293 rocks below the soil. When glaciations began, the ice advanced over these water-
1294 saturated soils, which deformed easily. Just as grease on a griddle allows batter poured on
1295 top to spread easily into a wide, thin pancake, deformation of the soils beneath the
1296 growing ice (Alley, 1991) would have produced an extensive ice sheet that did not
1297 contain a large volume of ice. As successive ice ages swept the loose materials to the
1298 edges of the ice sheet, and as rivers removed most of the materials to the sea, hard
1299 bedrock was exposed in the central region. And, just as the bumps and friction of an
1300 ungreased waffle iron slow spreading of the batter to give a thicker, not-as-wide breakfast
1301 than on a greased griddle, the hard, bumpy bedrock produced an ice sheet that did not
1302 spread as far but which contained more ice.

1303 Other hypotheses also exist for these changes. A complete explanation of the
1304 onset of extensive glaciation on North America and Eurasia as well as Greenland about
1305 2.8 Ma, or of the transition from 41 ka to 100 ka ice age cycles, remains the object of
1306 ongoing investigations.

1307

1308 **4.4.4 A link between ice volume, atmospheric temperature and greenhouse**
1309 **gases**

1310 The globally-averaged temperature change during one of the large 100-ka ice-age
1311 cycles was about 5°–6°C (Jansen et al., 2007). The larger changes were measured in the
1312 Arctic and close to the ice sheets, such as a change of 21°–23°C atop the *Greenland Ice*

1313 *Sheet* (Cuffey et al., 1995). The total change in sunshine reaching the planet during these
1314 cycles was near zero, and the orbital features served primarily to move sunshine from
1315 north to south and back, or from equator to poles and back, depending on the cycle
1316 considered (see Chapter 3, paleoclimate concepts).

1317 As discussed by Jansen et al. (2007), and in section 5.2.6 above, many factors
1318 probably contributed to the large temperature change despite very small global change in
1319 total sunshine. Cooling produced growth of reflective ice that reduced the amount of
1320 sunshine absorbed by the planet. Complex changes especially in the ocean reduced
1321 atmospheric carbon dioxide, and both oceanic and terrestrial changes reduced
1322 atmospheric methane and nitrous oxide, all of which are greenhouse gases; the changes in
1323 carbon dioxide were most important. Various changes produced additional dust that
1324 blocked sunshine from reaching the planet (e.g., Mahowald et al., 2006). Cooling caused
1325 regions formerly forested to give way to grasslands or **tundra** that also reflected more
1326 sunshine. While Earth's orbit features drove the ice-age cycles, these feedbacks are
1327 required to provide quantitatively accurate explanations of the changes.

1328 The relation between climate and carbon dioxide has been relatively constant for
1329 at least 650,000 years (Siegenthaler et al., 2005), and the growth and shrinkage of ice,
1330 cooling and warming of the globe, and other changes have repeated along similar
1331 although not identical paths. However, some of the small differences between successive
1332 cycles are of interest, as discussed next.

1333

1334 **4.4.5 Marine Isotopic Stage 11 – a long interglaciation**

1335 Following the mid-Pleistocene transition, the growth and decay of ice sheets
1336 followed a 100 ka cycle: brief, warm interglaciations lasted from 10 to ca. 40 ka, after
1337 which ice progressively extended to a maximum limit, and then the icy interval
1338 terminated rapidly by the transition into the next warm interglaciation (e.g., Kellogg,
1339 1977; Ruddiman et al., 1986; Jansen et al., 1988; Bauch and Erlenkeuser, 2003; Henrich
1340 and Baumann, 1994). As discussed above, this 100 ka cycle is unlikely to be linked to the
1341 100 ka variation of the eccentricity, or out-of-roundness, of Earth's orbit about the Sun,
1342 because there is so little change in solar isolation reaching the Earth because of this
1343 effect.

1344 The eccentricity exhibits an additional cycle of just greater than 400,000 years,
1345 such that the orbit goes from almost round to more eccentric to almost round in about
1346 100,000 years, but the maximum eccentricity reached in this 100,000-year cycle increases
1347 and decreases within a 400,000-year cycle (Berger and Loutre, 1991; Loutre, 2003).
1348 When the orbit is almost round, there is little effect from Earth's precession, which
1349 determines whether Earth is closer to the Sun or farther from the Sun during a particular
1350 season such as northern summer. About 400,000 years ago, during marine isotope stage
1351 (MIS) 11, the 400,000-year cycle caused a nearly round orbit to persist. The interglacial
1352 of MIS 11 lasted longer than previous or subsequent interglacials (see Droxler et al., 2003
1353 and references therein; Kandiano and Bauch, 2007; Jouzel et al., 2007), perhaps because
1354 the summer sunshine (insolation) at high northern latitudes did not become low enough at
1355 the end of the first 10,000 years of the interglacial to allow ice growth at high northern
1356 latitudes—because the persistently nearly round orbit (i.e., of low eccentricity) prevented
1357 adequate cooling during northern summer (Figure 4.28).

1358

1359

FIGURE 4.28 NEAR HERE

1360

1361

1362

1363

1364

1365

1366

1367

1368

1369

4.4.6 Marine Isotopic Stage (MIS) 5e: The Last Interglaciation

1370

1371

1372

1373

1374

1375

1376

1377

1378

1379

As discussed in Chapter 6 (Greenland Ice Sheet), indications of Arctic and subarctic temperatures at this time versus more-recent interglacials are inconsistent (also see Stanton-Frazee et al., 1999; Bauch et al., 2000; Droxler and Farrell, 2000; Helmke and Bauch, 2003). Sea level seems to have been higher at this time than at any time since, and data from Greenland are consistent with notable shrinkage or loss of the ice sheet accompanying the notable warmth, although the age of this shrinkage is not constrained well enough to be sure that the warm time recorded was indeed MIS 11 (Chapter 6).

The warmest millennia of at least the past 250,000 years occurred during MIS 5, and especially during the warmest part of that interglaciation, MIS 5e (e.g., McManus et al., 1994; Fronval and Jansen, 1997; Bauch et al., 1999; Kukla, 2000). At that time global ice volumes were smaller than they are today, and Earth's orbital parameters aligned to produce a strong positive anomaly in solar radiation during summer throughout the Northern Hemisphere (Berger and Loutre, 1991). Between 130 and 127 ka, the average solar radiation during the key summer months (May, June, and July) was about 11% greater than solar radiation at present throughout the Northern Hemisphere, and a slightly greater anomaly, 13%, has been measured over the Arctic. Greater solar energy in summer, melting of the large Northern Hemisphere ice sheets, and intensification of the

1380 North Atlantic Drift (Chapman et al., 2000; Bauch and Kandiano, 2007) combined to
1381 reduce Arctic Ocean sea ice, to allow expansion of **boreal** forest to the Arctic Ocean
1382 shore throughout large regions, to reduce permafrost, and to melt almost all glaciers in
1383 the Northern Hemisphere (CAPE Project Members, 2006).

1384 High solar radiation in summer during MIS 5e, amplified by key boundary-
1385 condition feedbacks (especially sea ice, seasonal snow cover, and atmospheric water
1386 vapor; see above), collectively produced summer temperature anomalies 4°–5°C above
1387 present over most Arctic lands, substantially above the average Northern Hemisphere
1388 summer temperature anomaly (0°–2°C above present; CLIMAP Project Members, 1984;
1389 Bauch and Erlenkeuser, 2003). MIS 5e demonstrates the strength of positive feedbacks
1390 on Arctic warming (CAPE Project Members, 2006; Otto-Bleisner et al., 2006).

1391

1392 **4.4.6a Terrestrial MIS 5e records** At high northern latitudes, summer
1393 temperatures exert the dominant control on glacier mass balance, unless they are
1394 accompanied by strong changes in precipitation (e.g., Oerlemans, 2001; Denton et al.,
1395 2005; Koerner, 2005). Summer temperature is also the most effective predictor of most
1396 biological processes, although seasonality and the availability of moisture very likely also
1397 influence some biological parameters such as dominance by evergreen or by deciduous
1398 vegetation (Kaplan et al., 2003). For these reasons, most studies of conditions during MIS
1399 5e have focused on reconstructing summer temperatures. Terrestrial MIS 5e climate,
1400 especially, has been reconstructed from diagnostic assemblages of biotic proxies
1401 preserved in lake, peat, river, and shallow marine archives and from isotopic changes
1402 preserved in ice cores and carbonate deposits in lakes. Estimated winter and summer

1403 temperatures, and hence seasonality, are well constrained for Europe but are poorly
1404 known for most other Arctic regions; likewise, precipitation reconstructions are limited to
1405 qualitative estimates in most cases where they are available, and they are not available for
1406 most regions.

1407 During MIS 5e, all sectors of the Arctic had summers that were warmer than at
1408 present, but the magnitude of warming differed from one place to another (Figure 4.29)
1409 (CAPE Last Interglacial Project Members, 2006). Positive summer temperature
1410 anomalies were largest around the Atlantic sector, where summer warming was typically
1411 4°–6°C. This anomaly extended into Siberia, but it decreased from Siberia westward to
1412 the European sector (0°–2°C), and eastward toward *Beringia* (2°–4°C). The *Arctic coast*
1413 *of Alaska* had sea-surface temperatures 3°C above recent values and considerably less
1414 summer sea ice than recently, but much of interior Alaska had smaller anomalies (0°–
1415 2°C) that probably extended into western Canada. In contrast, northeastern Canada and
1416 parts of Greenland had summer temperature anomalies of about 5°C and perhaps more
1417 (see Chapter 6 for a discussion of Greenland).

1418

1419

FIGURE 4.29 NEAR HERE

1420

1421 Precipitation and winter temperatures are more difficult to reconstruct for MIS 5e
1422 than are summer temperatures. In northeastern Europe, the latter part of MIS 5e was
1423 characterized by a marked increase in winter temperatures. A large positive winter
1424 temperature anomaly also occurred in Russia and western Siberia, although the timing is
1425 not as well constrained (Troitsky, 1964; Gudina et al., 1983; Funder et al., 2002).

1426 Qualitative precipitation estimates for most other sectors indicate wetter conditions than
1427 in the Holocene.

1428

1429 **4.4.6b Marine MIS 5e records** Low sedimentation rates in the central Arctic
1430 Ocean and the rare preservation of carbonate fossils limit the number of sites at which
1431 MIS 5e can be reliably identified in sediment cores. MIS 5e sediments from the central
1432 Arctic Ocean usually contain high concentrations of planktonic (surface-dwelling)
1433 foraminifers and coccoliths, which indicate a reduction in summer sea-ice coverage that
1434 permitted increased biological productivity (Gard, 1993; Spielhagen et al., 1997; 2004;
1435 Jakobsson et al., 2000; Backman et al., 2004; Polyak et al., 2004; Nørgaard-Pedersen et
1436 al., 2007a,b). However, occasional dissolution of carbonate fossils complicates the
1437 interpretation of microfossil concentrations. Also, marine sediments from MIS 5a,
1438 slightly younger and cooler than MIS 5e, sometimes have higher microfossil
1439 concentrations than do MIS 5e sediments (Gard, 1986; 1987).

1440 Arctic Ocean sediment cores recently recovered from the *Lomonosov Ridge*, north
1441 of Greenland, have revived the discussion of MIS 5e conditions in the Arctic Ocean.
1442 Unusually high concentrations of a subpolar foraminifer species, one which usually
1443 dwells in waters with temperatures well above freezing, were found in MIS 5e zones and
1444 interpreted to indicate warm interglacial conditions and much reduced sea-ice cover in
1445 the interior Arctic Ocean (Nørgaard-Pedersen et al., 2007a,b). Interpretation of these and
1446 other microfossils is complicated by the strong vertical stratification in the Arctic Ocean;
1447 today, warm Atlantic water (temperatures greater than 1°C) is in most areas isolated from
1448 the atmosphere by a relatively thin layer of cold (less than 1°C) fresher water; this cold

1449 water limits the transfer of heat to the atmosphere. It is not always possible to determine
1450 whether warm-water foraminifers found in marine sediment from the Arctic Ocean lived
1451 in warm waters that remained isolated from the atmosphere below the cold surface layer,
1452 or whether the warm Atlantic water had displaced the cold surface layer and was
1453 interacting with the atmosphere and affecting its energy balance.

1454 Landforms and fossils from the western Arctic and *Bering Strait* indicate vastly
1455 reduced sea ice during MIS 5 (Figure 4.30). The winter sea-ice limit is estimated to have
1456 been as much as 800 km farther north than its average 20th-century position, and summer
1457 sea ice was likely to have been much reduced relative to present (Brigham-Grette and
1458 Hopkins, 1995). These reconstructions are consistent with the northward migration of
1459 treeline by hundreds of kilometers throughout much of Alaska and nearby *Chukotka* and
1460 with the elimination of **tundra** from *Chukotka* to the Arctic Ocean coast (Lozhkin and
1461 Anderson, 1995).

1462

1463

FIGURE 4.30 NEAR HERE

1464

1465 Sufficient data are not yet available to allow unambiguous reconstruction of MIS
1466 5e conditions in the central Arctic Ocean. Key uncertainties are related to the extent and
1467 duration of Arctic Ocean sea ice. The vertical structure of the upper 500 m of the water
1468 column is also climatically important but poorly known, in particular whether the strong
1469 vertical stratification characteristic of the modern regime persisted throughout MIS 5e, or
1470 whether reduced sea ice and changes in the hydrologic cycle and winds destabilized this

1471 stratification and allowed Atlantic water to reside at the surface in larger areas of the
1472 Arctic Ocean.

1473

1474 **4.4.7 MIS 3 Warm Intervals**

1475 The temperature and precipitation history of MIS 3 (about 70–30 ka) is difficult to
1476 reconstruct because of the paucity of continuous records and the difficulty in providing a
1477 secure time frame. The $\delta^{18}\text{O}$ record of temperature change over the *Greenland Ice Sheet*
1478 and other ice-core data show that the North Atlantic region experienced repeated episodes
1479 of rapid, high-magnitude climate change, that temperatures rapidly increased by as much
1480 as 15°C (reviewed by Alley, 2007 and references therein), and that each warm period
1481 lasted several hundred to a few thousand years. These brief climate excursions are found
1482 not only in the *Greenland Ice Sheet* but are also recorded in cave sediments in China
1483 (Wang et al., 2001; Dykoski, et al., 2005) and in high-resolution marine records off
1484 California (Behl and Kennett, 1996), and in the Caribbean Sea’s Cariaco Basin (Hughen
1485 et al., 1996.), the Arabian Sea (Schulz et al., 1998) and the Sea of Okhotsk (Nürnberg and
1486 Tiedmann, 2004), among many other sites. The ice-core records from Greenland contain
1487 indications of climate change in many regions on the same time scale (for example, the
1488 methane trapped in ice-core bubbles was in part produced in tropical wetlands and was
1489 essentially all produced beyond the *Greenland Ice Sheet*; Severinghaus et al., 1998).
1490 These ice-core records demonstrate clearly that the climate-change events were
1491 synchronous throughout widespread areas, and that the ages of events from many regions
1492 agree within the stated uncertainties. These events were thus hemispheric to global in
1493 nature (see review by Alley, 2007) and are considered a sign of large-scale coupling

1494 between the ocean and the atmosphere (Bard, 2002). The cause of these events is still
1495 debated. However, Broecker and Hemming (2001) and Bard (2002) among others
1496 suggested that they were likely the result of major and abrupt reorganizations of the
1497 ocean's thermohaline circulation, probably related to ice sheet instabilities that
1498 introduced large quantities of fresh water into the North Atlantic (Alley, 2007). Such
1499 large and abrupt oscillations, which were linked to changes in North Atlantic surface
1500 conditions and probably to the large-scale oceanic circulation, persisted into the Holocene
1501 (MIS 1); the youngest was only about 8.2 ka (Alley and Ágústadóttir, 2005). However, it
1502 appears that the abrupt 8.2 ka cooling was linked to an ice-age cause, a catastrophic flood
1503 from a very large lake that had been dammed by the melting *Laurentide Ice Sheet*.

1504 Within MIS 3, land ice was somewhat reduced compared with the colder times of
1505 MIS 2 and MIS 4, but Arctic temperatures generally were much lower and ice more
1506 extensive than in MIS 1 (with certain exceptions). Sea level was lower at that time, the
1507 coastline was well offshore in many places, and the increased continentality very likely
1508 contributed to warmer summer temperatures that presumably were offset by colder winter
1509 temperatures.

1510 For example, on the *New Siberian Islands* in the *East Siberian Sea*, Andreev et al.
1511 (2001) documented the existence of graminoid-rich **tundra** thought to have covered wide
1512 areas of the emergent shelf while summer temperatures were perhaps as much as 2°C
1513 warmer than during the 20th century. At Elikchan 4 Lake in the upper *Kolyma* drainage,
1514 the sediment record contains at least three intervals (especially one about 38 ka) when
1515 summer temperatures and treeline reached late Holocene conditions (Anderson and
1516 Lozhkin, 2001). Insect faunas nearby in the lower *Kolyma* are thought to have thrived in

1517 summers that were 1°–4.5°C warmer than recently for similar intervals of MIS 3 Alfimov
1518 et al., 2003). In general, variable paleoenvironmental conditions were typical of the
1519 traditional Karaginskii-MIS 3 period throughout Arctic Russia; however, stratigraphic
1520 confusion within the limits of radiocarbon-dating precludes the widespread correlation of
1521 events.

1522 Relative warmth during MIS 3 appears to have been strongest in eastern *Beringia*;
1523 some evidence suggests that between 45 and 33 ka temperatures were only 1°–2°C lower
1524 than at present (Elias, 2007). The warmest interval in interior Alaska is known as the Fox
1525 Thermal Event, about 40–35 ka, which was marked by spruce forest **tundra** (Anderson
1526 and Lozhkin, 2001). Yet in the Yukon forests were most dense a little earlier, about 43–
1527 39 ka. In general (Anderson and Lozhkin, 2001), the warmest interstadial interval in all
1528 of *Beringia* possibly was 44–35 ka; it is well represented in proxies from interior sites
1529 and little or no vegetation response in areas closest to Bering Strait. Climatic conditions
1530 in eastern *Beringia* appear to have been harsher than modern conditions for all of MIS 3.
1531 In contrast, MIS 3 climates of western *Beringia* achieved modern or near modern
1532 conditions during several intervals. Moreover, although the transition from MIS 3 to MIS
1533 2 was clearly marked by a transition from warm-moist to cold-dry conditions in western
1534 *Beringia*, this transition is absent or subtle in all but a few records in Alaska (Anderson
1535 and Lozhkin, 2001).

1536

1537 **4.4.8 MIS 2, The Last Glacial Maximum (30 to 15 ka)**

1538 The last glacial maximum was particularly cold both in the Arctic and globally,
1539 and it provides useful constraints on the magnitude of Arctic amplification (see below).

1540 During peak cooling of the last glacial maximum, planetary temperatures were about 5°–
1541 6°C lower than at present (Farrera et al., 1999; Braconnot et al., 2007, Jansen et al.,
1542 2007), whereas Arctic temperatures in central Greenland were depressed more than 20°C
1543 (Cuffey et al., 1995; Dahl-Jensen et al., 1998)and similarly in *Beringia* (Elias et al.,
1544 1996).

1545

1546 **4.4.9 MIS 1, The Holocene: The Present Interglaciation**

1547 In the face of rising solar energy in summer that was tied to orbital features and to
1548 rising greenhouse gases, Northern Hemisphere ice sheets began to recede from near their
1549 largest extent shortly after 20 ka, and the rate of recession noticeably increased after
1550 about 16 ka (see, e.g., Alley et al., 2002 for the timing of various events during the
1551 deglaciation). Most coastlines became ice-free before 12 ka, and ice continued to melt
1552 rapidly as summer insolation reached a peak (about 9% above modern insolation) about
1553 11 ka. The transition from MIS 2 to MIS 1, which marks the start of the Holocene
1554 interglaciation, is commonly placed at the abrupt termination of the cold event called the
1555 Younger Dryas; that termination recently was estimated at about 11.7 ka (Rasmussen et
1556 al., 2006).

1557 A wide variety of evidence from terrestrial and marine archives indicates that
1558 peak Arctic summertime warmth was achieved during the early Holocene, when most
1559 regions of the Arctic experienced sustained temperatures that exceeded observed 20th
1560 century values. This period of peak warmth, which is geographically variable in its
1561 timing, is generally referred to as the Holocene Thermal Maximum. The ultimate driver
1562 of the warming was orbital forcing, which produced increased summer solar radiation

1563 across the Northern Hemisphere. At 70°N., insolation in June now is near a local
1564 minimum (the maximum was recorded about 11–12 ka). June insolation about 4 ka was
1565 about 15 W/m² larger than recently, and June insolation at the Holocene peak was about
1566 45 W/m² larger than recently, for a total change of about 10% (Figure 4.31; Berger and
1567 Loutre, 1991). Winter (January) insolation about 11 ka was only slightly lower than
1568 today, in large part because there is almost zero insolation that far north in January.

1569

1570

FIGURE 4.31 NEAR HERE

1571

1572 By 6 ka, sea level and ice volumes were close to those observed more recently,
1573 and climate forcings such as atmospheric carbon-dioxide concentration differed little
1574 from pre-industrial conditions (e.g., Jansen et al., 2007). (The exception is that far-
1575 northern summer insolation steadily decreased throughout the Holocene.) High-resolution
1576 (decades to centuries) archives containing many climate proxies are available for most of
1577 the Holocene throughout the Arctic. Consequently, the mid- to late-Holocene record
1578 allows evaluation of the range of natural climate variability and of the magnitude of
1579 climate change in response to relatively small changes in forcings.

1580

1581

4.4.9a The Holocene Thermal Maximum

1582

1583

1584

1585

Many of the Arctic paleoenvironmental records for the Holocene Thermal
Maximum appear to have recorded primarily summertime conditions. Many different
proxies have been exploited to derive these reconstructions by use of biological indicators
such as pollen, diatoms, chironomids, dinoflagellate cysts, and other microfossils;

1586 elemental and isotopic geochemical indexes from lacustrine sediments, marine sediments,
1587 and ice cores; borehole temperatures; and age distributions of radiocarbon-dated tree
1588 stumps north of (or above) current treeline, marine mollusks, and whale bones (Kaufman
1589 et al., 2004).

1590 A recent synthesis of 140 Arctic paleoclimatic and paleoenvironmental records
1591 extending from *Beringia* westward to Iceland (Kaufman et al., 2004) outlines the nature
1592 of the Holocene Thermal Maximum in the western Arctic (Figure 4.32). Fully 85% of
1593 the sites included in the synthesis contained evidence of a Holocene thermal maximum.
1594 Its average duration extended from 2100 years in *Beringia* to 3500 years in Greenland.
1595 The interval 10–4 ka contains the greatest number of sites recording Holocene Thermal
1596 Maximum conditions and the greatest spatial extent of those conditions in the western
1597 Arctic (Figure 4.32b). In the western Arctic the timing of this thermal maximum begins
1598 and ends along a strong geographic gradient (Figure 4.32c). The thermal maximum
1599 began first in *Beringia*, where warmer-than-present summer conditions became
1600 established at 14–13 ka. Intermediate ages for its initiation (10–8 ka) are apparent in the
1601 *Canadian Arctic islands* and in central Greenland. The Holocene Thermal Maximum on
1602 *Iceland* occurred a bit later, 8–6 ka. The onset on Svalbard was earlier, by 10.8 ka
1603 (Svendsen and Mangerud, 1997). The latest general onset (7–4 ka) of Holocene Thermal
1604 Maximum conditions affected the continental portions of central and eastern Canada
1605 experienced. Similarly, the earliest termination of the Holocene Thermal Maximum
1606 occurred in *Beringia*, although most regions registered summer cooling by 5 ka. Much of
1607 the pattern of the onset of the Holocene Thermal Maximum can be explained at least in
1608 part by proximity to cold winds blowing off the melting *Laurentide Ice Sheet* in Canada,

1609 which depressed temperatures nearby until the ice melted back. Milankovitch cycling has
1610 also been suggested to explain the spatial variability of the Holocene Thermal Maximum
1611 (Maximova and Romanovsky, 1988).

1612

1613

FIGURE 4.32 NEAR HERE

1614

1615 Records for sea-ice conditions in the Arctic Ocean and adjacent channels have
1616 been developed by radiocarbon-dating indicators including the remains of open-water
1617 proxies such as whales and walrus, warm-water marine mollusks, and changes in the
1618 microfauna preserved in marine sediments. These reconstructions, presented in more
1619 detail in Chapter 7 (Arctic sea ice), parallel the terrestrial record for the most part. The
1620 data demonstrate that an increased mass of warm Atlantic water moved into the Arctic
1621 Ocean beginning about 11.5 ka. It peaked about 8–5 ka which, coupled with increased
1622 summer insolation, decreased the area of perennial sea-ice cover during the early
1623 Holocene. Decreased sea-ice cover in the western Arctic during the early Holocene also
1624 may be indicated by changes in concentrations of sodium from sea salt in the *Penny Ice*
1625 *Cap* (eastern Canadian Arctic; Fisher et al., 1998) and the *Greenland Ice Sheet*
1626 (Mayewski et al., 1997). In most regions, perennial sea ice increased in the late Holocene,
1627 although it has been suggested that sea ice declined in the *Chukchi Sea* (de Vernal et al.,
1628 2005), possibly in response to changing rates of Atlantic water inflow in *Fram Strait*.

1629 As summer temperatures increased through the early Holocene, in North America
1630 treeline expanded northward into regions formerly mantled by **tundra**, although the
1631 northward extent appears to have been limited to perhaps a few tens of kilometers beyond

1632 its recent position (Seppä et al., 2003; Gajewski and MacDonald, 2004). In contrast,
1633 treeline advanced much farther across the Eurasian Arctic. Tree macrofossils
1634 (Kremenetski et al., 1998; MacDonald et al., 2000a,b; 2007) collected at or beyond the
1635 current treeline indicate that tree genera such as birch (*Betula*) and larch (*Larix*) advanced
1636 beyond the modern limits of treeline across most of northern Eurasia between 11 and 10
1637 ka (Figures 5.33 and 5.34). Spruce (*Picea*) advanced slightly later than the other two
1638 genera. Interestingly, pine (*Pinus*), which now forms the conifer treeline in *Fennoscandia*
1639 and the *Kola Peninsula*, does not appear to have established appreciable forest cover at or
1640 beyond the present treeline in those regions at the far west of Europe until around 7 ka
1641 (MacDonald et al. 2000a). However, quantitative reconstructions of temperature from the
1642 *Kola Peninsula* and adjacent *Fennoscandia* suggest that summer temperatures were
1643 warmer than modern temperatures by 9 ka (Seppä and Birks, 2001; 2002; Hammarlund et
1644 al., 2002; Solovieva et al., 2005), and the development of extensive pine cover at and
1645 north of the present treeline appears to have been delayed relative to this warming. In the
1646 *Taimyr Peninsula* of *Siberia* and across nearby regions, the most northerly limit reached
1647 by trees during the Holocene was more than 200 km north of the current treeline. The
1648 treeline appears to have begun its retreat across northern Eurasia about 4 ka. The timing
1649 of the Holocene Thermal Maximum in the *Eurasian Arctic* overlaps the widest
1650 expression of the Holocene Thermal Maximum in the western Arctic (Figure 4.33), but it
1651 differs in two respects. The timing of onset and termination in Eurasia show much less
1652 variability than in North America, and the magnitude of the treeline expansion and retreat
1653 is far greater in the *Eurasian Arctic*. Fossil pollen and other indicators of vegetation or
1654 temperature from the northern Eurasian margin also support the contention of a

1655 prolonged warming and northern extension of treeline during the early through middle
1656 Holocene (see for example Hyvärinen, 1975; Seppä, 1996; Clayden et al., 1997; Velichko
1657 et al., 1997; Kaakinen and Eronen, 2000; Pisaric et al., 2001; Seppä and Birks, 2001,
1658 2002; Gervais et al., 2002; Hammarlund et al., 2002; Solovieva et al., 2005).

1659

1660 FIGURE 4.33 NEAR HERE

1661 FIGURE 4.34 NEAR HERE

1662

1663 Changes in landforms suggest that during the early to middle Holocene,
1664 permafrost in Siberia degraded. A synthesis of Russian data by Astakhov (1995) indicates
1665 that melting permafrost was apparent north of the Arctic Circle only in the European
1666 North, not in *Siberia*. In the Siberian North, permafrost partially thawed only very
1667 locally, and thawing was almost entirely confined to areas under thermokarst lakes that
1668 actively formed there during the early through middle Holocene. Areas south of the
1669 Arctic Circle appear to have experienced deep thawing (100–200 m depth) from the early
1670 Holocene until about 4–3 ka, when cooler summer conditions led permafrost to develop
1671 again. The deep thawing and subsequent renewal of surface permafrost in these regions
1672 produced an extensive thawed layer sandwiched between shallow (20–80 m deep) more
1673 recently frozen ground and deeper Pleistocene permafrost throughout much of
1674 northwestern *Siberia*.

1675 Quantitative estimates of the Holocene Thermal Maximum summer temperature
1676 anomaly along the northern margins of Eurasia and adjacent islands typically range from
1677 1° to 3°C. The geographic position of northern treeline across Eurasia is largely

1678 controlled by summer temperature and the length of the growing season (MacDonald et
1679 al., 2007), and in some areas the magnitude of treeline displacement there suggests a
1680 summer warming equivalent of 2.5°–7.0°C (see for example Birks, 1991; Wohlfarth et
1681 al., 1995; MacDonald et al., 2000a; Seppä and Birks, 2001, 2002; Hammarlund et al.,
1682 2002; Solovieva et al., 2005). Sea-surface temperature anomalies during the Holocene
1683 Thermal Maximum were as much as 4°–5°C higher than during the late Holocene for the
1684 eastern *North Atlantic sector* and adjacent Arctic Ocean (Salvigsen, 1992; Koç et al.,
1685 1993). Anomalies in summer temperature in the western Arctic during the Holocene
1686 Thermal Maximum ranged from 0.5° to 3°C (mean, 1.65°C). The largest anomalies were
1687 in the *North Atlantic sector* (Kerwin et al., 1999; Kaufman et al., 2004; Flowers et al.,
1688 2008).

1689

1690 **4.4.9b Neoglaciation**

1691 Many climate proxies are available to characterize the overall pattern of Late
1692 Holocene climate change. Following the Holocene Thermal Maximum, most proxy
1693 summer temperature records from the Arctic indicate an overall cooling trend through the
1694 late Holocene. Cooling is first recognized between 6 and 3 ka, depending on the threshold
1695 for change of each particular proxy. Records that exhibit a shift by 6–5 ka typically
1696 reflect intensified summer cooling about 3 ka (Figure 4.34).

1697 Summer cooling during the second half of the Holocene led to the expansion of
1698 mountain glaciers and ice caps around the Arctic. The term “Neoglaciation” is widely
1699 applied to this episode of glacier growth, and in some cases re-formation, following the
1700 maximum glacial retreat during the Holocene Thermal Maximum (Porter and Denton,

1701 1967). The former extent of glaciers is inferred from dated moraines and proglacial
1702 sediments deposited in lakes and marine settings. For example, ice-rafted detritus
1703 (Andrews et al., 1997) and the glacial geologic record (Funder, 1989) indicate that outlet
1704 glaciers of the *Greenland Ice Sheet* advanced during 6–4 ka (see Chapter 6, Greenland
1705 Ice Sheet). Multiproxy records from 10 glaciers or glaciated areas in Norway show
1706 evidence for increased activity by 5 ka (Nesje et al., 2001; Nesje et al., 2008). Major
1707 advances of outlet glaciers of northern Icelandic ice caps begin by 5 ka (Stötter et al.,
1708 1999; Geirsdottir et al., in press). In the *European Arctic*, glaciers expanded on *Franz*
1709 *Josef Land* (Lubinski et al., 1999) and *Svalbard* (Svendsen and Mangerud, 1997) by 4 ka,
1710 although sustained growth primarily began around 3 ka. An early Neoglacial advance of
1711 mountain glaciers is registered in *Alaska*, most prominently in the *Brooks Range*, the
1712 highest-latitude mountains in the state (Ellis and Calkin, 1984; Calkin, 1988). In
1713 southwest Alaska, mountain glaciers in the Ahklun Mountains did not reform until about
1714 3 ka (Levy et al., 2003). Neoglacial advances began in Arctic Canada by 5 ka (Miller et
1715 al., 2005)

1716 Additional evidence of Neoglacial seasonal cooling comes from several localities:
1717 a reduction in melt layers in the *Agassiz Ice Cap* (Koerner and Fisher, 1990) and in
1718 Greenland (Alley and Anandakrishnan, 1995); the decrease in $\delta^{18}\text{O}$ values in ice cores
1719 such as those from the *Devon Island* (Fisher, 1979) and Greenland (Johnsen et al., 1992)
1720 and indications of cooling from borehole thermometry (Cuffey et al., 1995); the retreat of
1721 large marine mammals and warm-water-dependent mollusks from the Canadian Arctic
1722 (Dyke and Savelle, 2001); the southward migration of the northern treeline across central
1723 Canada (MacDonald et al., 1993), Eurasia (MacDonald et al., 2000b), and Scandinavia

1724 (Barnekow and Sandgren, 2001); the expansion of sea-ice cover along the shores of the
1725 Arctic Ocean on *Ellesmere Island* (Bradley, 1990), in *Baffin Bay* (Levac et al., 2001), and
1726 in the *Bering Sea* (Cockford and Frederick, 2007); and the shift in vegetation
1727 communities inferred from plant macrofossils and pollen around the Arctic (Bigelow et
1728 al., 2003). The assemblage of microfossils and the stable isotope ratios of foraminifers
1729 indicate a shift toward colder, lower salinity conditions about 5 ka along the East
1730 Greenland Shelf (Jennings et al., 2002) and the western Nordic seas (Koç and Jansen,
1731 1994), suggesting increased influx of sea ice from the Arctic. Where quantitative
1732 estimates of temperature change are available, they generally indicate that summer
1733 temperature decreased by 1°–2°C during this initial phase of cooling.

1734 The general pattern of an early- to middle-Holocene Thermal Maximum followed
1735 by Neoglacial cooling forms a multi-millennial trend that, in most places, culminated in
1736 the 19th century. Superposed on the long-term cooling trend were many centennial-scale
1737 warmer and colder summer intervals, which are expressed to a varying extent and are
1738 interpreted with various levels of confidence in different proxy records. In northern
1739 Scandinavia, evidence for notable late Holocene cold intervals before the 16th century
1740 includes narrow tree rings (Grudd et al., 2002), lowered treeline (Eronen et al., 2002), and
1741 major glacier advances (Karlén, 1988) between 2.6 and 2.0 ka. An extended analysis of
1742 these many centennial-scale warmer and colder intervals in Russia was published by
1743 Velichko and Nechaev (2005).

1744

1745 **4.4.9c The Medieval Climate Anomaly (MCA)** Probably the most oft-cited
1746 warm interval of the late Holocene is the Medieval Climate Anomaly (MCA), earlier

1747 referred to as the Medieval Warm Period (MWP). The anomaly was recognized on the
1748 basis of several lines of evidence in Western Europe, but the term is commonly applied to
1749 other regions to refer to any of the relatively warm intervals of various magnitudes and at
1750 various times between about 950 and 1200 AD (Lamb, 1977) (Figure 4.35). In the
1751 Arctic, evidence for climate variability, such as relative warmth, during this interval is
1752 based on glacier extents, marine sediments, **speleothems**, ice cores, borehole
1753 temperatures, tree rings, and archaeology. The most consistent records of an Arctic
1754 Medieval Climate Anomaly come from the *North Atlantic sector* of the Arctic. The
1755 summit of Greenland (Dahl-Jensen et al., 1998), western Greenland (Crowley and
1756 Lowery, 2000), Swedish Lapland (Grudd et al., 2002), northern Siberia (Naurzbaev et al.,
1757 2002), and Arctic Canada (Anderson et al., 2008) were all relatively warm around 1000
1758 AD. During Medieval time, Inuit populations moved out of Alaska into the eastern
1759 Canadian Arctic and hunted whale from skin boats in regions perennially ice-covered in
1760 the 20th century (McGhee, 2004).

1761

1762

FIGURE 4.35 NEAR HERE

1763

1764 The evidence for Medieval warmth throughout the rest of the Arctic is less clear.
1765 However, some indications of Medieval warmth include the general retreat of glaciers in
1766 southeastern Alaska (Reyes et al., 2006; Wiles et al., 2008) and the wider tree rings in
1767 some high-latitude tree-ring records from Asia and North America (D'Arrigo et al.,
1768 2006). However D'Arrigo et al. (2006) emphasized the uncertainties involved in
1769 estimating Medieval Climate Anomaly warmth relative to that of the 20th century, owing

1770 in part to the sparse geographic distribution of proxy data as well as to the less coherent
1771 variability of tree growth temperature estimates for this anomaly. Hughes and Diaz
1772 (1994) argued that the Arctic as a whole was not anomalously warm throughout Medieval
1773 time (also see Bradley et al., 2003b, and National Research Council, 2006). Warmth
1774 during the Medieval interval is generally ascribed to lack of explosive volcanoes that
1775 produce particles that block the Sun and perhaps to greater brightness of the Sun
1776 (Crowley, 2000; Goosse et al., 2005; also see Jansen et al., 2007). Warming around the
1777 North Atlantic and adjacent regions may have been linked to changes in oceanic
1778 circulation as well (Broecker, 2001).

1779

1780 **4.4.9d Climate of the past millennium and the Little Ice Age**

1781 Given the importance of understanding climate in the most recent past and the
1782 richness of the available evidence, intensive scientific effort has resulted in numerous
1783 temperature reconstructions for the past millennium (Jones, et al., 1998; Mann et al.,
1784 1998; Briffa et al., 2001; Esper et al., 2002; Crowley et al., 2003; Mann and Jones, 2003;
1785 Moberg et al., 2005; National Research Council, 2006; Jansen et al., 2007), and
1786 especially the last 500 years (Bradley and Jones, 1992; Overpeck et al., 1997). Most of
1787 these reconstructions are based on annually resolved proxy records, primarily from tree
1788 rings, and they attempt to extract a record of air-temperature change over large regions or
1789 entire hemispheres. Data from Greenland ice cores and a few annually laminated lake
1790 sediment records are typically included in these compilations, but few other records of
1791 quantitative temperature changes spanning the last millennium are available from the
1792 Arctic. In general, the temperature records are broadly similar: they show modest summer

1793 warmth during Medieval times, a variable, but cooling climate from about 1250 to 1850
1794 AD, followed by warming as shown by both paleoclimate proxies and the instrumental
1795 record. Less is known about changes in precipitation, which is spatially and temporally
1796 more variable than temperature.

1797 The trend toward colder summers after about 1250 AD coincides with the onset of
1798 the Little Ice Age (LIA), which persisted until about 1850 AD, although the timing and
1799 magnitude of specific cold intervals were different in different places. Proxy climate
1800 records, both glacial and non-glacial from around the Arctic and for the Northern
1801 Hemisphere as a whole, show that the coldest interval of the Holocene was sustained
1802 sometime between about 1500 and 1900 AD (Bradley et al., 2003a). Recent evidence
1803 from the *Canadian Arctic* indicates that, following their recession in Medieval times,
1804 glaciers and ice sheets began to expand again between 1250 and 1300 AD. Expansion
1805 was further amplified about 1450 AD (Anderson et al., 2008).

1806 Glacier mass balances throughout most of the Northern Hemisphere during the
1807 Holocene are closely correlated with summer temperature (Koerner, 2005), and the
1808 widespread evidence of glacier re-advances across the Arctic during the Little Ice Age is
1809 consistent with estimates of summer cooling that are based on tree rings. The climate
1810 history of the Little Ice Age has been extensively studied in natural and historical
1811 archives, and it is well documented in Europe and North America (Grove, 1988).
1812 Historical evidence from the Arctic is relatively sparse, but it generally agrees with
1813 historical records from northwest Europe (Grove, 1988). Icelandic written records
1814 indicate that the duration and extent of sea ice in the *Nordic Seas* were high during the
1815 Little Ice Age (Ogilvie and Jónsson, 2001).

1816 The average temperature of the Northern Hemisphere during the Little Ice Age
1817 was less than 1°C lower than in the late 20th century (Bradley and Jones, 1992; Hughes
1818 and Diaz, 1994; Crowley and Lowery, 2000), but regional temperature anomalies varied.
1819 Little Ice Age cooling appears to have been stronger in the Atlantic sector of the Arctic
1820 than in the Pacific (Kaufman et al., 2004), perhaps because ocean circulation promoted
1821 the development of sea ice in the North Atlantic, which further amplified Little Ice Age
1822 cooling there (Broecker, 2001; Miller et al., 2005).

1823 The Little Ice Age also shows evidence of multi-decadal climatic variability, such
1824 as widespread warming during the middle through late 18th century (e.g., Cronin et al.,
1825 2003). Although the initiation of the Little Ice Age and the structure of climate
1826 fluctuations during this multi-centennial interval vary around the Arctic, most records
1827 show warming beginning in the late 19th century (Overpeck et al., 1997). The end of the
1828 Little Ice Age was apparently more uniform both spatially and temporally than its
1829 initiation (Overpeck et al., 1997).

1830 The climate change that led to the Little Ice Age is manifested in proxy records
1831 other than those that reflect temperature. For example, it was associated with a positive
1832 shift in transport of dust and other chemicals to the summit of Greenland (O'Brien et al.,
1833 1995), perhaps related to deepening of the Icelandic low-pressure system (Meeker and
1834 Mayewski, 2002). According to modeling studies, the negative phase [see
1835 <http://www.ldeo.columbia.edu/res/pi/NAO/>] of the North Atlantic Oscillation could have
1836 been amplified during the Little Ice Age (Shindell et al., 2001) whereas, in the North
1837 Pacific, the Aleutian low was significantly weakened during the Little Ice Age (Fisher et
1838 al., 2004; Anderson et al., 2005).

1839 Seasonal cooling into the Little Ice Age resulted from the orbital changes as
1840 described above, together with increased explosive volcanism and probably also
1841 decreased solar luminosity as recorded by sunspot numbers as far back as 1600 AD
1842 (Renssen et al., 2005; Ammann et al., 2007; Jansen et al., 2007).

1843

1844 **4.4.10 Placing 20th century warming in the Arctic in a millennial perspective**

1845 Much scientific effort has been devoted to learning how 20th-century and 21st-
1846 century warmth compares with warmth during earlier times (e.g., National Research
1847 Council, 2006; Jansen et al., 2007). Owing to the orbital changes affecting midsummer
1848 sunshine (a drop in June insolation of about 1 W/m^2 at 75°N . and 2 W/m^2 at 90°N . during
1849 the last 1000 years; Berger and Loutre, 1991), additional forcing was needed in the 20th
1850 century to give the same summertime temperatures as achieved in the Medieval Warm
1851 Period.

1852 After it evaluated globally or even hemispherically averaged temperatures, the
1853 National Research Council (2006) found that “Presently available proxy evidence
1854 indicates that temperatures at many, but not all, individual locations were higher during
1855 the past 25 years than during any period of comparable length since A.D. 900” (p. 3).
1856 Greater uncertainties for hemispheric or global reconstructions were identified in
1857 assessing older comparisons. As reviewed next, some similar results are available for the
1858 Arctic.

1859 Thin, cold ice caps in the eastern Canadian Arctic preserve intact—but frozen—
1860 vegetation beneath them that was killed by the expanding ice. As these ice caps melt,
1861 they expose this dead vegetation, which can be dated by radiocarbon with a precision of a

1862 few decades. A recent compilation of more than 50 radiocarbon dates on dead vegetation
1863 emerging from beneath thin ice caps on northern *Baffin Island* shows that some ice caps
1864 formed more than 1600 years ago and persisted through Medieval times before melting
1865 early in the 21st century (Anderson et al., 2008).

1866 Records of the melting from ice caps offer another view by which 20th century
1867 warmth can be placed in a millennial perspective. The most detailed record comes from
1868 the *Agassiz Ice Cap* in the Canadian High Arctic, for which the percentage of summer
1869 melting of each season's snowfall is reconstructed for the past 10 ka (Fisher and Koerner,
1870 2003). The percent of melt follows the general trend of decreasing summer insolation
1871 from orbital changes, but some brief departures are substantial. Of particular note is the
1872 significant increase in melt percentage during the past century; current percentages are
1873 greater than any other melt intensity since at least 1700 years ago, and melting is greater
1874 than any in sustained interval since 4–5 ka.

1875 As reviewed by Smol and Douglas (2007b), changes in lake sediments record
1876 climatic and other changes in the lakes. Extensive changes especially in the post-1850
1877 interval are most easily interpreted in terms of warming above the Medieval warmth on
1878 *Ellesmere Island* and probably in other regions, although other explanations cannot be
1879 excluded (also see Douglas et al., 1994). D'Arrigo et al. (2006) show tree-ring evidence
1880 from a few North American and Eurasian records that imply that summers were cooler in
1881 the Medieval Warm Period than in the late 20th century, although the statistical
1882 confidence is weak. Tree-ring and treeline studies in western *Siberia* (Esper and
1883 Schweingruber, 2004) and Alaska (Jacoby and D'Arrigo, 1995) suggest that warming
1884 since 1970 is has been optimal for tree growth and follows a circumpolar trend.

1885 Hantemirov and Shiyatov (2002) records from the Russian *Yamal Peninsula*, well north of
1886 the Arctic Circle, show that summer temperatures of recent decades are the most
1887 favorable for tree growth within the past 4 millennia.

1888 Whole-Arctic reconstructions are not yet available to allow confident comparison
1889 of late 20th century warmth with Medieval temperatures, nor has the work been done to
1890 correct for the orbital influence and thus to allow accurate comparison of the remaining
1891 forcings.

1892

1893 **4.5 Summary**

1894

1895 **4.5.1 Major features of Arctic Climate in the past 65 Ma**

1896 Section 5.4 summarized some of the extensive evidence for changes in Arctic
1897 temperatures, and to a lesser extent in Arctic precipitation, during the last 65 m.y. To
1898 some degree it also discussed “attribution”—the best scientific understanding of the
1899 causes of the climate changes. In this subsection, a brief synopsis is provided; for
1900 citations, the reader is referred to the extensive discussion just above.

1901 At the start of the Cenozoic, 65 Ma, the Arctic was much warmer year around
1902 than it was recently; forests grew on all land regions and no perennial sea ice or
1903 *Greenland Ice Sheet* existed. Gradual but bumpy cooling has dominated most of the last
1904 65 million years, and falling atmospheric CO₂ concentration apparently is the most
1905 important contributor to the cooling—although possible changing continental positions
1906 and their effect on atmospheric or oceanic circulation may also contribute. One especially
1907 prominent “bump,” the Paleocene-Eocene Thermal Maximum about 55 Ma, warmed the

1908 Arctic Ocean more than 5°C and the Arctic landmass about 8°C, probably in a few
1909 centuries to a millennium or so, followed by cooling for about 100 ka. Warming from
1910 release of much CO₂ (possibly initially as sea-floor methane that was then oxidized to
1911 CO₂) is the most likely explanation. In the middle Pliocene (about 3 Ma) a modest
1912 warming was sufficient to allow deciduous trees on Arctic land that at present supports
1913 only High Arctic polar-desert vegetation; whether this warming originated from changes
1914 to circulation, CO₂, or some other cause remains unclear.

1915 About 2.7 Ma, the cooling reached the threshold beyond which extensive
1916 continental ice sheets developed in the North American and Eurasian Arctic, and it
1917 marked the onset of the Quaternary Ice Age. Initially, the growth and shrinkage of the
1918 ice ages were directly controlled by changes in northern sunshine caused by features of
1919 Earth's orbit (the 41-k.y. cycle of sunshine that is tied to the obliquity (tilt) of Earth's
1920 axis is especially prominent). More recently, a 100-ka cycle has become more
1921 prominent, perhaps because the ice sheets became large enough that their behavior
1922 became important. Short, warm interglacials (usually lasting about 10,000 years,
1923 although the one about 440,000 years ago lasted longer) have alternated with longer
1924 glacial intervals. Recent work suggests that, in the absence of human influence, the
1925 current interglacial would continue for a few tens of thousands of years before the start
1926 of a new ice age (Berger and Loutre, 2002). Although driven by the orbital cycles, the
1927 large temperature differences between glacials and interglacials, and the globally
1928 synchronous response, reflect the effects of strong positive feedbacks, such as changes
1929 in atmospheric CO₂ and other greenhouse gases and in the areal extent of reflective
1930 snow and ice.

1931 Interactions among the various orbital cycles have caused small differences
1932 between successive interglacials. More summer sunshine was received in the Arctic
1933 during the interglacial of about 130–120 ka than has been received in the current
1934 interglacial. Thus, summer temperatures in many places were about 4°–6°C warmer than
1935 recently, and these higher temperatures reduced ice on Greenland (Chapter 6, Greenland
1936 Ice Sheet), raised sea level, and melted widespread small glaciers and ice caps.

1937 The seasonal cooling into and warming out of the most recent glacial were
1938 punctuated by numerous abrupt climate changes, and conditions persisted for millennia
1939 between jumps that were completed in years to decades. These events were very
1940 pronounced around the North Atlantic, but they had a much smaller effect on
1941 temperature elsewhere in the Arctic. Temperature changes extended to equatorial
1942 regions and caused a seesaw response in the far south (i.e., mean annual warming in the
1943 south when the north cooled). Large changes in extent of sea ice in the North Atlantic
1944 were probably responsible, linked to changes in regional to global patterns of ocean
1945 circulation; freshening of the North Atlantic favored expansion of sea-ice.

1946 These abrupt temperature changes also were a feature of the current interglacial,
1947 the Holocene, but they ended as the *Laurentide Ice Sheet* on Canada melted away. Arctic
1948 temperatures in the Holocene broadly responded to orbital changes, and temperatures
1949 warmed during the middle Holocene when there was more summer sunshine. Warming
1950 generally led to northward migration of vegetation and to shrinkage of ice on land and
1951 sea. Smaller oscillations in climate during the Holocene, including the so-called
1952 Medieval Warm Period and the Little Ice Age, were linked to variations in the sun-
1953 blocking effect of particles from explosive volcanoes and perhaps to small variations in

1954 solar output, or in ocean circulation, or other factors. The warming from the Little Ice
1955 Age began for largely natural reasons, but it appears to have been accelerated by human
1956 contributions and especially by increasing CO₂ concentrations in the atmosphere
1957 (Jansen, 2007).

1958

1959 **4.5.2. Arctic Amplification**

1960 The scientific understanding of climate processes shows that Arctic climate
1961 operates by use of many strong positive feedbacks (Serreze and Francis, 2006; Serreze et
1962 al., 2007a). As outlined in section 5.2, these feedbacks especially depend on the
1963 interactions of snow and ice with sunlight, the ocean, and the land surface (including its
1964 vegetation). For example, higher temperature tends to remove reflective ice and snow,
1965 more solar heat is then absorbed, and absorption of that heat promotes further warming
1966 (ice-albedo feedback). Also, higher temperature tends to remove sea ice that insulates the
1967 cold wintertime air from the warmer ocean beneath, further warming the air (ice-
1968 insolation feedback). Furthermore, higher temperature tends to allow dark shrubs to
1969 replace low-growing **tundra** that is easily covered by snow, intensifying the ice-albedo
1970 feedback. Similarly strong negative feedbacks are not known to stabilize Arctic climate,
1971 so physical understanding indicates that climate changes should be amplified in the
1972 Arctic as compared with lower latitude sites. This expectation is confirmed by the
1973 available data, as shown in Figure 4.36.

1974

1975

FIGURE 4.36 NEAR HERE

1976

1977 As we consider Arctic amplification, we must account for forcings. For the three
1978 younger time intervals shown in Figure 4.36, the Holocene Thermal Maximum (about 6
1979 ka ago), the Last Glacial Maximum (LGM, about 20 ka ago), and marine isotope stage
1980 5e, also known as the last interglaciation (LIG, about 130–120 ka ago), the climate
1981 changes were primarily forced by regular variations in Earth’s orbital parameters. The
1982 anomalies of incoming solar radiation (insolation) averaged throughout the whole planet
1983 for a year are less than 0.4% for all times considered, and the orbital changes serve
1984 primarily to shift sunlight around on the planet seasonally or geographically. However,
1985 during these intervals the insolation forcing was relatively uniform throughout the
1986 Northern Hemisphere, and insolation anomalies north of 60°N typically were only 10–
1987 20% greater than the anomalies for corresponding times averaged throughout the
1988 Northern Hemisphere as a whole. For example, at the peak of the last interglaciation
1989 (130–125 ka), the Arctic (60°–90°N.) summer (May-June-July) insolation anomaly was
1990 12.7% above present, while the Northern Hemisphere anomaly was 11.4% above present
1991 (Berger and Loutre, 1991). At the same time, the Southern Hemisphere summer (Nov.,
1992 Dec., Jan.) insolation anomaly at 60 °S was 6% less than present.

1993 To assess the geographic differences in the climate response to this relatively
1994 uniform forcing, the Arctic can be compared to the Northern Hemisphere average
1995 summer temperature anomalies for the three younger time periods because of the similar
1996 forcing in the Arctic and Northern Hemisphere. During the Pliocene (and during earlier
1997 warm times discussed below but not plotted in the figure), warmth persisted much longer
1998 than the cycle time of insolation changes resulting from Earth’s orbital irregularities

1999 (about 20 ka and about 40 ka). Consequently, Arctic anomalies are compared to global
2000 temperature anomalies.

2001 A difficulty is that for some of those younger times, global and Arctic estimates
2002 of temperature anomalies are available but hemispheric estimates are not. (The global
2003 estimates clearly include hemispheric data, but those data have not been summarized in
2004 anomaly maps or hemispheric anomaly estimates that were published in the refereed
2005 scientific literature.) To obtain hemispheric estimates here, note (as described in more
2006 detail below) that climate models driven by the known forcings show considerable
2007 fidelity in reproducing the global anomalies shown by the data for the relevant times, and
2008 that hemispheric anomalies can be assessed within these models. The hemispheric
2009 anomalies so produced are consistent with the available paleoclimate data, and so they
2010 are used here.

2011 The Palaeoclimate Modelling Intercomparison Project (PMIP2; Harrison et al.,
2012 2002, and see <http://pmip2.lsce.ipsl.fr/>) coordinates an international effort to compare
2013 paleoclimate simulations produced by a range of climate models, and to compare these
2014 climate model simulations with data-based paleoclimate reconstructions for a middle
2015 Holocene warm time (6 ka) and for the last glacial maximum (LGM; 21 ka). A
2016 comparison of simulations for 6 and 21 ka by the project is reported by Braconnot et al.
2017 (2007).

2018 As part of this Palaeoclimate Modelling Intercomparison Project effort, Harrison
2019 et al. (1998) compared global (mostly Northern Hemisphere) vegetation patterns
2020 simulated by using the output of 10 different climate model simulations for 6 ka. The
2021 model simulations closely agreed with the vegetation reconstructed from paleoclimate

2022 records. Similar comparisons on a regional basis for the Northern Hemisphere north of
2023 55°N. (Kaplan et al., 2003), the Arctic (CAPE Project Members, 2001), Europe (Brewer
2024 et al., 2007), and North America (Bartlein et al., 1998) also showed close matches
2025 between paleoclimate data and models for the early Holocene. Comparison of models and
2026 data for the Last Glacial Maximum (Bartlein et al., 1998; Kaplan et al., 2003), and Last
2027 Interglaciation (CAPE Last Interglacial Project Members, 2006; Otto-Bliesner et al.,
2028 2006) reached similar conclusions. (Also see Pollard and Thompson, 1997; Farrera et al.,
2029 1999; Pinot et al., 1999; Kageyama et al., 2001.) Paleoclimate data corresponded closely
2030 with model simulations of the Holocene Thermal Maximum, Last Interglaciation warmth,
2031 and Last Glacial Maximum cold. This agreement provides confidence that climate-model
2032 simulations of past times may be compared with paleoclimate-based reconstructions of
2033 summer temperatures for the Arctic in order to evaluate the magnitude of Arctic
2034 amplification. Figure 4.34 shows such a comparison. Clearly, however, additional data
2035 and additional analyses of existing as well as new data would improve confidence in the
2036 results and perhaps reduce the error bars.

2037 The forcing of the warmth of the middle Pliocene remains unclear. Orbital
2038 oscillations have continued throughout Earth history, but the Pliocene warmth persisted
2039 long enough to cross many orbital oscillations, which thus cannot have been responsible
2040 for the warmth. The most likely explanation is an elevated level of CO₂ that is estimated
2041 to be between 380 and 400 ppmv, coupled with smaller Greenland and Antarctic ice
2042 sheets (Haywood and Valdes, 2004).

2043 The data indicate that Arctic temperature anomalies were much larger than global
2044 ones (Figure 4.34). The regression line through the four data points has a slope of $3.6 \pm$

2045 0.6, suggesting that the change in Arctic summer temperatures tends to be 3 to 4 times as
2046 large as the global change.

2047 This trend of larger Arctic anomalies was already well established during the
2048 greater warmth of the early Cenozoic peak warming and of the Cretaceous before that.
2049 Somewhat greater uncertainty is attached to these more ancient times in which continents
2050 were differently configured, so these data are not plotted in Figure 5.34; even so, the
2051 leading result is fully consistent with the regression. Barron et al. (1995) estimated
2052 global-average temperatures about 6°C warmer in the Cretaceous than recently. As
2053 reviewed by Alley (2003) (also see Bice et al., 2006), subsequent work suggests upward
2054 revision of tropical sea-surface temperatures by as much as a few degrees. The
2055 Cretaceous peak warmth seems to have been somewhat higher than early Cenozoic
2056 values, or perhaps similar (Zachos et al., 2001). In the Arctic, as discussed in section
2057 5.4.1, the early Cenozoic (late Paleocene) temperature records probably mostly recorded
2058 summertime conditions of about 18°C in the ocean and about 17°C on land, followed
2059 during the short-lived Paleocene-Eocene Thermal Maximum by warming to about 23°C
2060 in the summer ocean and 25°C on land (Moran et al., 2006; Sluijs et al.; 2006; 2008;
2061 Weijers et al., 2007). No evidence of wintertime ice exists, and temperatures very likely
2062 remained higher than during the mid-Pliocene. Recently, the oceanic site has remained
2063 ice covered; it is near or below freezing during the summer and much colder in winter.
2064 Hence, changes in the Arctic were much larger than the globally averaged change.

2065 Figure 4.34 does not include quantitative estimates for the pre-Pliocene warm
2066 times, but a 3-fold Arctic amplification is consistent with the data within the broad
2067 uncertainties. The Cretaceous and early-Cenozoic warmth seems to have been forced by

2068 increased greenhouse-gas concentration, as discussed above, so the Arctic amplification
2069 seems to be independent of the forcing. This conclusion is expectable; many of the strong
2070 Arctic feedbacks serve to amplify temperature change without regard to causation—
2071 warmer summer temperatures melt reflective snow and ice, regardless of whether the
2072 warmth came from changing solar output, orbital configuration, greenhouse-gas
2073 concentrations, or other causes. Global warmth and an ice-free Arctic during the early
2074 Eocene occurred without albedo feedbacks at the same time that the tropics experienced
2075 sustained warmth (Pearson et al., 2007).

2076 Targeted studies designed to quantitatively assess Arctic amplification of climate
2077 change remain relatively rare, and they could be clarified. The available data, as assessed
2078 here, point to 3-fold to 4-fold Arctic amplification, such that, in response to the same
2079 forcing, Arctic temperature changes are 3 to 4 times as large as hemispheric-average
2080 changes, which are dominated by changes in the much larger lower latitude regions.

2081

2082 **4.5.3 Implications for the future**

2083 Paleoclimatology shows that climate has changed greatly in the Arctic with time,
2084 and that the changes typically have been much larger in the Arctic than in lower latitudes.
2085 Strong feedbacks have promoted these Arctic changes, such as the ice-albedo feedback in
2086 which summer cooling expands reflective snow and ice that in turn amplify the cooling,
2087 or warming causes melting that amplifies the warming. Changes in sea-ice coverage of
2088 the Arctic Ocean have also been critical—open water cannot fall below the freezing
2089 point, but air above ice-covered water can become very cold in the dark Arctic winter.

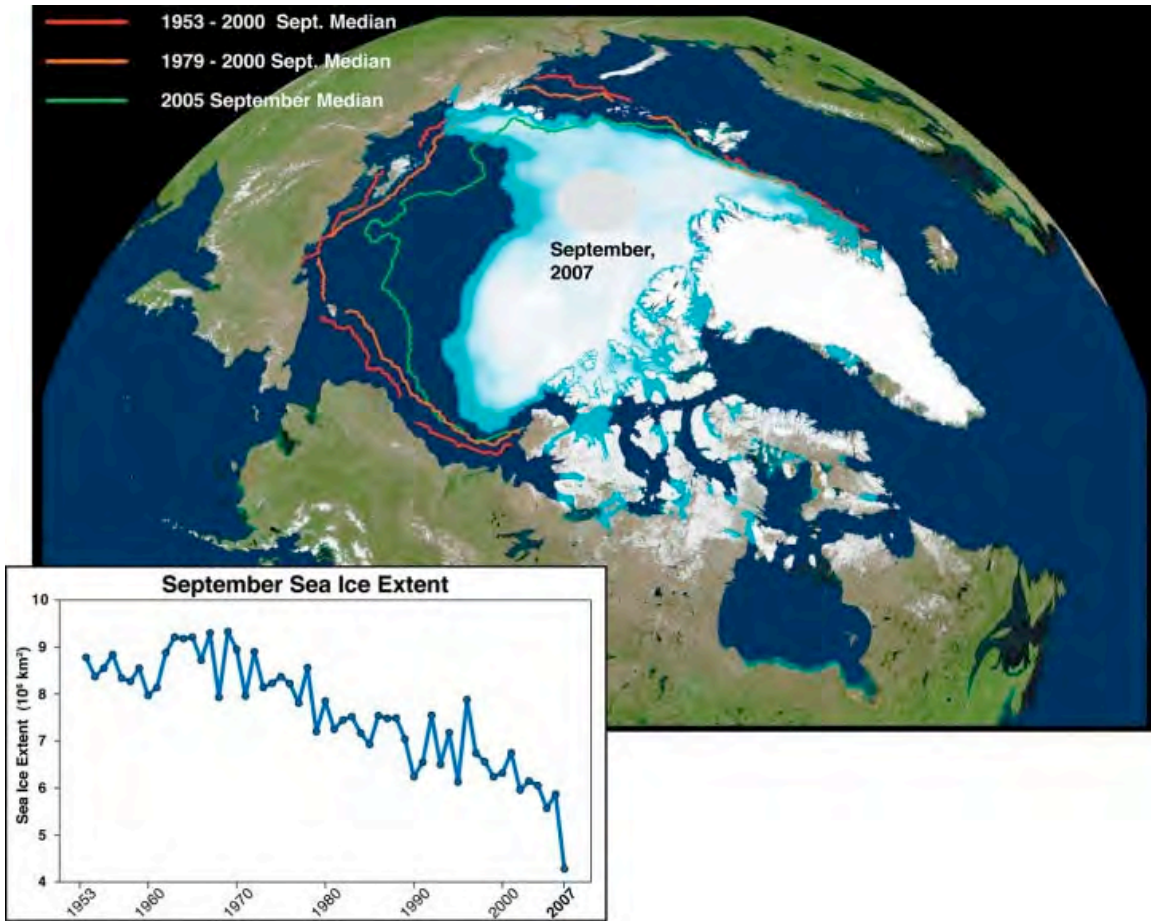
2090 Thus, sustained changes in sea-ice coverage very likely contribute to the largest
2091 temperature changes observed on the planet (see, e.g., Denton et al., 2005).

2092 These feedbacks have served to amplify climate changes with various causes,
2093 including those forced primarily by greenhouse-gas changes, consistent with physical
2094 understanding of the nature of the feedbacks. By simple analogy, and taken together with
2095 physical understanding, this knowledge indicates that climate changes will continue to be
2096 amplified in the Arctic. In turn, this knowledge indicates that continuing greenhouse-gas
2097 forcing of global climate or other human influences will change climate more in the
2098 Arctic than in lower latitude regions.

2099

2099

2100



2101

2102

2103

2104

Figure 4.1 Median extent of sea ice in September, 2007, compared with averaged

2105 intervals during recent decades. Red curve, 1953–2000; orange curve, 1979–2000; green

2106 curve, September 2005. Inset: Sea ice extent time series plotted in square kilometers,

2107 shown from 1953–2007 in the graph below (Stroeve et al., 2008). The reduction in Arctic

2108 Ocean summer sea ice in 2007 was greater than that predicted by most recent climate

2109 models.

2110

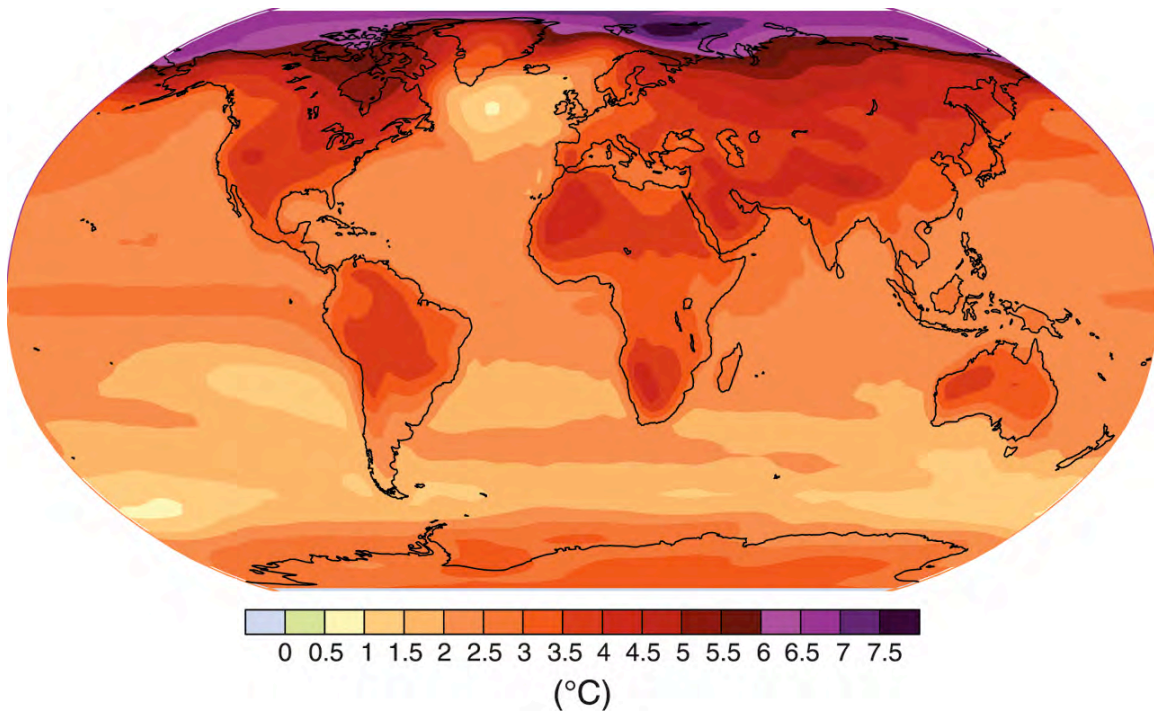
2111

2112

2112

2113

Geographical pattern of surface warming

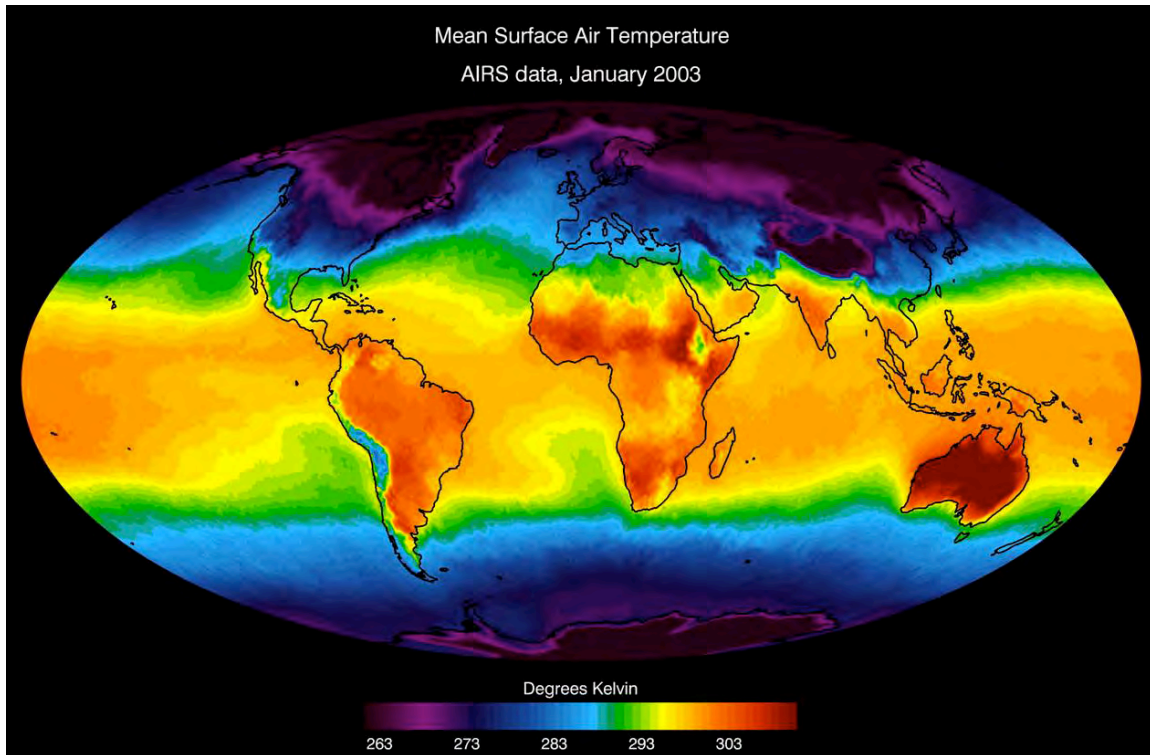


2114

2115 **Figure 4.2** Projected surface temperature changes for the last decade of the 21st century
2116 (2090-2099) relative to the period 1980-1999. The map shows the IPCC multi-
2117 Atmosphere-Ocean coupled Global Climate Model average projection for the A1B
2118 (balanced emphasis on all energy resources) scenario. The most significant warming is
2119 projected to occur in the Arctic. (IPCC, 2007; Figure SPM6)

2120

2120



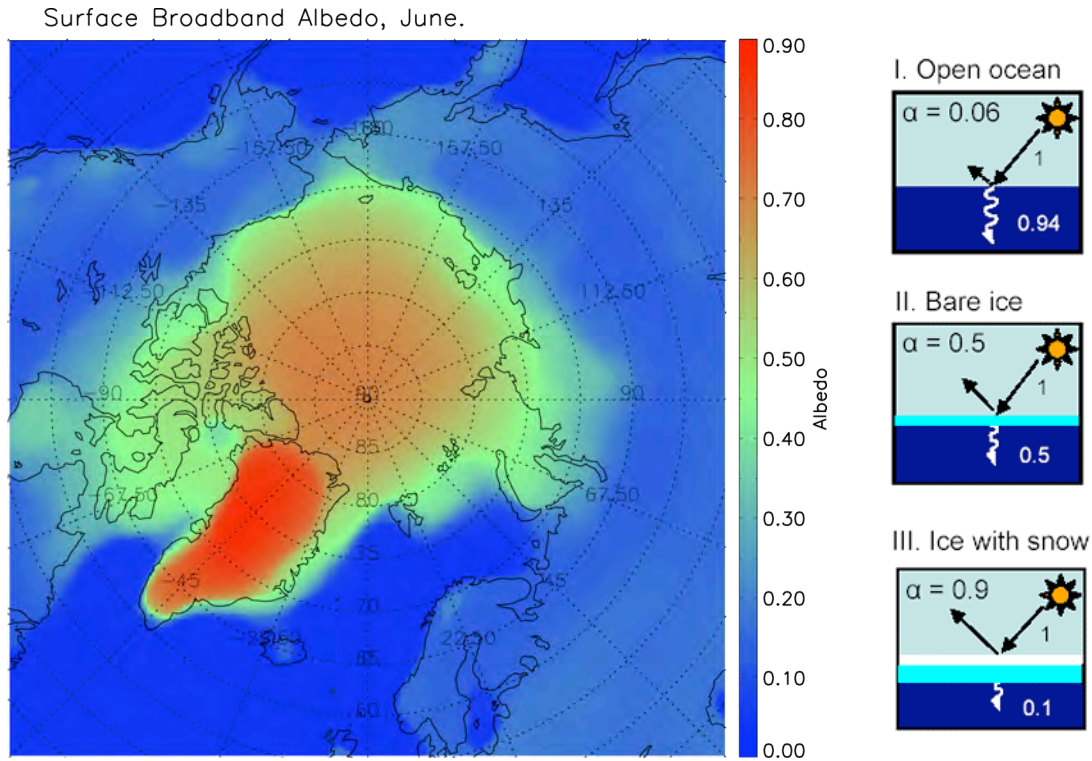
2121

2122 **Figure 4.3** Global mean observed near-surface air temperatures for the month of
2123 January, 2003 derived from the Atmospheric Infrared Sounder (AIRS) data. Contrast
2124 between equatorial and Arctic temperatures is greatest during the northern hemisphere
2125 winter. The transfer of heat from the tropics to the polar regions is a primary feature of
2126 the Earth's climate system (Color scale is in Kelvin degrees such that $0^{\circ}\text{C}=273.15$
2127 Kelvin.)

2128 (Source: http://www-airs.jpl.nasa.gov/graphics/features/airs_surface_temp1_full.jpg)

2129

2129



2130

2131

2132

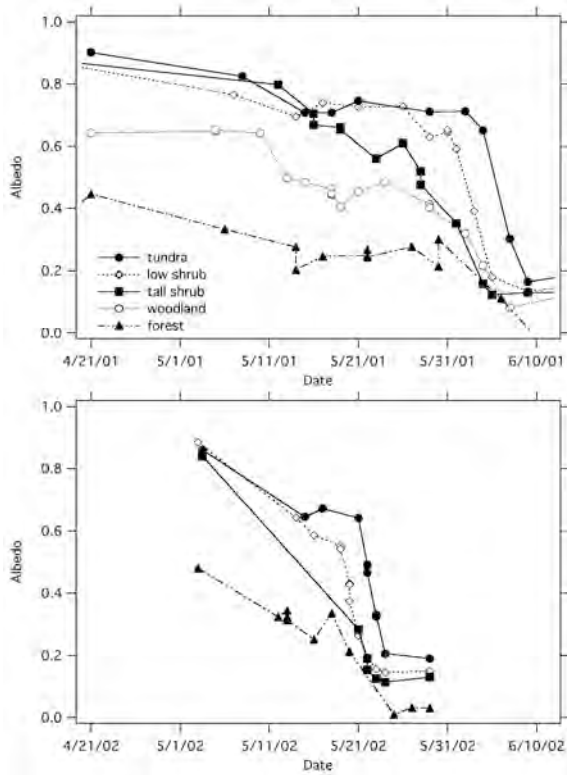
2133 **Figure 4.4** Albedo values in the Arctic

2134 **5a.** Advanced Very High Resolution Radiometry (AVHRR)-derived Arctic albedo
 2135 values in June, 1982-2004 multi-year average, showing the strong contrast between snow
 2136 and ice covered areas (green through red) and open water or land (blue). (Image courtesy
 2137 of X. Wang, University of Wisconsin-Madison, CIMSS/NOAA)

2138 **5b.** Albedo feedbacks. Albedo is the fraction of incident sunlight that is reflected. Snow,
 2139 ice, and glaciers have high albedo. Dark objects such as the open ocean, which absorbs
 2140 some 93% of the Sun’s energy, have low albedo (about 0.06), absorbing some 93% of the
 2141 Sun’s energy. Bare ice has an albedo of 0.5; however, sea ice covered with snow has an
 2142 albedo of nearly 90% (Source: <http://nsidc.org/seaice/processes/albedo.html>).

2143

2143



2144

a

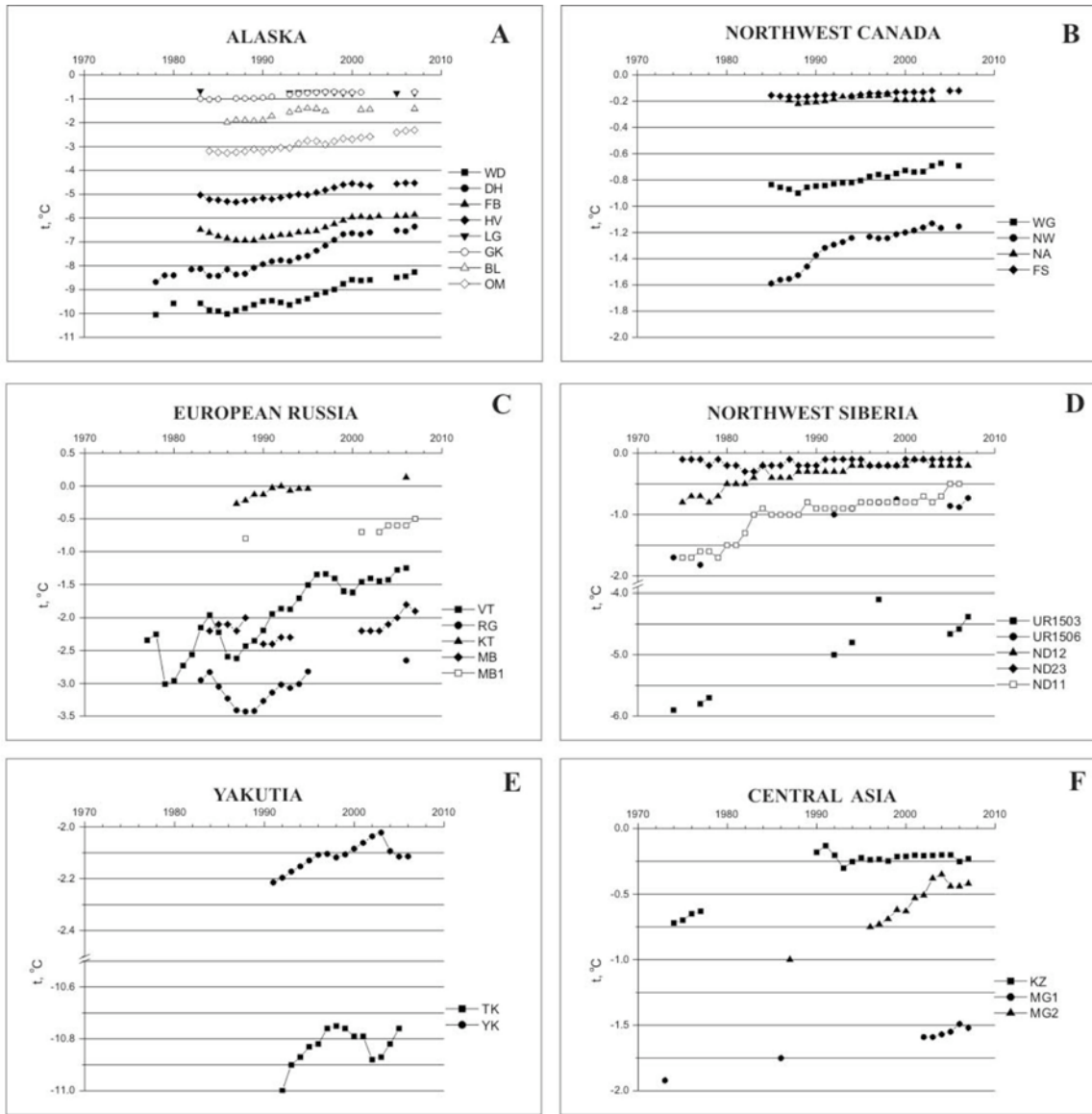
b

2145

2146

2147 **Figure 4.5** Changes in vegetation cover throughout the Arctic can influence albedo, as
 2148 can altering the onset of snow melt in spring. a) Progression of the melt season in
 2149 northern Alaska, May 2001 (top) and May 2002 (bottom), demonstrates how areas with
 2150 exposed shrubs show earlier snow melt. b) Dark branches against reflective snow alter
 2151 albedo (Sturm et al., 2005; Photograph courtesy of Matt Sturm).

2152



2153

2154 **Figure 4.6** Warming trend in Arctic permafrost (permanently frozen ground), 1970–
 2155 present. Local effects can modify this trend. A) Sites in Alaska: WD, West Dock; DH,
 2156 Deadhorse; FB, Franklin Bluffs; HV, Happy Valley; LG, Livengood; GK, Gulkana; BL,
 2157 Birch Lake; OM, Old Man. B) Sites in northwest Canada: WG, Wrigley; NW, Norman
 2158 Wells; NA, Northern Alberta; FS, Fort Simpson. C) Sites in European Russia: VT,
 2159 Vorkuta; RG, Rogovoi; KT, Karataikha; MB, Mys Bolvansky. D) Northwest Siberia: UR,

2160 Urengoi; ND, Nadym. E) Sites in Yakutia: TK, Tiksi; YK, Yakutsk. F) Sites in central
2161 Asia: KZ, Kazakhstan; MG, Mongolia (Brown and Romanovsky, 2008).
2162



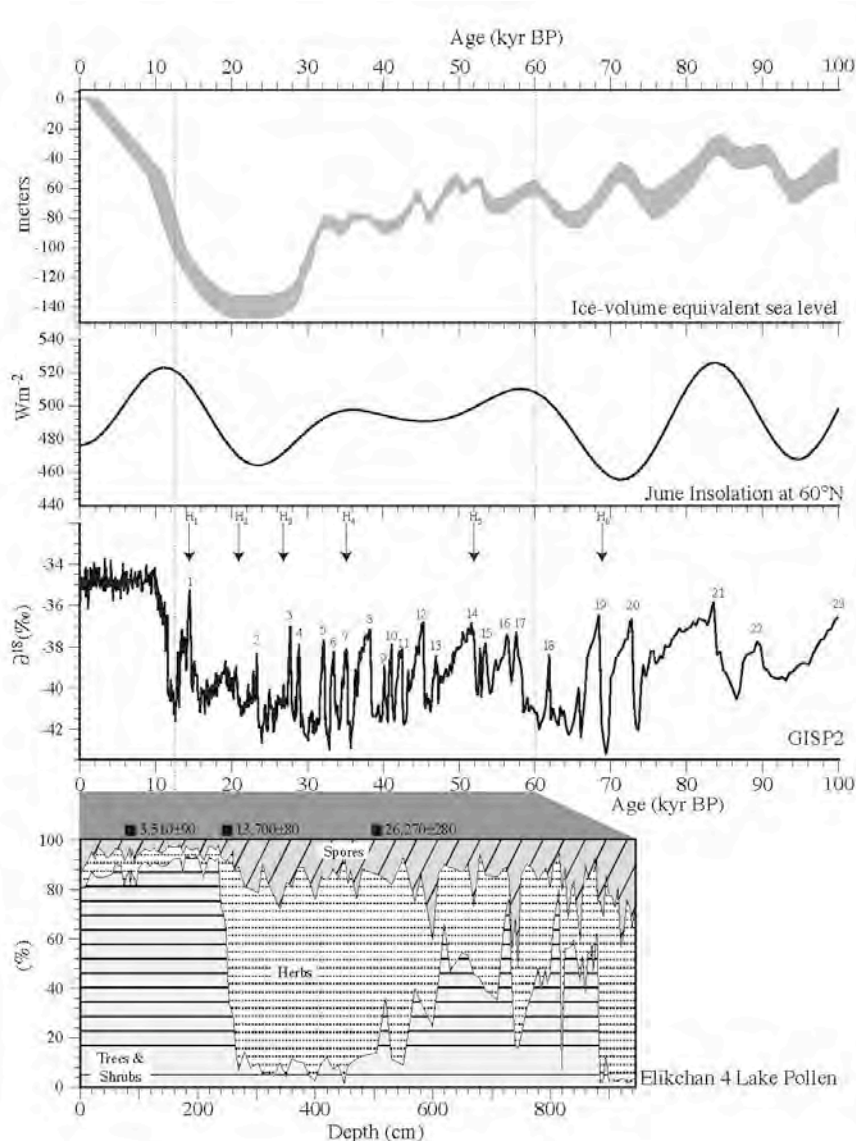
2162

2163

2164 **Figure 4.7** Inflows and outflows of water in the Arctic Ocean. Red lines, components
 2165 and paths of the surface and Atlantic Water layer in the Arctic; black arrows, pathways of
 2166 Pacific water inflow from 50–200 m depth; blue arrows, surface-water circulation; green,
 2167 major river inflow; red arrows, movements of density-driven Atlantic water and
 2168 intermediate water masses into the Arctic (AMAP, 1998).

2169

2169



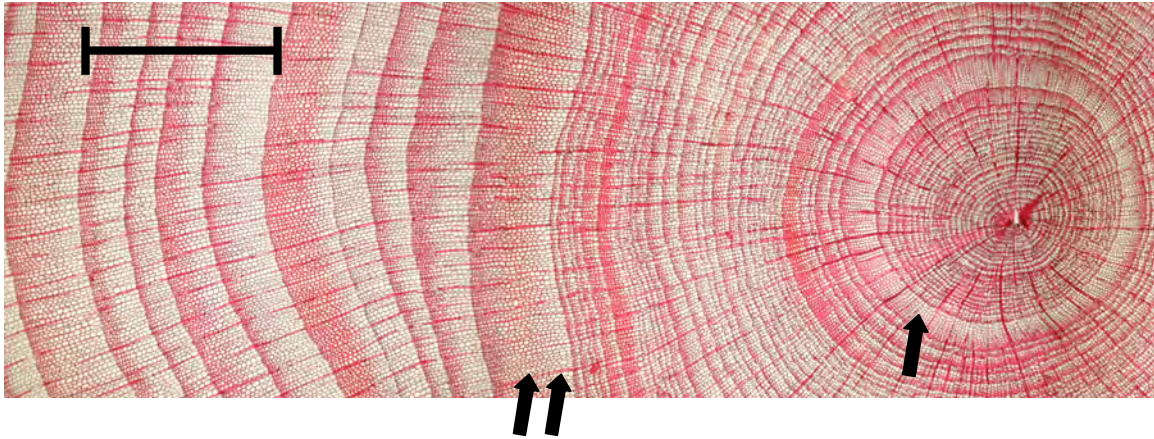
2170

2171 **Figure 4.8** Upper three panels: Correlation of global sea-level curve (Lambeck et al.,
 2172 2002), Northern Hemisphere summer insolation (Berger and Loutre, 1991), and the
 2173 Greenland Ice Sheet (GISP2) $\delta^{18}\text{O}$ record (Grootes et al., 1993), ages all given in
 2174 calendar years. Bottom panel: temporal changes in the percentages of the main taxa of
 2175 trees and shrubs, herbs and spores at Elikchan 4 Lake in the Magadan region of
 2176 Chukotka, Russia. Lake core x-axis is depth, not time (Brigham-Grette et al., 2004).
 2177 Habitat was reconstructed on the basis of modern climate range of collective species
 2178 found in fossil pollen assemblages. The reconstruction can be used to estimate past

2179 temperatures or the seasonality of a particular site. The GISP2 record: Base of core
2180 roughly 60 ka (Lozhkin and Anderson, 1996). H1 above arrow, timing of Heinrich event
2181 event 1 (and so on); number 1 above curve, Dansgaard-Oscheger event (and so on).
2182 During approximately 27 ka to nearly 55 ka, vegetation, especially treeline, recovered for
2183 short intervals to nearly Holocene conditions at the same time that the isotopic record in
2184 Greenland suggests repeated warm warm-cold cycles of change. kyr BP, thousands of
2185 years before the present.

2186

2187



2188

2189

2190 **Figure 4.9** Annual tree rings composed of seasonal early and late wood are clear in this a
2191 64-year year-old *Larix siberica* from western Siberia (Esper and Schweingruber, 2004).

2192 Initial growth was restricted; narrow rings average 0.035 mm/year, punctuated by one

2193 thicker ring (one single arrow). Later (two arrows), tree-ring width abruptly at least

2194 doubled for more than three years. Ring widths increased to 0.2 mm/year (Photograph

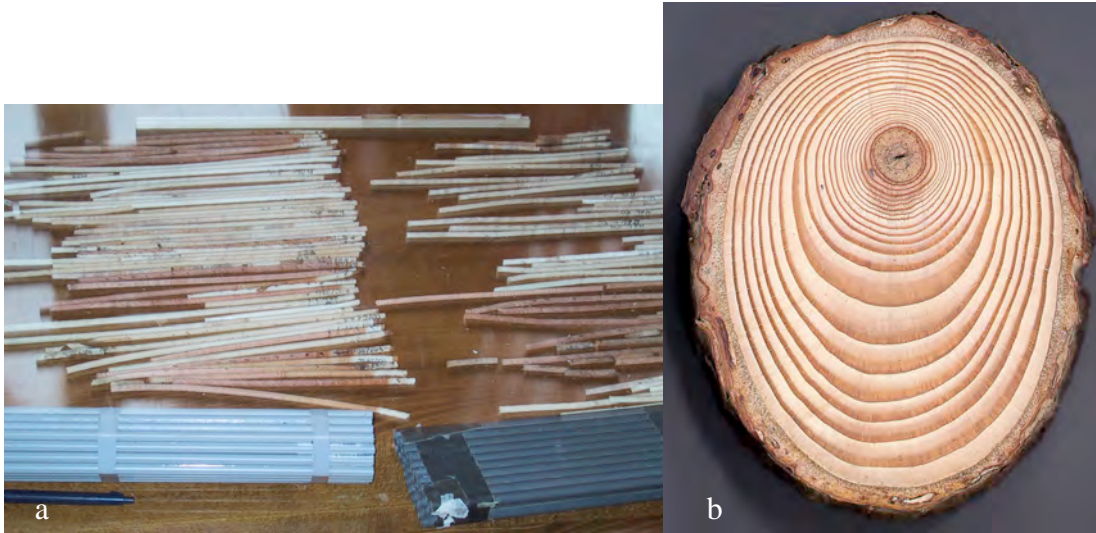
2195 courtesy of Jan Esper, Swiss Federal Research Institute).

2196

2197

2197

2198



2199

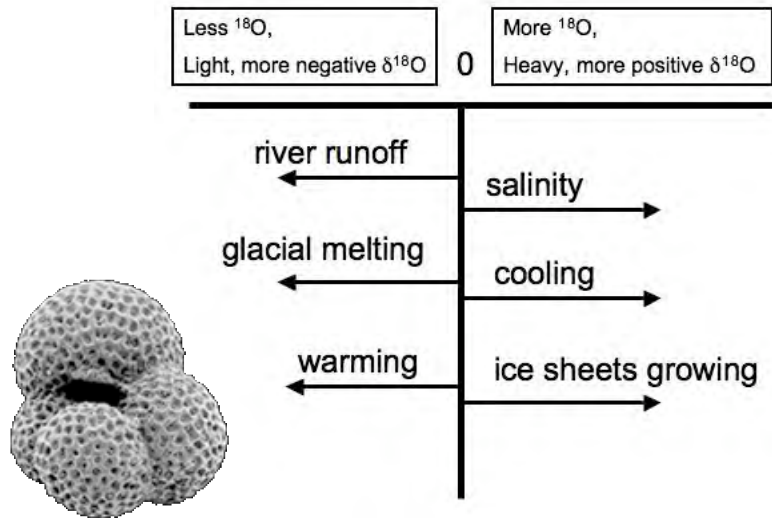
2200

2201 **Figure 4.10** Typical tree ring samples. a) Increment cores taken from trees with a small
2202 small-bore hollow drill. They can be easily stored and transported in plastic soda straws
2203 for analysis in the laboratory. b) Alternatively, cross sections or disks can be sanded for
2204 study. A cross section of *Larix decidua* root shows differing wood thickness within single
2205 rings, caused by exposure. (Photographs courtesy of Jan Esper and Holger Gärtner, Swiss
2206 Federal Research Institute, respectively).

2207

2208

2208



2209

2210 **Figure 4.11** 14 Microscopic marine plankton known as (foraminifera) (see inset)
 2211 grow a shell of calcium carbonate (CaCO_3) in or near isotopic equilibrium with ambient
 2212 sea water. The oxygen isotope ratio measured in these shells can be used to determine the
 2213 temperature of the surrounding waters. (The oxygen-isotope ratio is expressed in $\delta^{18}\text{O}$
 2214 parts per million (ppm) = $10^3[(R_{\text{sample}}/R_{\text{standard}}) - 1]$, where $R_x = (^{18}\text{O})/(^{16}\text{O})$ is the ratio of
 2215 isotopic composition of a sample compared to that of an established standard, such as
 2216 ocean water) However, factors other than temperature can influence the ratio of ^{18}O to
 2217 ^{16}O . Warmer seasonal temperatures, glacial meltwater, and river runoff with depleted
 2218 values all will produce a more negative (lighter) $\delta^{18}\text{O}$ [should the Greek letter be δ ?] ratio. On the
 2219 other hand, cooler temperatures or higher salinity waters will drive the ratio up, making it
 2220 heavier, or more positive. The growth of large continental ice sheets selectively removes
 2221 the lighter isotope (^{16}O), leaving the ocean enriched in the heavier isotope (^{18}O).
 2222

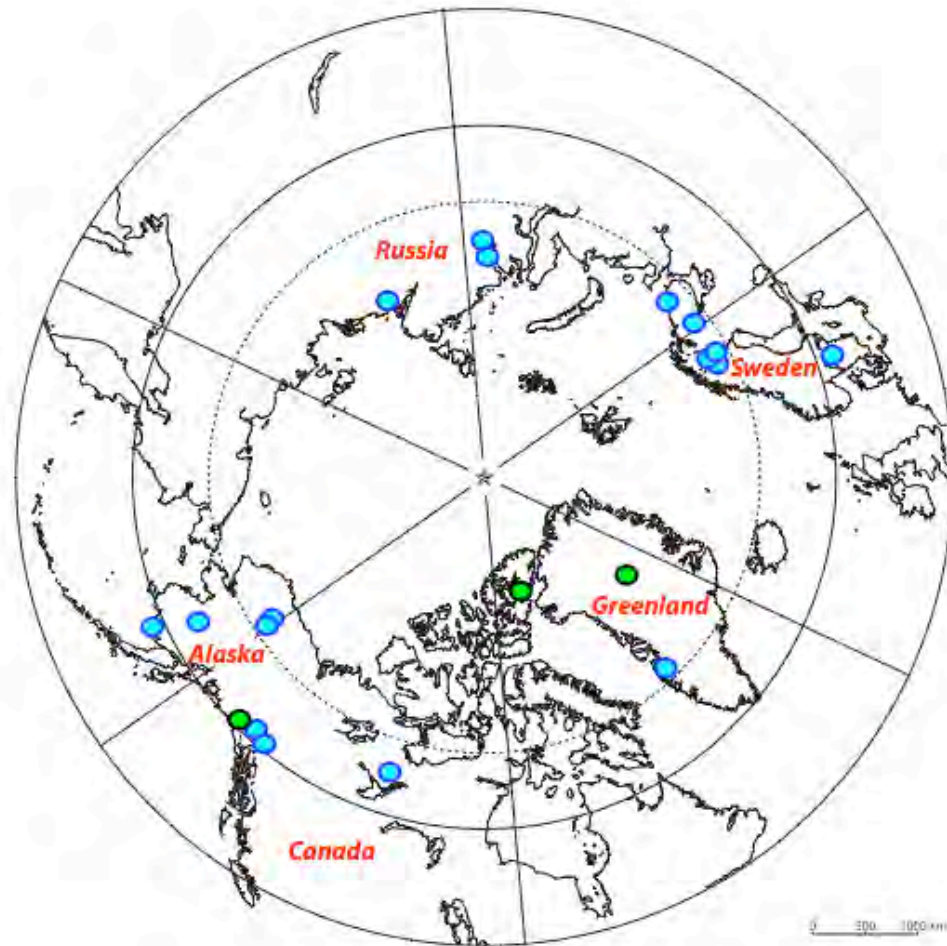
2222



2223

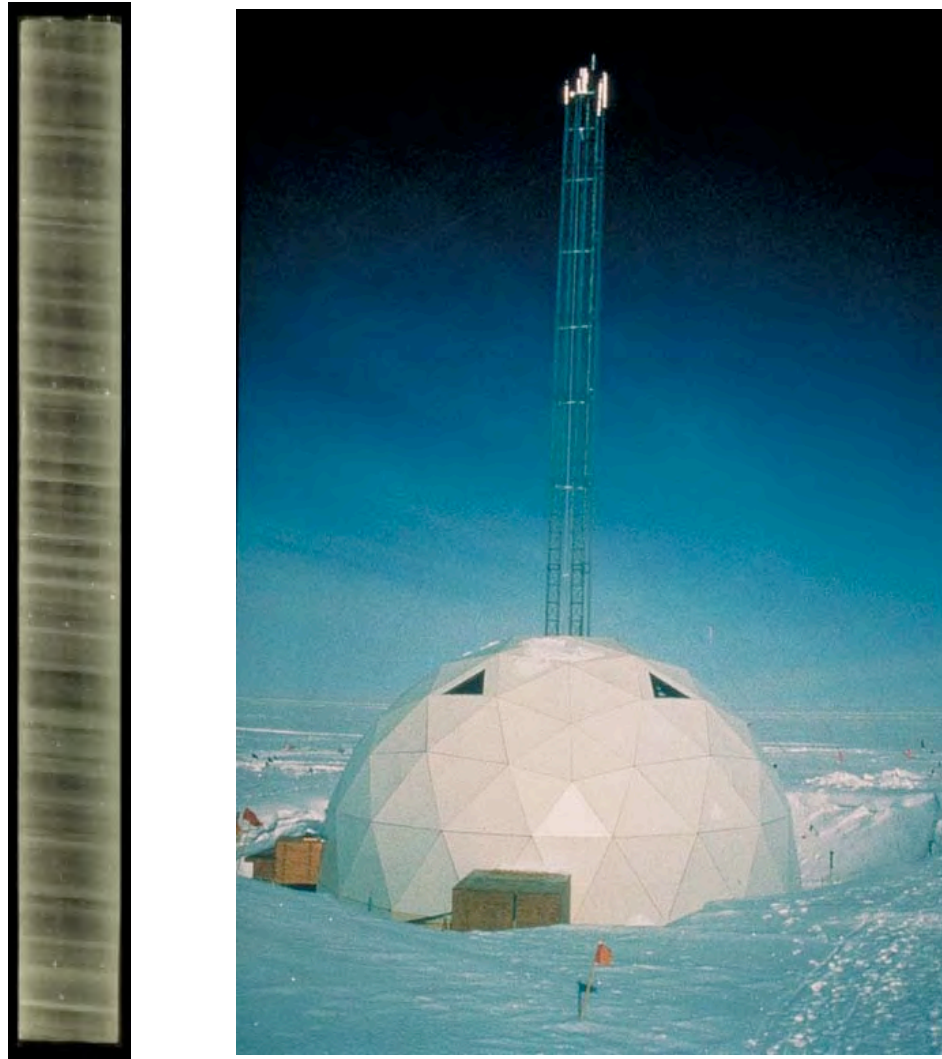
2224 **Figure 4.12** Lake El'gygytgyn in the Arctic Far East of Russia. Open and closed lake
2225 systems in the Arctic differ hydrologically according to the balance between inflow,
2226 outflow, and the ratio of precipitation to evaporation. These parameters are the dominant
2227 influence on lake stable stable-isotopic chemistry and on the depositional character of the
2228 sediments and organic matter. Lake El'gygytgyn is annually open and flows to the Bering
2229 Sea during July and August, but the outlet closes by early September as lake level drops
2230 and storms move beach gravels that choke the outlet. (Photograph by J. Brigham-Grette).
2231

2231



2232

2233 **Figure 4.13** Locations of Arctic and sub-Arctic lakes (blue) and ice cores (green) whose
2234 oxygen isotope records have been used to reconstruct Holocene paleoclimate. (Map
2235 adapted from the Atlas of Canada, © 2002. Her Majesty the Queen in Right of Canada,
2236 Natural Resources Canada. / Sa Majesté la Reine du chef du Canada, Ressources
2237 naturelles Canada.)



2238

a

b

2239

2240

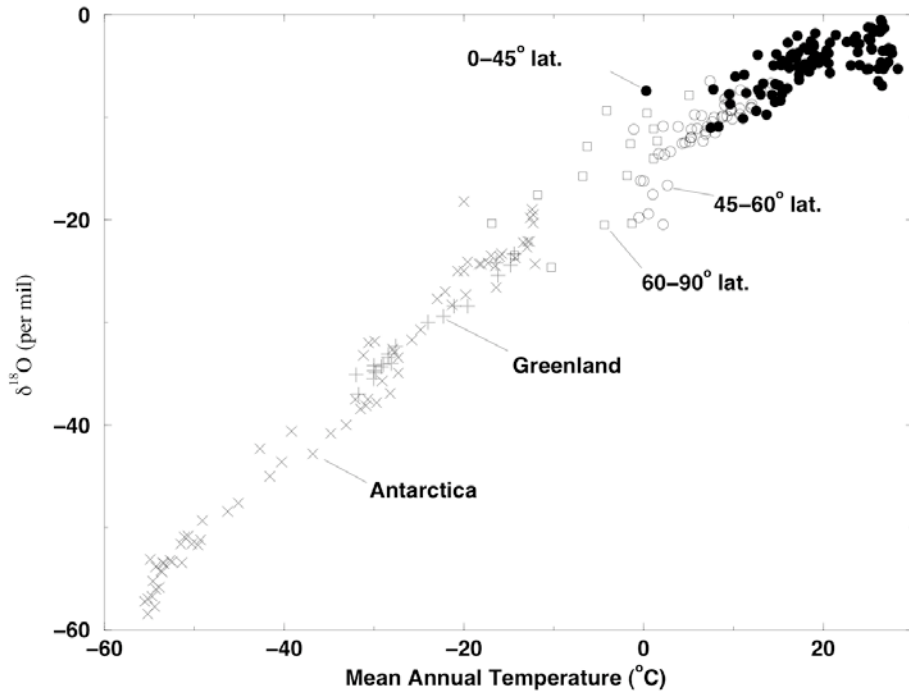
2241

2242

2243

2244

Figure 4.14 a) One-meter section of Greenland Ice Core Project-2 core from 1837 m depth showing annual layers. (Photograph courtesy of Eric Cravens, Assistant Curator, U.S. National Ice Core Laboratory). b) Field site of Summit Station on top of the Greenland Ice Sheet (Photograph by Michael Morrison, GISP2 SMO, University of New Hampshire; NOAA Paleoslide Set)

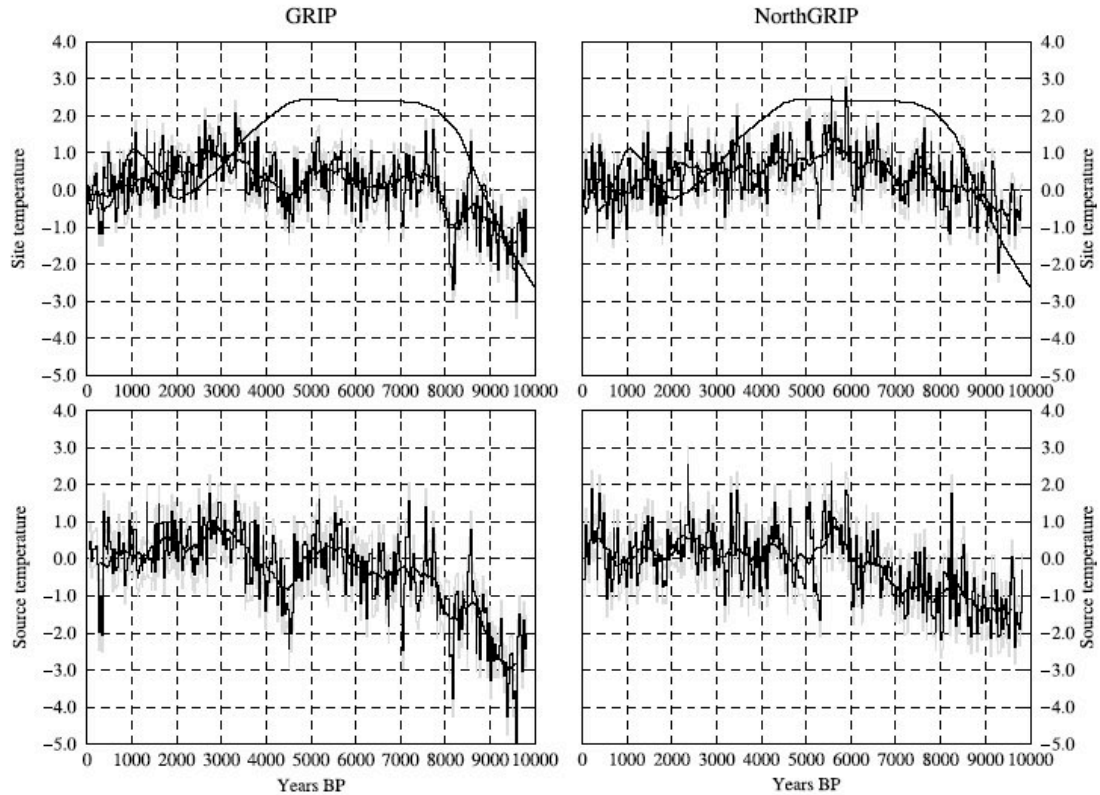


2245

2246 **Figure 4.15** Relation between isotopic composition of precipitation and temperature in
 2247 the parts of the world where ice sheets exist. Sources of data as follows: International
 2248 Atomic Energy Agency (IAEA) network (Fricke and O'Neil, 1999; calculated as the
 2249 means of summer and winter data of their Table 1 for all sites with complete data. Open
 2250 squares, poleward of 60° latitude (but with no inland ice-sheet sites); open circles, 45°–
 2251 60° latitude; filled circles, equatorward of 45° latitude. x, data from Greenland (Johnsen
 2252 et al., 1989); +, data from Antarctica (Dahe et al., 1994). About 71% of Earth's surface
 2253 area is equatorward of 45°, where dependence of $\delta^{18}\text{O}$ on temperature is weak to
 2254 nonexistent. Only 16% of Earth's surface falls in the 45°–60° band, and only 13% is
 2255 poleward of 60°. The linear array is clearly dominated by data from the ice sheets.
 2256 (Source: Alley and Cuffey, 2001)

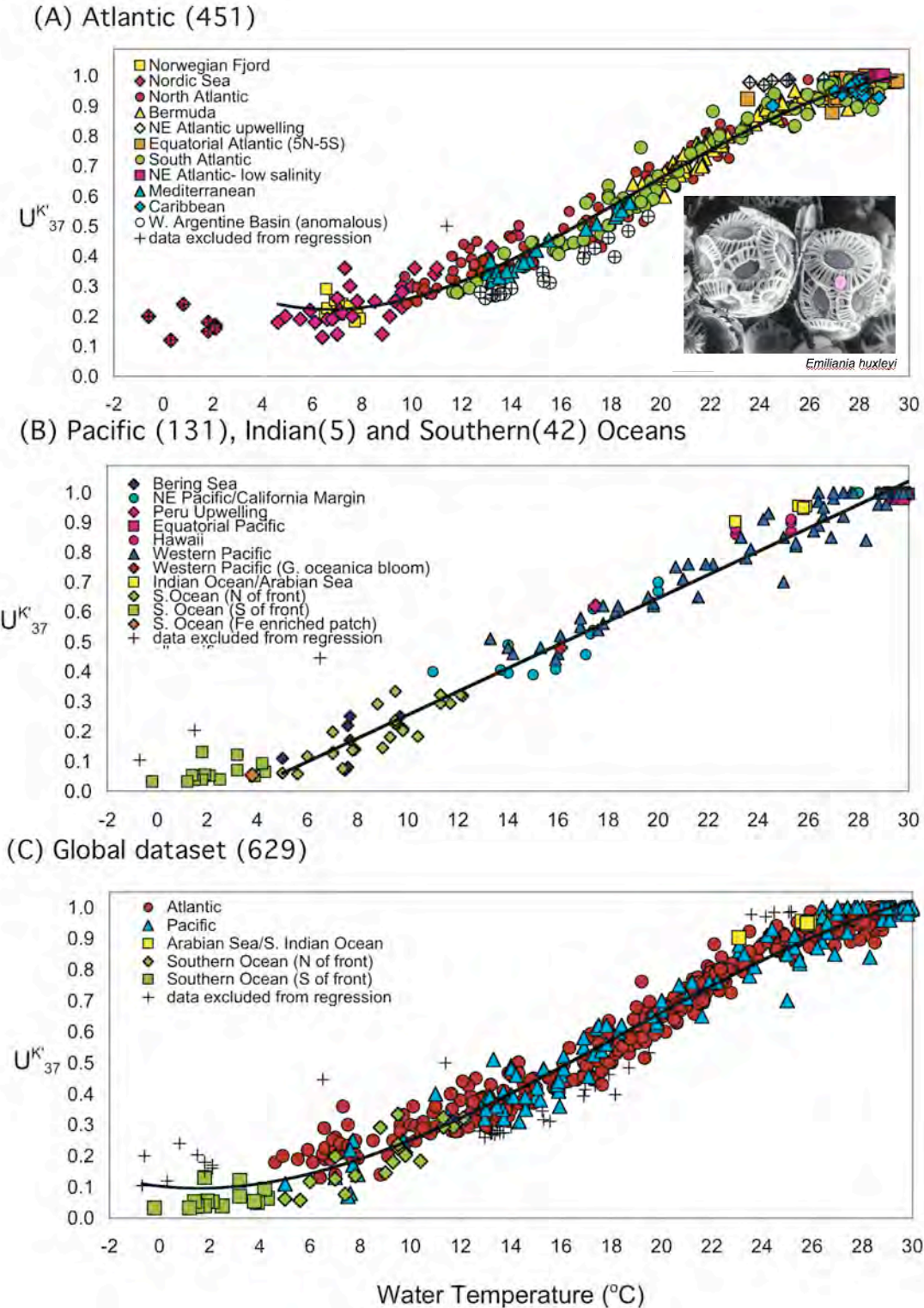
2257

2257



2258

2259 **Figure 4.16** Paleotemperature estimates of site and source waters from on Greenland:
 2260 GRIP and NorthGrip, Masson-Delmotte et al., 2005). GRIP (left) and NorthGRIP (right)
 2261 site (top) and source (bottom) temperatures derived from GRIP and NorthGRIP $\delta^{18}\text{O}$ and
 2262 deuterium excess corrected for seawater $\delta^{18}\text{O}$ (until 6000 BP). Shaded lines in gray
 2263 behind the black line provide an estimate of uncertainties due to the tuning of the isotopic
 2264 model and the analytical precision. Solid line (in part above zigzag line), GRIP
 2265 temperature derived from the borehole-temperature profile (Dahl-Jensen et al., 1998).



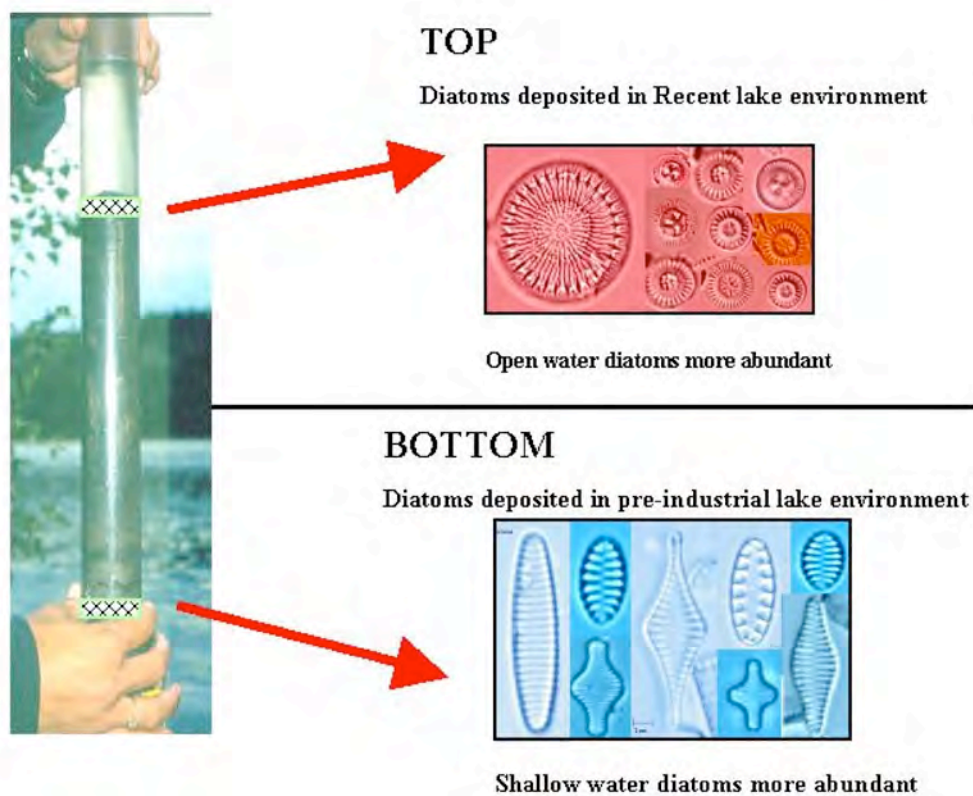
2266

2267 **Figure 4.17** Biomarker alkenone. U_{37}^K versus measured water temperature for ocean-

2268 water surface mixed layer (0–30 m) samples. A) Atlantic region: Empirical 3rd-order

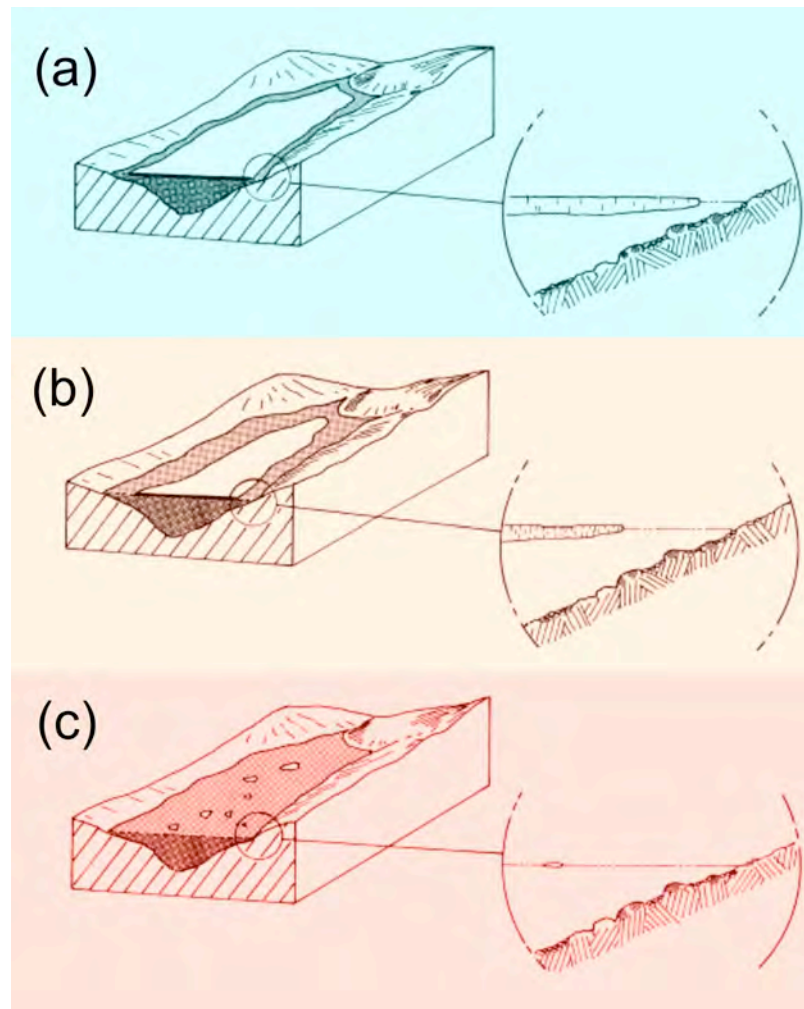
2269 polynomial regression for samples collected in warmer-than-4°C waters is $U_{37}^K = 1.004$
2270 $10^{-4}T^3 + 5.744 \cdot 10^{-3}T^2 - 6.207 \cdot 10^{-2}T + 0.407$ ($r^2 = 0.98$, $n = 413$) (Outlier data from
2271 the southwest Atlantic margin and northeast Atlantic upwelling regime is excluded.). B)
2272 Pacific, Indian, and Southern Ocean regions: The empirical linear regression of Pacific
2273 samples is $U_{37}^K = 0.0391T - 0.1364$ ($r^2 = 0.97$, $n = 131$). Pacific regression does not
2274 include the Indian and Southern Ocean data. C) Global data: The empirical 3rd order
2275 polynomial regression, excluding anomalous southwest Atlantic margin data, is $U_{37}^K =$
2276 $5.256 \cdot 10^{-5}T^3 + 2.884 \cdot 10^{-3}T^2 - 8.4933 \cdot 10^{-2}T + 9.898$ ($r^2 = 0.97$, $n = 588$). +, sample
2277 excluded from regressions. (Conte et al, 2006).

2278



2279 **Figure 4.18** Diatom assemblages reflect a variety of environmental conditions in Arctic
 2280 lake systems. Transitions, especially rapid change from one assemblage to another, can
 2281 reflect large changes in conditions such as light, nutrient availability, or temperature, for
 2282 example. Biogenic silica, chiefly the silica skeletal framework constructed by diatoms, is
 2283 commonly measured in lake sediments and used as an index of past changes in aquatic
 2284 primary productivity.

2285



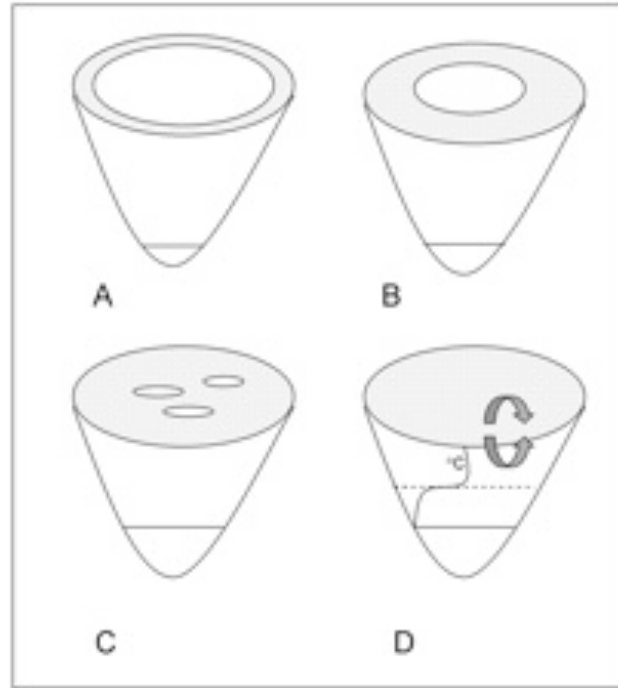
2286

2287 **Figure 4.19** Changing ice and snow conditions on an Arctic lake during relatively (a)
2288 cold, (b) moderate, and (c) warm conditions. During colder years, a permanent raft of ice
2289 may persist throughout the short summer, precluding the development of large
2290 populations of phytoplankton, and restricting much of the primary production to a
2291 shallow, open open-water moat. Many other physical, chemical and biological changes
2292 occur in lakes that are either directly or indirectly affected by snow and ice cover (see
2293 Table 1; Douglas and Smol, 1999). Modified from Smol (1988).

2294

2294

2295

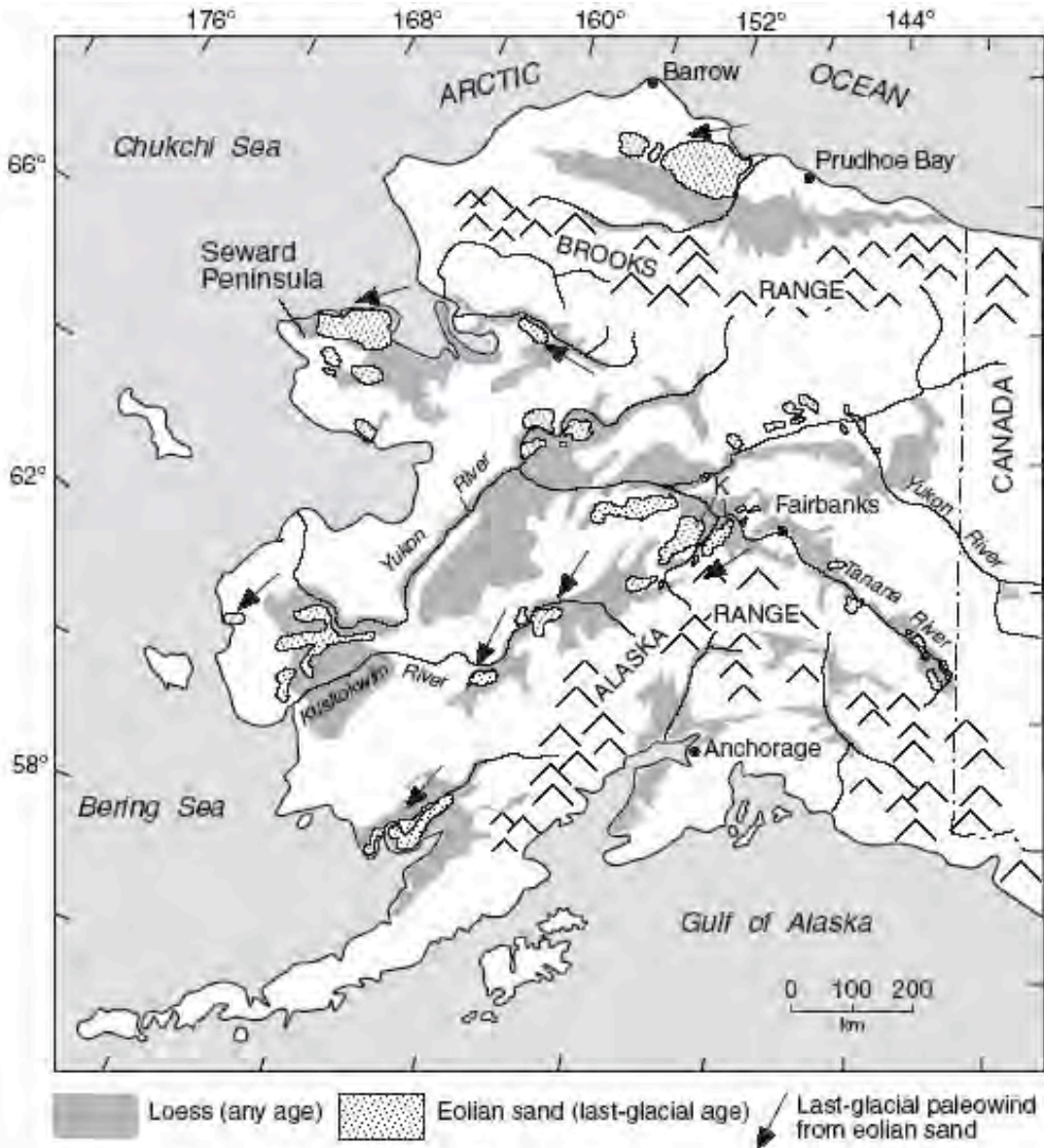


2296

2297 **Figure 4.20** Lake ice melts as it continues to warm (A – D). Eventually, in deeper lakes
2298 (vs ponds) thermal stratification (horizontal lines) may also occur (or be prolonged)
2299 during the summer months (D), further altering the limnological characteristics of the
2300 lake. Modified from Douglas (2007).

2301

2301



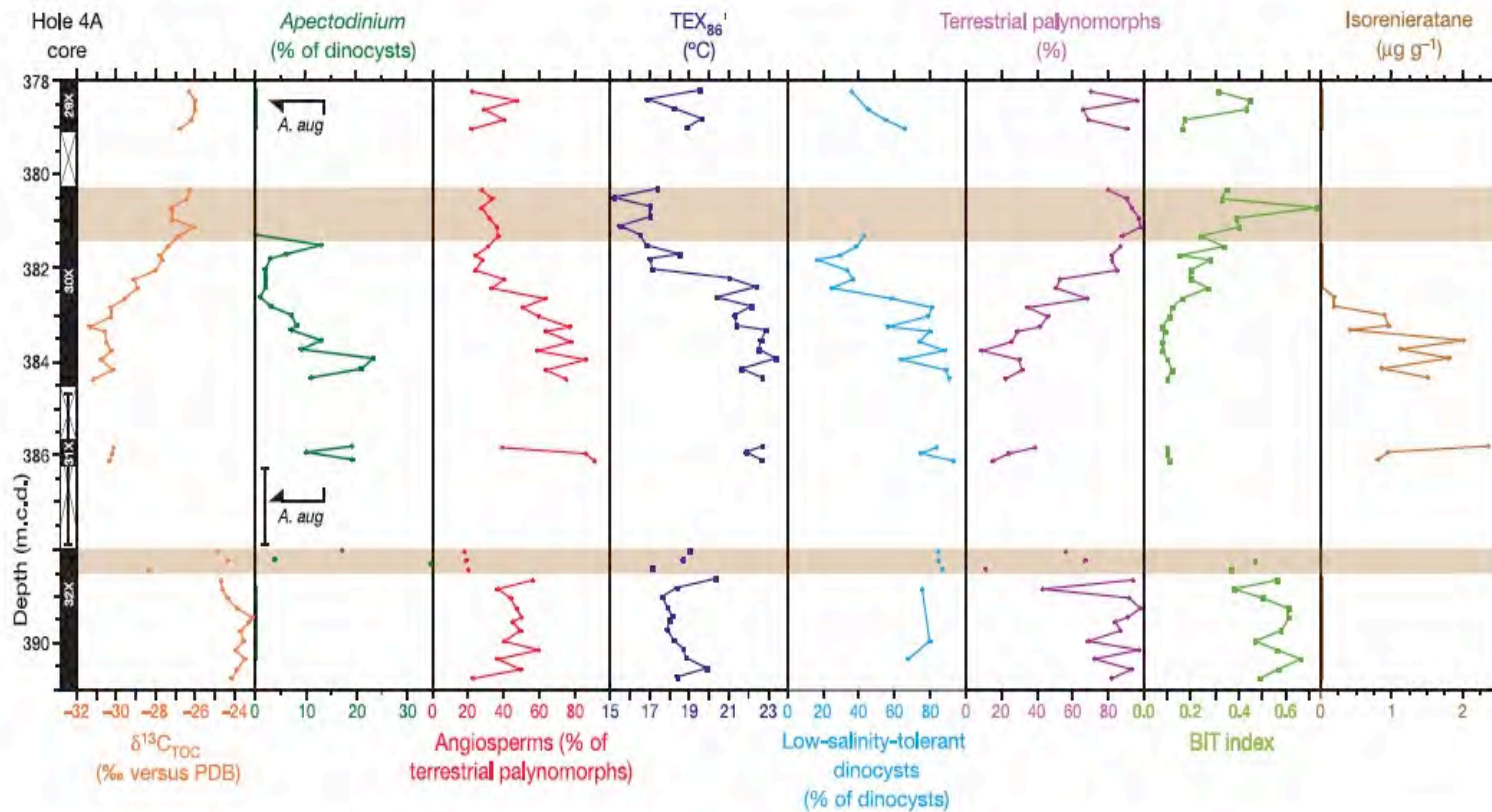
2302 **Figure 4.21** The form and distribution of wind-blown silt (loess), wind-blown sand
 2303 (dunes), and other deposits of wind-blown sediment in Alaska, have been use to infer
 2304 both Holocene and last-glacial past wind directions. (Compiled from multiple sources by
 2305 Muhs and Budahn, 2006).
 2306



2306

2307 **Figure 4.22** Unnamed, hydrologically closed lake in the Yukon Flats Wildlife Refuge,
2308 Alaska. Concentric rings of vegetation developed progressively inward as water level fell,
2309 owing to a negative change in the lake's overall water balance. Historic Landsat imagery
2310 and air photographs indicate that these shorelines formed during within the last 40 years
2311 or so. (Photograph by Lesleigh Anderson.)

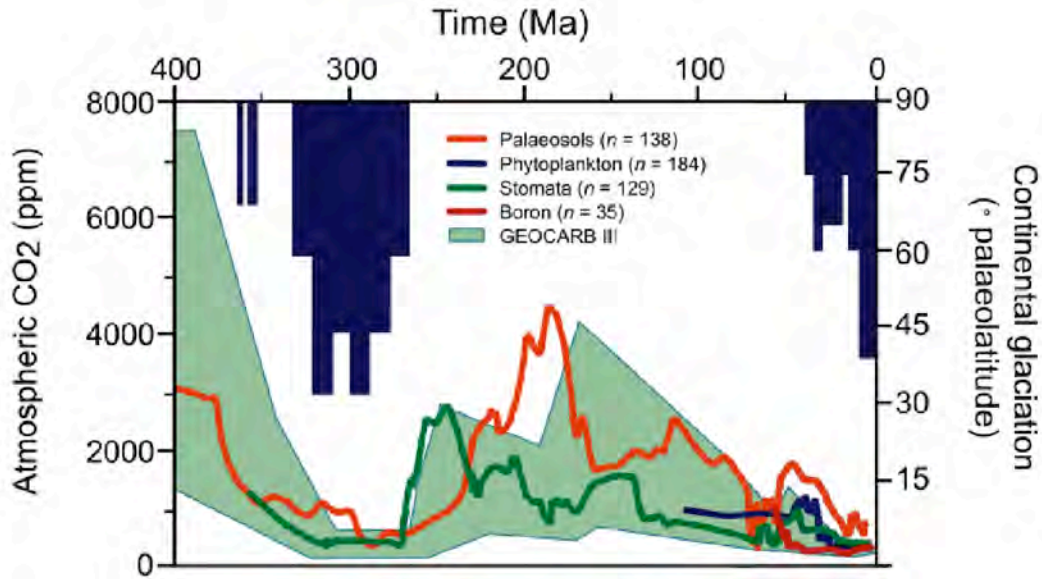
2312



2313

2314 **Figure 4.23** Recovered sections and palynological and geochemical results across the Paleocene-Eocene Thermal Maximum about 55
 2315 Ma; IODP Hole 302-4A (87° 52.00' N.; 136° 10.64' E.; 1288 m water depth, in the central Arctic Ocean basin). Mean annual surface-
 2316 water temperatures (as indicated in the TEX₈₆' column) are estimated to have reached 23°C, similar to water in the tropics today.

2317 (Error bars for Core 31X show the uncertainty of its stratigraphic position. Orange bars, indicate intervals affected by drilling
2318 disturbance.) Stable carbon isotopes are expressed relative to the PeeDee Belemnite standard. Dinocysts tolerant of low salinity
2319 comprise *Senegalinium* spp., *Cerodinium* spp., and *Polysphaeridium* spp., whereas *Membranosphaera* spp., *Spiniferites ramosus*
2320 complex, and *Areoligera-Glaphyrocysta* cpx. represent typical marine species. Arrows and *A. aug* (second column) indicate the first
2321 and last occurrences of dinocyst *Apectodinium augustum*—a diagnostic indicator of Paleocene-Eocene Thermal Maximum warm
2322 conditions. (Sluijs et al., 2006).



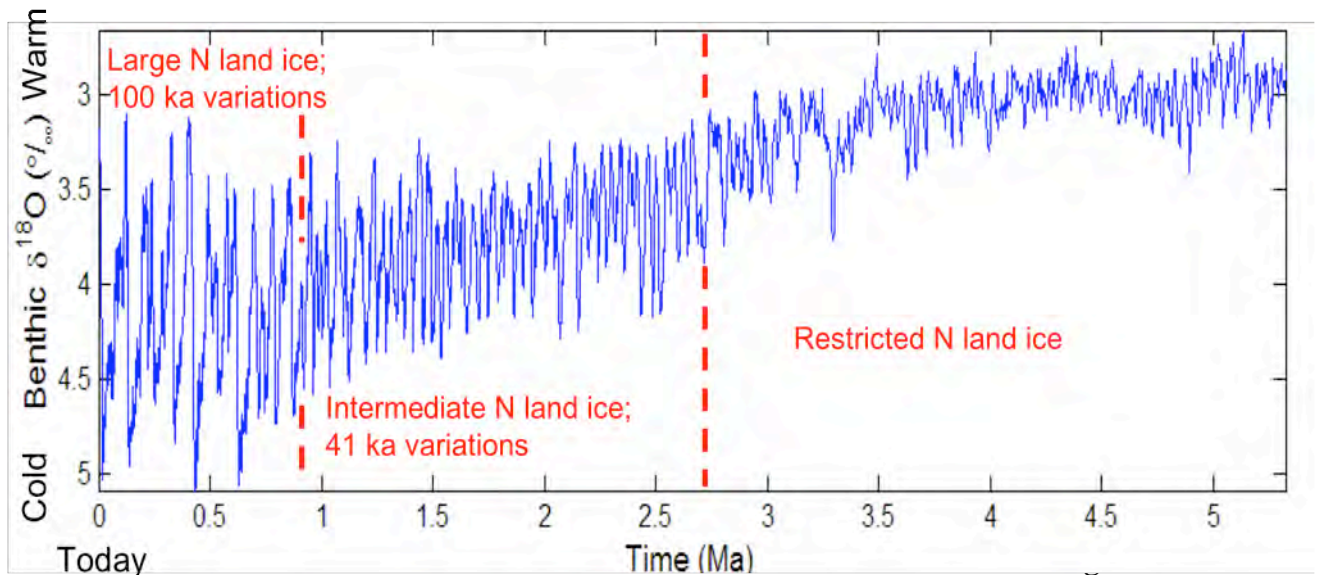
2323

2324

2325 **Figure 4.24** Atmospheric CO₂ and continental glaciation 400 Ma to present. Vertical
 2326 blue bars, timing and palaeolatitude extent of ice sheets (after Crowley, 1998). Plotted
 2327 CO₂ records represent five-point running averages from each of four major proxies (see
 2328 Royer, 2006 for details of compilation). Also plotted are the plausible ranges of CO₂
 2329 derived from the geochemical carbon cycle model GEOCARB III (Bernier and Kothavala,
 2330 2001). All data adjusted to the Gradstein et al. (2004) time scale. Continental ice sheets
 2331 grow extensively when CO₂ is low. (after Jansen, 2007, that report's Figure 6.1)

2332

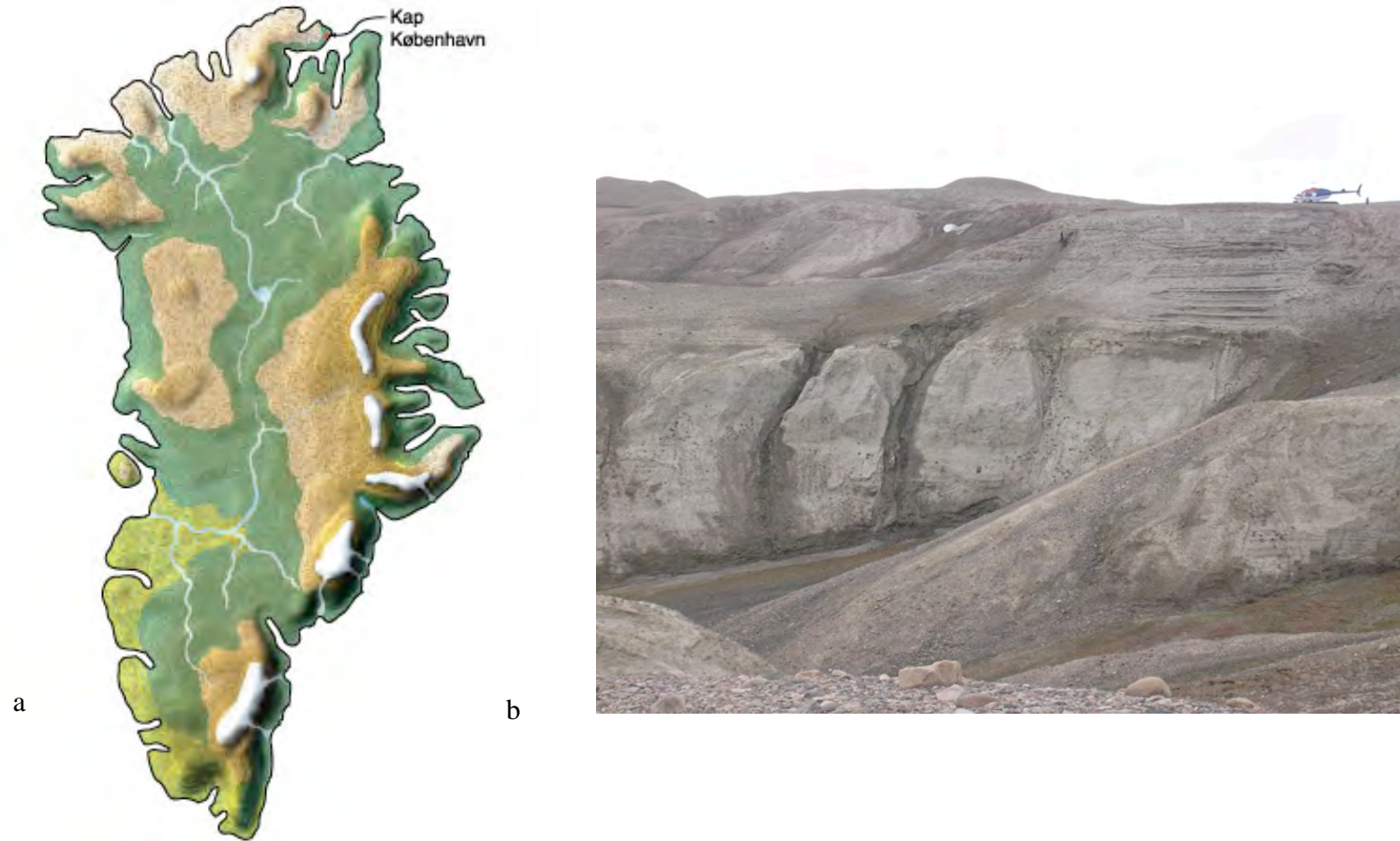
2334



2351

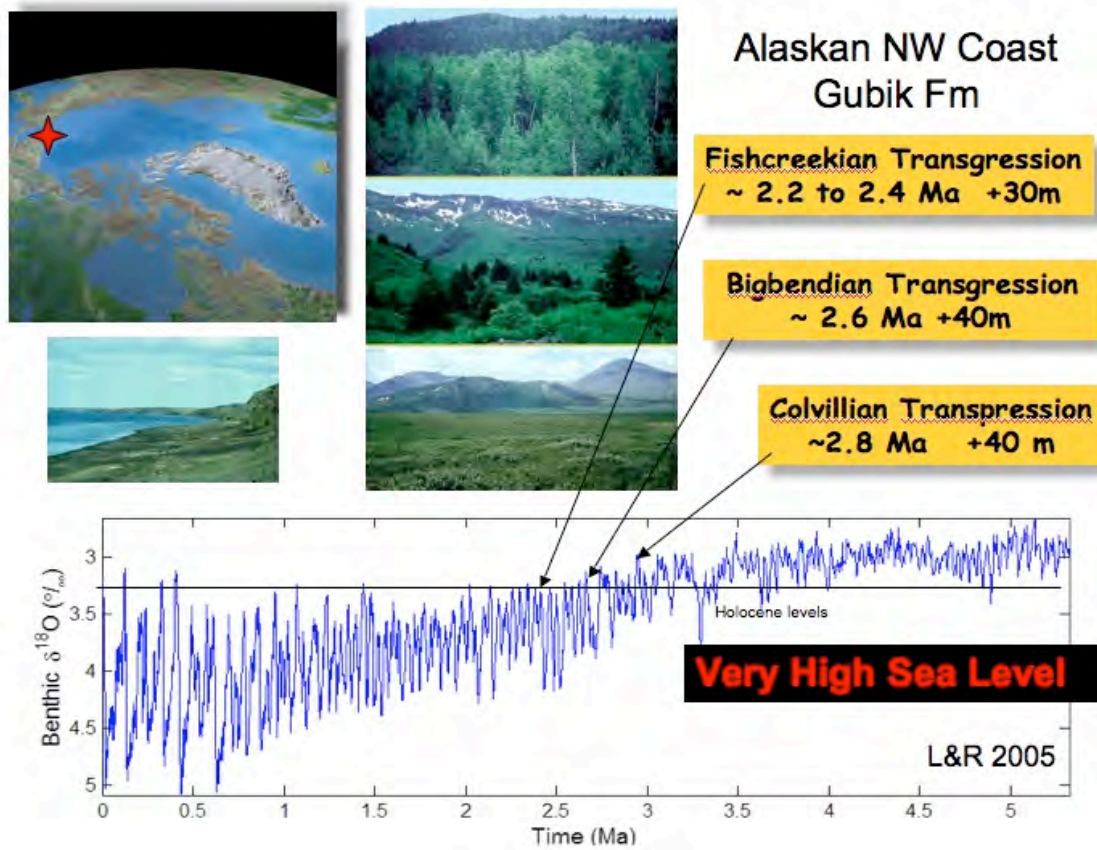
2352 **Figure 4.25** The average isotopic composition ($\delta^{18}\text{O}$) of bottom-dwelling
 2353 foraminifera from in a globally distributed set of 57 sediment cores that record the
 2354 last 5.3 Ma (modified from Lisiecki and Raymo, 2005). The $\delta^{18}\text{O}$ is controlled primarily
 2355 by global ice volume and deep-ocean temperature, with less ice or warmer temperatures
 2356 (or both) upward in the core. The influence of Milankovitch frequencies of Earth's orbital
 2357 variation are present throughout, but glaciation increased about 2.7 Ma ago concurrently
 2358 with establishment of a strong 41 ka variability linked to Earth's obliquity (changes in tilt
 2359 of Earth's spin axis), and the additional increase in glaciation about 1.2–0.7 Ma parallels
 2360 a shift to stronger 100 ka variability. Dashed lines are used because the changes seem to
 2361 have been gradual. The general trend toward higher $\delta^{18}\text{O}$ that runs through this series
 2362 reflects the long-term drift toward a colder Earth that began in the early Cenozoic (see
 2363 Figure 4.8).

2364



2365 **Figure 4.26** a) Greenland without ice for the last time? Dark green, **boreal** forest; light green, deciduous forest; brown, **tundra** and
2366 alpine heaths; white, ice caps. The north-south temperature gradient is constructed from a comparison between North Greenland and

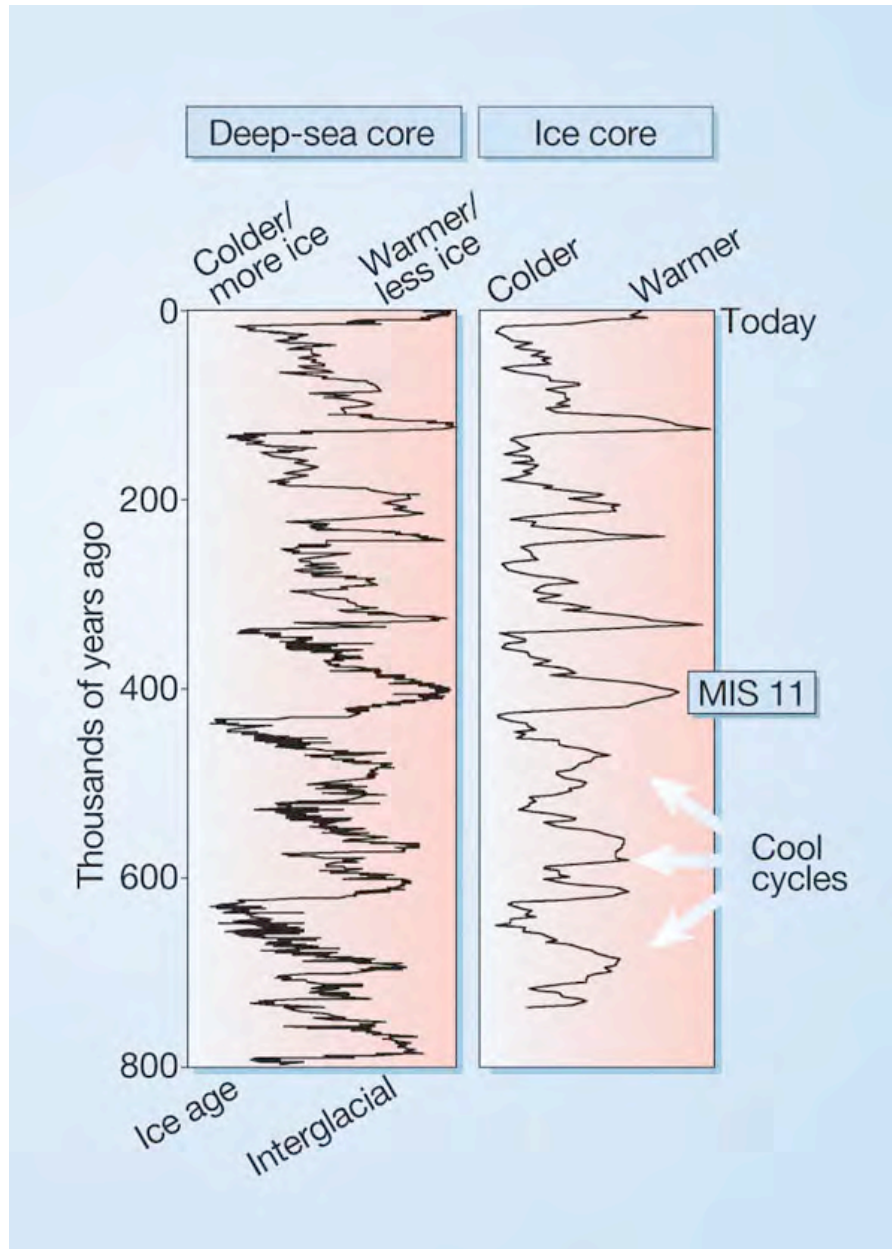
2367 northwest European temperatures, using standard lapse rate; distribution of precipitation assumed to retain the Holocene pattern.
2368 Topographical base, from model by Letreguilly et al. (1991) of Greenland's sub-ice topography after isostatic recovery. b) Upper part
2369 of the Kap København Formation, North Greenland. The sand was deposited in an estuary about 2.4 Ma; it contains abundant well-
2370 preserved leaves, seeds, twigs, and insect remains. (Figure and Photograph of by S.V. Funder.).



2371

2372

2373 **Figure 4.27** The largely marine Gubik Formation, North Slope of Alaska, contains three
 2374 superposed lower units that record relative sea level as high +30-+ to +40 m. Pollen in
 2375 these deposits suggests that borderland vegetation at each of these times was less
 2376 forested; **boreal** forests or spruce-birch woodlands at 2.7 Ma gave way to larch and
 2377 spruce forests at about 2.6 Ma and to open **tundra** by about 2.4 Ma (see photographs by
 2378 Robert Nelson, Colby College, who analyzed the pollen; oldest at top). Isotopic reference
 2379 time series of Lisecki and Raymo (2005) suggests best as assignments for these sea level
 2380 events (Brigham and Carter, 1992).

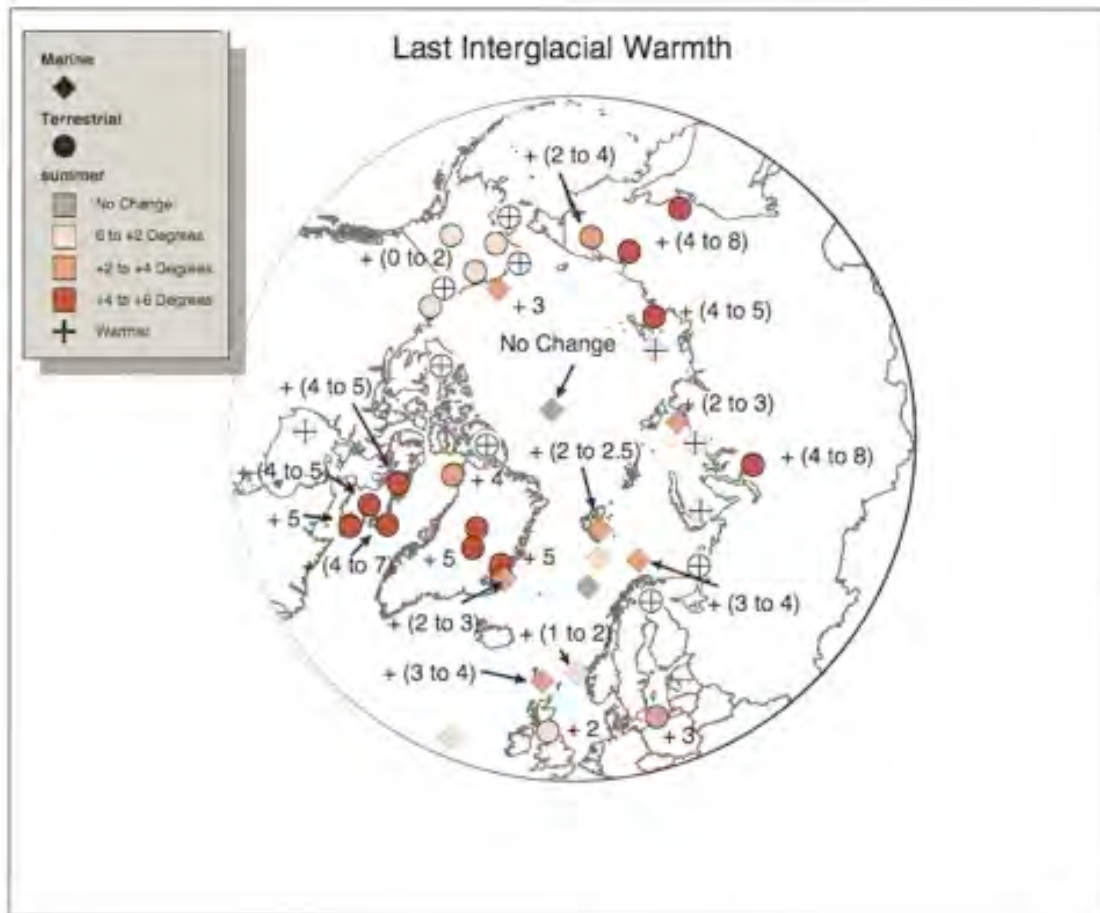


2381

2382 **Figure 4.28** Glacial cycles of the past 800 ka derived from marine-sediment and ice
 2383 cores (McManus, 2004). The history of deep-ocean temperatures and global ice volume
 2384 inferred from $\delta^{18}\text{O}$ measured in bottom-dwelling foraminifera shells preserved in Atlantic
 2385 Ocean sediments. Air temperatures over Antarctica inferred from the ratio of deuterium
 2386 to hydrogen in ice from central Antarctica (EPICA, 2004). Marine isotope stage 11 (MIS
 2387 11) is an interglacial whose orbital parameters were similar to those of the Holocene, yet
 2388 it lasted about twice as long as most interglacials. Note the smaller magnitude and less-
 2389 pronounced interglacial warmth of the glacial cycles that preceded MIS 11.

2390 Interglaciations older than MIS 11 were less warm than subsequent interglaciations.

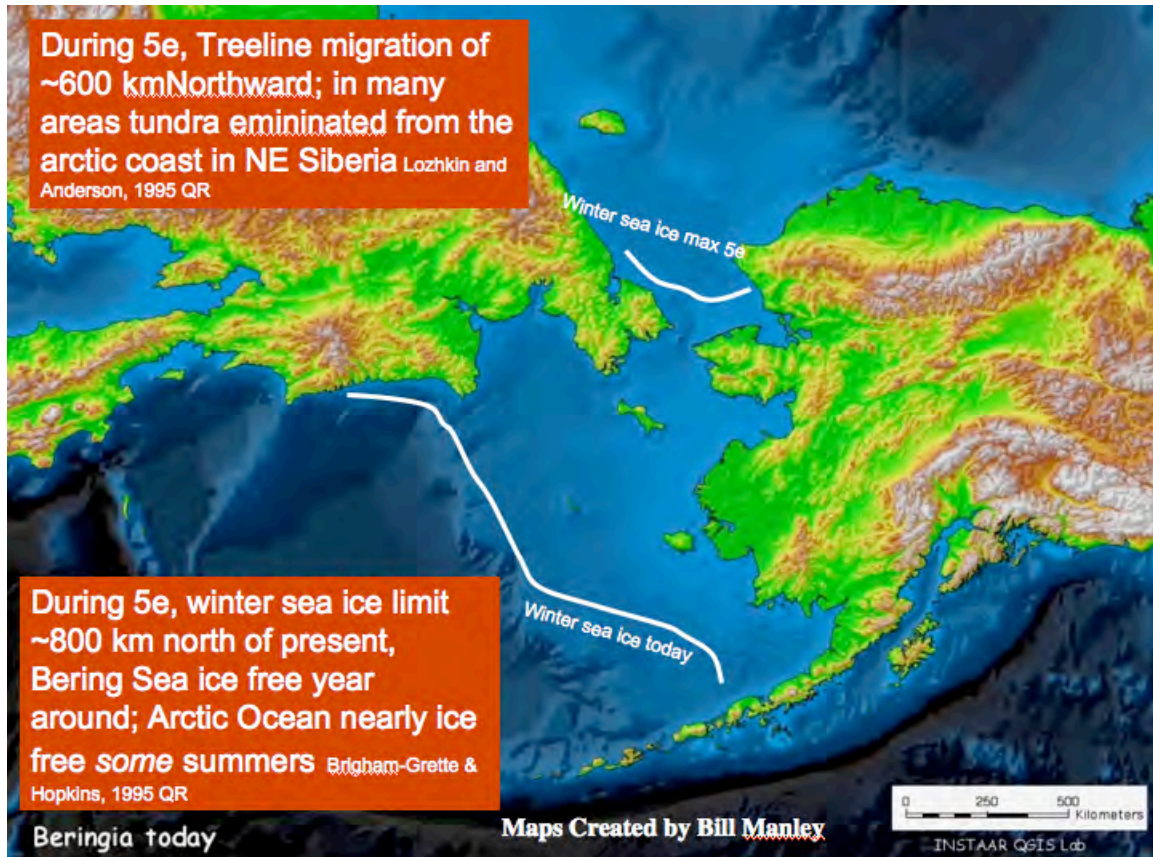
2391



2392

2393 **Figure 4.29** Polar projection showing regional maximum LIG last interglacial summer
 2394 temperature anomalies relative to present summer temperatures; derived from
 2395 paleotemperature proxies (see tables Tables 1 and 2, in from CAPE Last Interglacial
 2396 Project Members, 2006). Circles, terrestrial; squares, marine sites.

2397

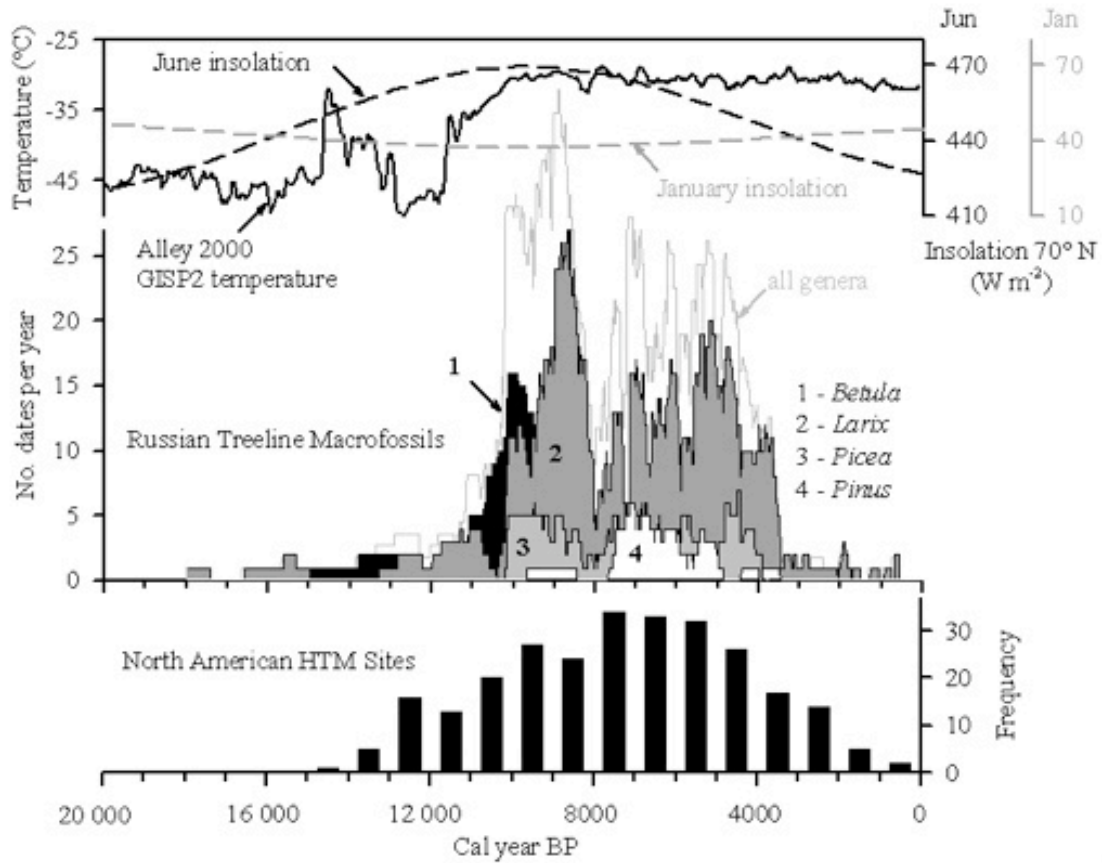


2398

2399

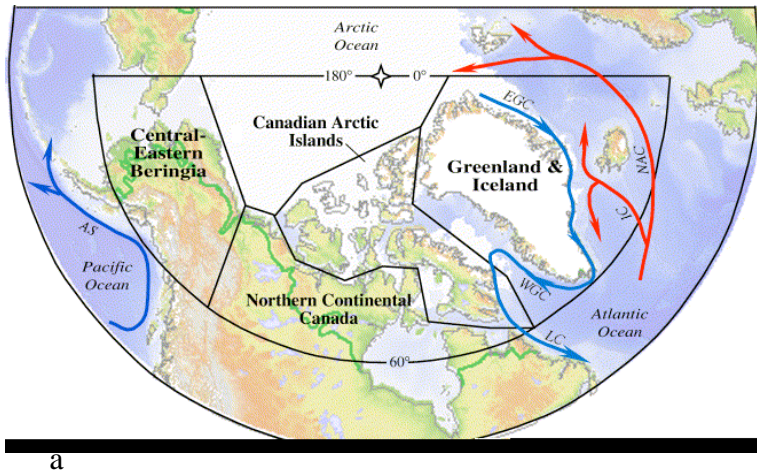
2400 **Figure 4.30** Winter sea-ice limit during MIS 5e and at present. Fossiliferous
 2401 paleoshorelines and marine sediments were used by Brigham-Grette and Hopkins (1995)
 2402 to evaluate the seasonality of coastal sea ice on both sides of the Bering Strait during the
 2403 Last Last Interglaciatiion. Winter sea limit is estimated to have been north of the
 2404 narrowest section of the strait, 800 km north of modern limits. Pollen data derived from
 2405 Last Interglacial lake sediments suggest that **tundra** was nearly eliminated from the
 2406 Russian coast at this time (Lozhkin and Anderson, 1995). In Chukotka during the warm
 2407 interglaciatiion, additional open water favored some taxa tolerant of deeper winter snows.
 2408 (Map of William Manley, <http://instaar.colorado.edu/QGISL/>).
 2409

2409

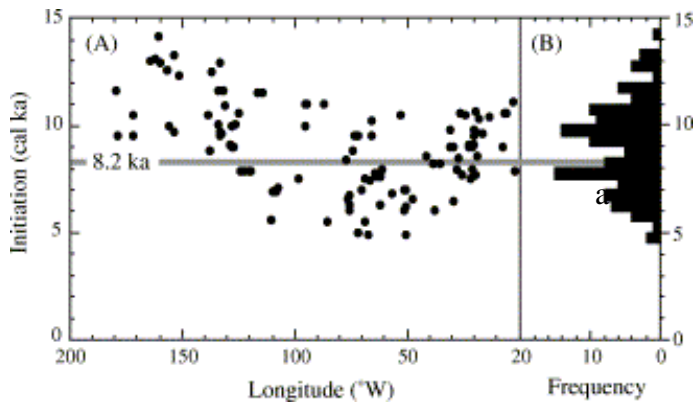


2410

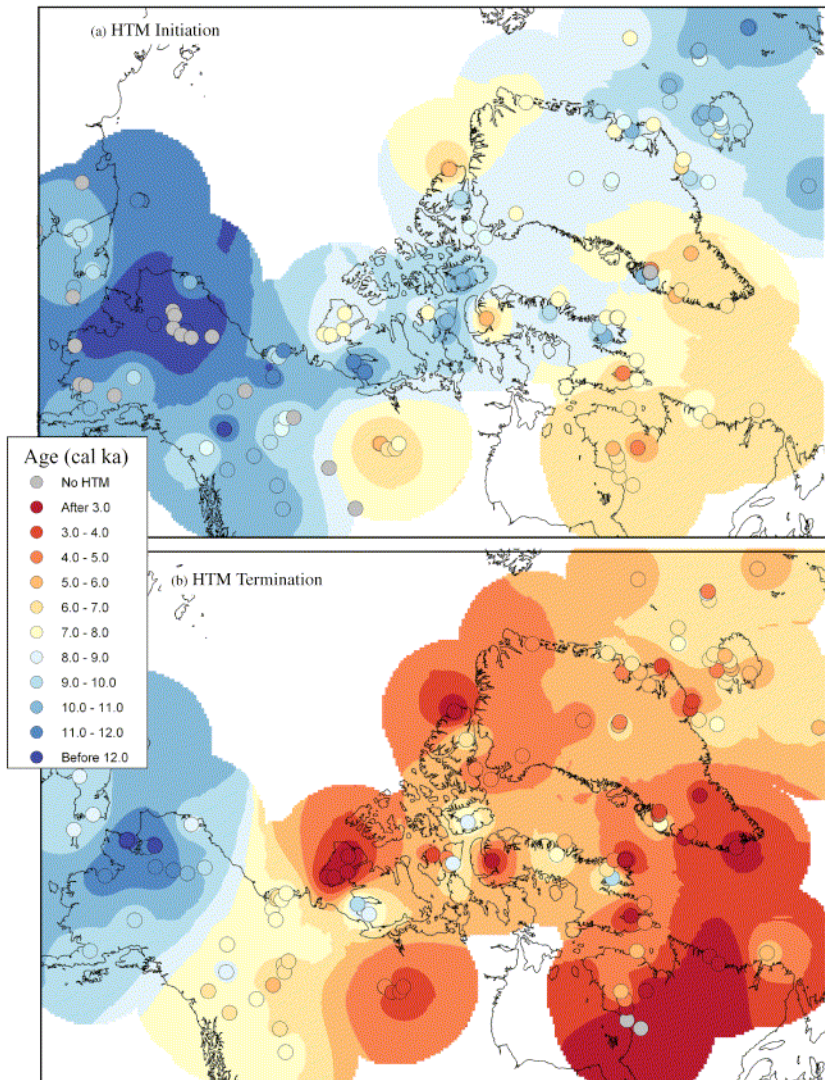
2411 **Figure 4.31** The Arctic Holocene Thermal Maximum. Items compared, top to bottom:
 2412 seasonal insolation patterns at 70° N. (Berger & Loutre, 1991), and reconstructed
 2413 Greenland air temperature from the GISP2 drilling project (Alley 2000); age distribution
 2414 of radiocarbon-dated fossil remains of various tree genera from north of present treeline
 2415 (MacDonald et al., 2007),); and the frequency of Western Arctic sites that experienced
 2416 Holocene Thermal Maximum conditions. (Kaufman et al. 2004).



a



b

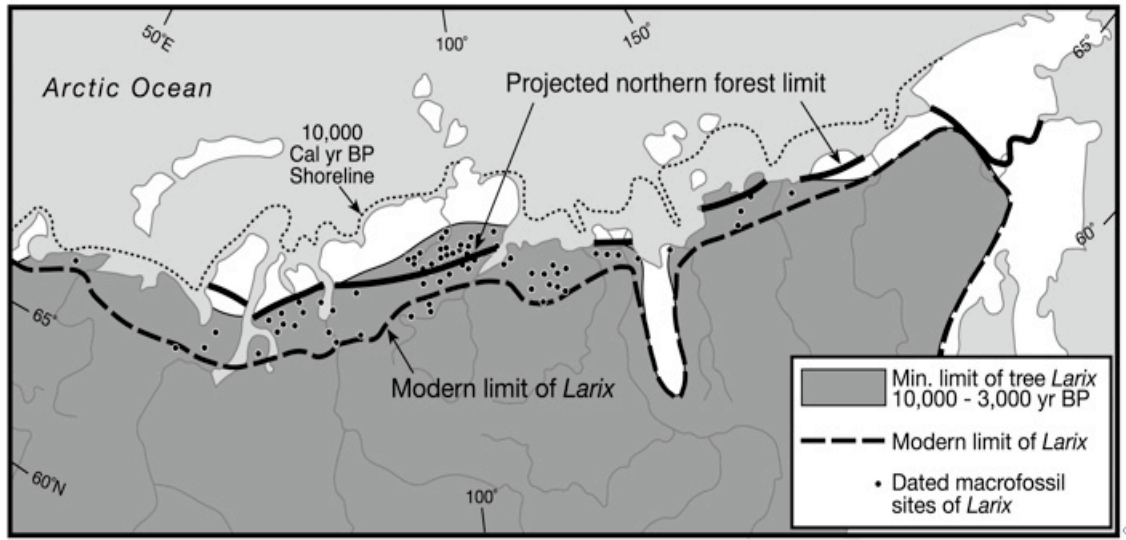


c

2417

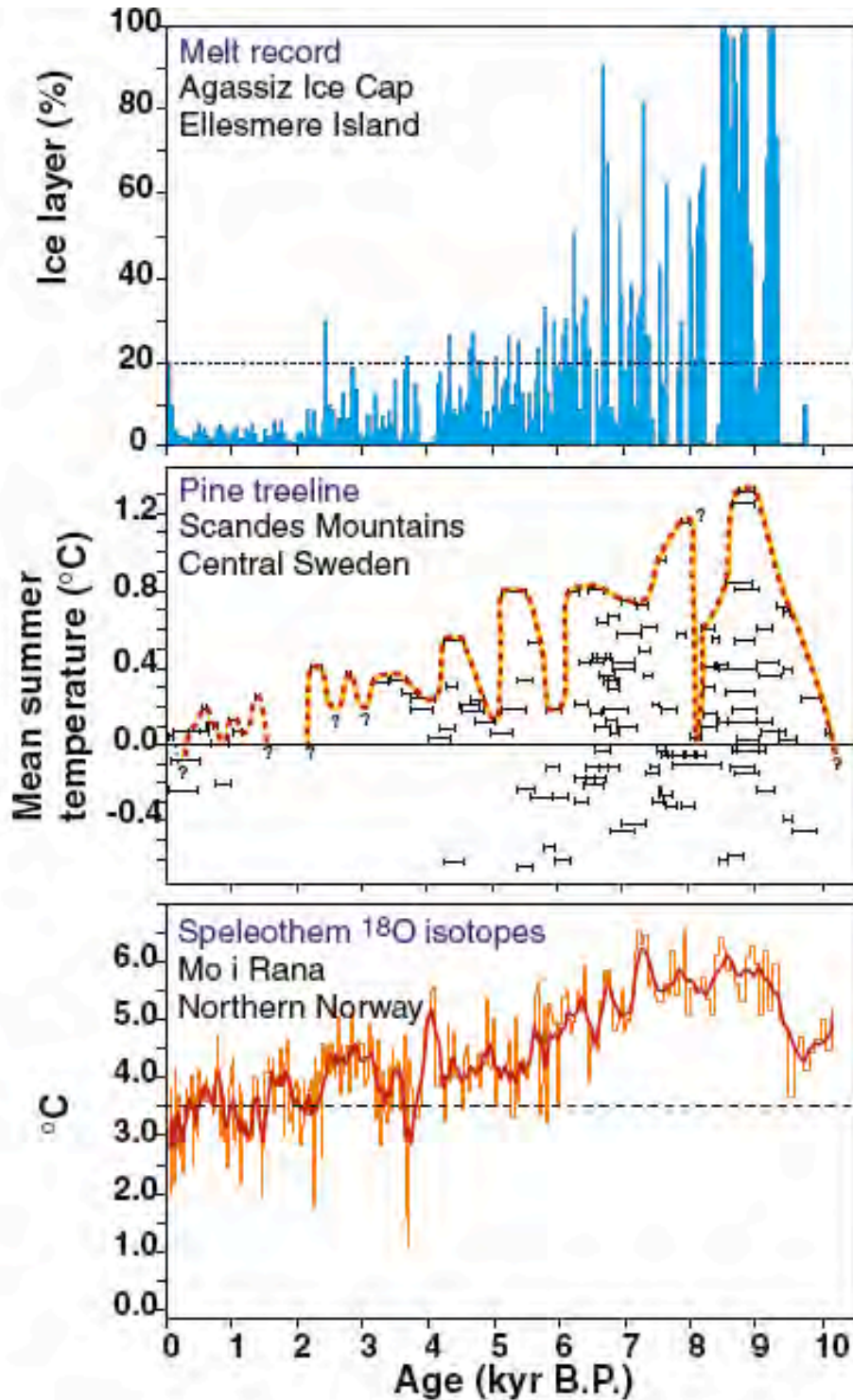
2418 **Figure. 5.32** The timing of initiation and termination of the Holocene Thermal Maximum in the western Arctic (Kaufman et al.,
2419 2004). a) Regions reviewed in Kaufman et al., 2004. b) Initiation of the Holocene Thermal Maximum in the western Arctic.
2420 Longitudinal distribution (left) and frequency distribution (right). c) Spatial-temporal pattern of the Holocene Thermal Maximum in
2421 the western Arctic. Upper panel, initiation; lower panel, termination. Dot colors bracket ages of the Holocene Thermal Maximum;
2422 ages contoured using the same color scheme. Gray dots, equivocal evidence for the Holocene Thermal Maximum.
2423

2424



2425

2426 **Figure 4.33** The northward extension of larch (*Larix*) treeline across the Eurasian Arctic.
 2427 Treeline today compared with treeline during the Holocene Thermal Maximum and with
 2428 anticipated northern forest limits (Arctic Climate Impact Assessment, 2005) due to climate
 2429 warming (MacDonald et al., 2007).



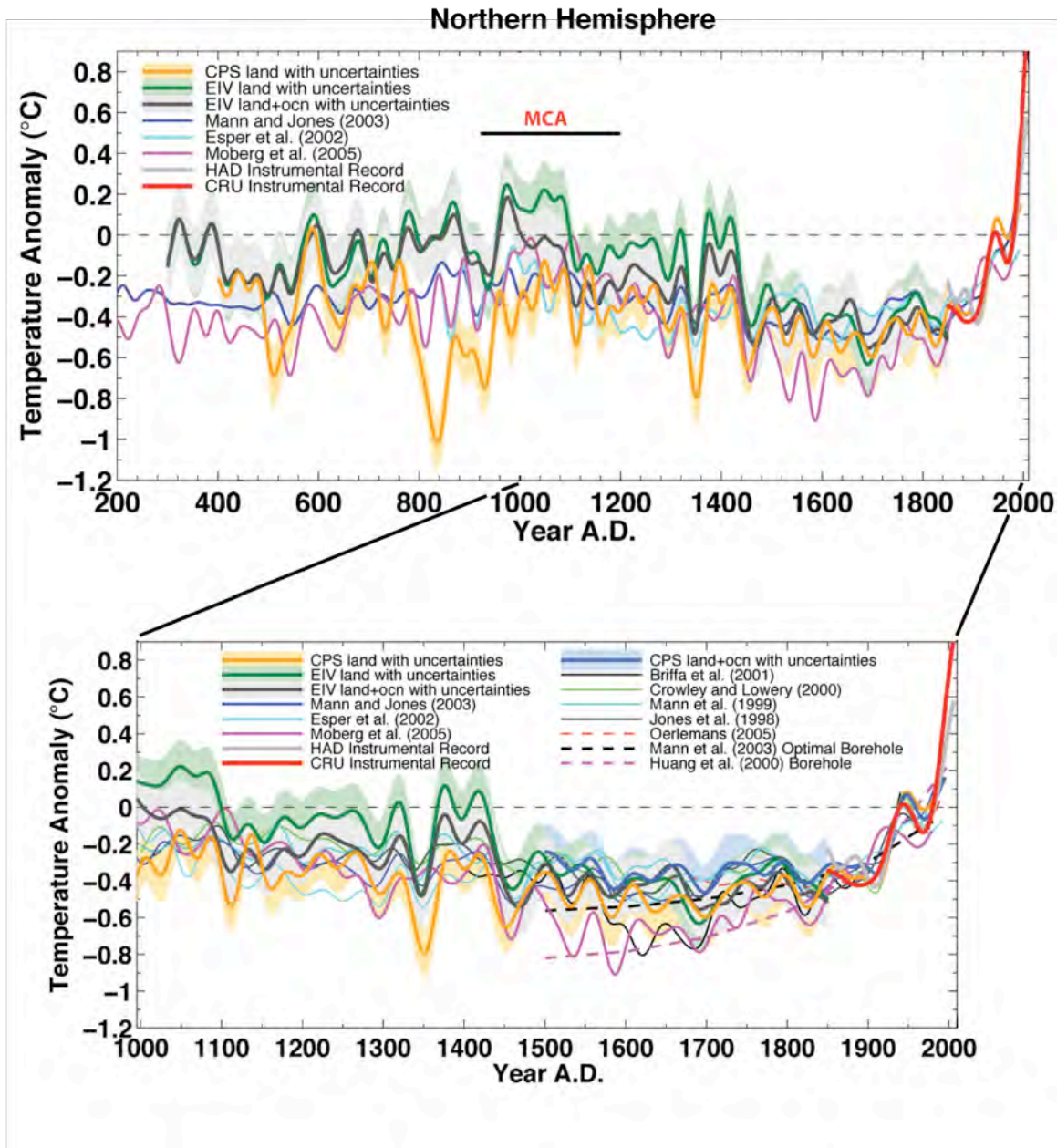
2430

2431 **Figure 4.34** Arctic temperature reconstructions. Upper panel: Holocene summer melting on the
 2432 Agassiz Ice Cap, northern Ellesmere Island, Canada. “Melt” indicates the fraction of each core
 2433 section that contains evidence of melting (from Koerner and Fisher, 1990). Middle panel:

2434 Estimated summer temperature anomalies in central Sweden. Black bars, elevation of ^{14}C - dated
2435 sub-fossil pine wood samples (*Pinus sylvestris* L.) in the Scandes Mountains, central Sweden,
2436 relative to temperatures at the modern pine limit in the region. Dashed line, upper limit of pine
2437 growth is indicated by the dashed line. Changes in temperature estimated by assuming a lapse
2438 rate of $6\text{ }^{\circ}\text{C km}^{-1}$ (from Dahl and Nesje, 1996, ; based on samples collected by L. Kullman and
2439 by G. and J. Lundqvist). Lower panel: Paleotemperature reconstruction from oxygen isotopes in
2440 calcite sampled along the growth axis of a stalagmite from a cave at Mo i Rana, northern
2441 Norway. Growth ceased around A.D. 1750 (from Lauritzen 1996; Lauritzen and Lundberg 1998;
2442 2002). Figure from Bradley (2000).

2443

2444



2445

2446

2447

2448

2449

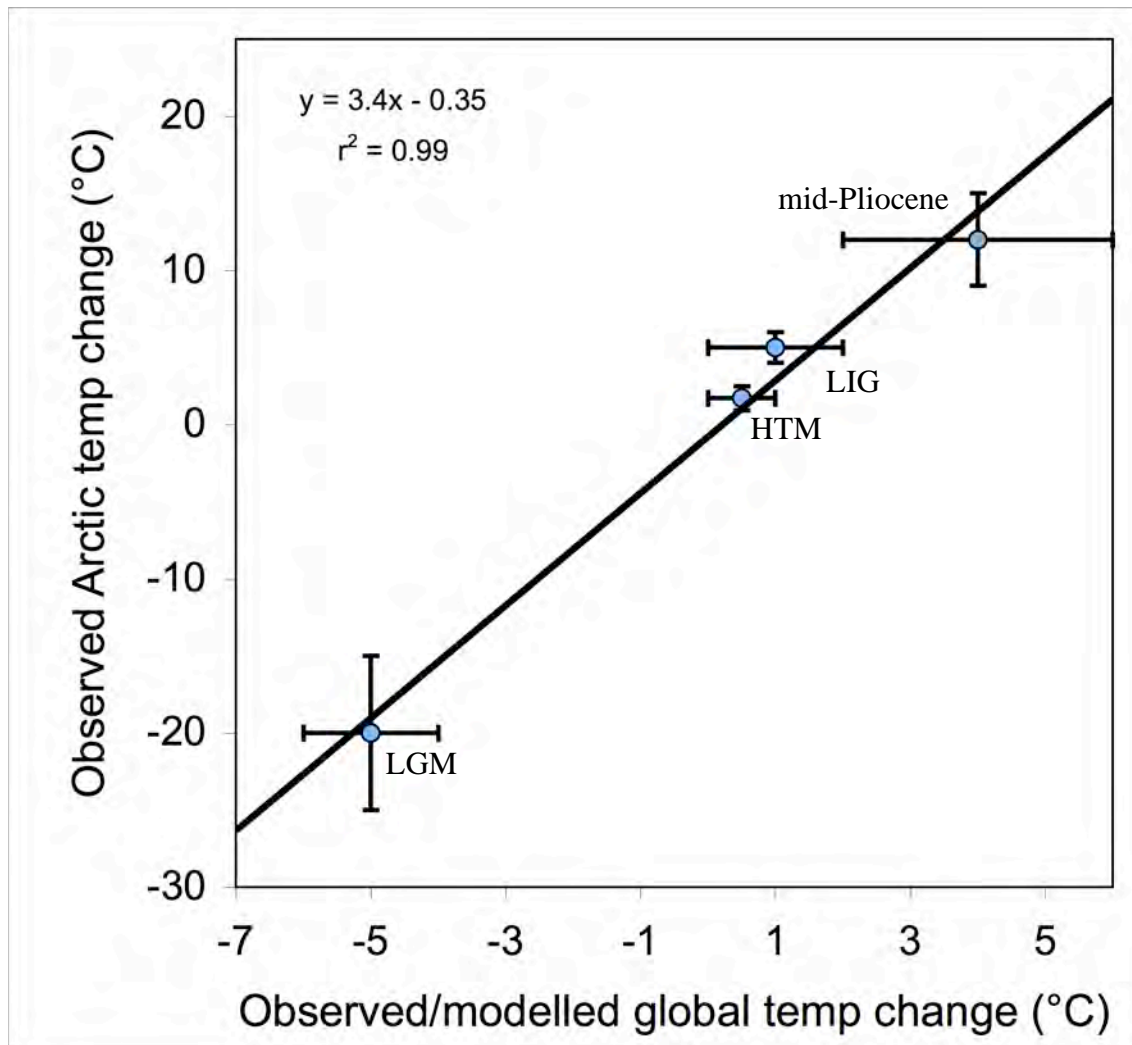
2450

2451

2452

Figure 4.35. Updated composite proxy-data reconstruction of Northern Hemisphere temperatures for most of the last 2000 years, compared with other published reconstructions. Estimated confidence limits, 95%. All series have been smoothed with a 40-year lowpass filter. The Medieval Climate Anomaly (MCA), about 950–1200 AD. The array of reconstructions demonstrate that the warming documented by instrumental data during the past few decades exceeds that of any warm interval of the past 2000 years, including that estimated for the MCA.

2453 (Figure from Mann et al. (in press). CPS, composite plus scale methodology; CRU, East Anglia
2454 Climate Research unit, a source of instrumental data; EIV, error-in-variables); HAD, Hadley
2455 Climate Center.



2456

2457

Figure 4.36 Paleoclimate data quantify the magnitude of Arctic amplification. Shown

2458

are paleoclimate estimates of Arctic summer temperature anomalies relative to recent, and the

2459

appropriate Northern Hemisphere or global summer temperature anomalies, together with their

2460

uncertainties, for the following: the last glacial maximum (LGM; about 20 ka), Holocene thermal

2461

maximum (HTM; about 8 ka), last interglaciation (LIG; 130–125 ka ago) and middle Pliocene

2462

(about 3.5–3.0 Ma). The trend line suggests that summer temperature changes are amplified 3 to

2463

4 times in the Arctic. Explanation of data sources follows, for the different times for each time

2464

considered, beginning with the most recent.

2465 **Holocene Thermal Maximum (HTM):** Arctic $\Delta T = 1.7 \pm 0.8^{\circ}\text{C}$; Northern Hemisphere
2466 $\Delta T = 0.5 \pm 0.3^{\circ}\text{C}$; Global $\Delta T = 0^{\circ} \pm 0.5^{\circ}\text{C}$.

2467 A recent summary of summer temperature anomalies in the western Arctic (Kaufman et
2468 al., 2004) built on earlier summaries (Kerwin et al., 1999; CAPE Project Members, 2001) and is
2469 consistent with more-recent reconstructions (Kaplan and Wolfe, 2006; Flowers et al., 2007).
2470 Although the Kaufman et al. (2004) summary considered only the western half of the Arctic, the
2471 earlier summaries by Kerwin et al., (1999) and CAPE Project Members (2001) indicated that
2472 similar anomalies characterized the eastern Arctic, and all syntheses report the largest anomalies
2473 in the North Atlantic sector. Although few data are available for the central Arctic Ocean, the
2474 circumpolar dataset provides an adequate reflection of air temperatures over the Arctic Ocean as
2475 well.

2476 Climate models suggest that the average planetary anomaly was concentrated over the
2477 Northern Hemisphere. Braconnot et al. (2007) summarized the simulations from 10 different
2478 climate model contributions to the PMIP2 project that compared simulated summer temperatures
2479 at 6 ka with recent temperatures. The global average summer temperature anomaly at 6 ka was
2480 $0^{\circ} \pm 0.5^{\circ}\text{C}$, whereas the Northern Hemisphere anomaly was $0.5^{\circ} \pm 0.3^{\circ}\text{C}$. These patterns are
2481 similar to patterns in model results described by Hewitt and Mitchell (1998) and Kitoh and by
2482 Murakami (2002) for 6 ka, and a global simulation for 9 ka (Renssen et al., 2006). All simulate
2483 little difference in summer temperature outside the Arctic when those temperatures are compared
2484 to with pre-industrial temperatures.

2485 **Last Glacial Maximum (LGM):** Arctic $\Delta T = 20^{\circ} \pm 5^{\circ}\text{C}$; global and Northern
2486 Hemisphere $\Delta T = -5^{\circ} \pm 1^{\circ}\text{C}$

2487 Quantitative estimates of temperature reductions during the peak of the Last Glacial
2488 Maximum are less widespread in for the Arctic than are estimates of temperatures during warm
2489 times. Ice-core borehole temperatures, which offer the most compelling evidence (Cuffey et al.,
2490 1995; Dahl-Jensen et al., 1998), are supported by evidence from biological proxies in the North
2491 Pacific sector (Elias et al., 1996a), where no ice cores are available that extend back to the Last
2492 Glacial Maximum. Because of the limited datasets for temperature reduction in the Arctic during
2493 the Last Glacial Maximum, a large uncertainty is specified. The global-average temperature
2494 decrease during peak glaciations, based on paleoclimate proxy data, was 5° – 6°C , and little
2495 difference existed between the Northern and Southern Hemispheres (Farrera et al., 1999;
2496 Braconnot et al., 2007; Braconnot et al., 2007). A similar temperature anomaly is derived from
2497 climate-model simulations (Otto-Bliesner et al., 2007).

2498 **Last Interglaciation (LIG):** Arctic $\Delta T = 5^{\circ} \pm 1^{\circ}\text{C}$; global and Northern Hemisphere ΔT
2499 $= 1^{\circ} \pm 1^{\circ}\text{C}$)

2500 A recent summary of all available quantitative reconstructions of summer-temperature
2501 anomalies for in the Arctic during peak Last Interglaciation warmth shows a spatial pattern
2502 similar to that shown by Holocene Thermal Maximum reconstructions. The largest anomalies are
2503 in the North Atlantic sector and the smallest anomalies are in the North Pacific sector, but those
2504 small anomalies are substantially larger ($5^{\circ} \pm 1^{\circ}\text{C}$) than they were during the Holocene Thermal
2505 Maximum (CAPE Last Interglacial Project Members, 2006). A similar pattern of Last
2506 Interglaciation summer-temperature anomalies is apparent in climate model simulations (Otto-
2507 Bliesner et al., 2006). Global and Northern Hemisphere summer-temperature anomalies are
2508 derived from summaries in CLIMAP Project Members (1984), Crowley (1990), Montoya et al.
2509 (2000), and Bauch and Erlenkeuser (2003).

2510 **Middle Pliocene:** Arctic $\Delta T = 12^{\circ} \pm 3^{\circ}\text{C}$; global $\Delta T = 4^{\circ} \pm 2^{\circ}\text{C}$)
2511 Widespread forests throughout the Arctic in the middle Pliocene offer a glimpse of a
2512 notably warm time in the Arctic, which had essentially modern continental configurations and
2513 connections between the Arctic Ocean and the global ocean. Reconstructed Arctic temperature
2514 anomalies are available from several sites that show much warmth and no summer sea ice in the
2515 Arctic Ocean basin. These sites include the *Canadian Arctic Archipelago* (Dowsett et al., 1994;
2516 Elias and Matthews, 2002; Ballantyne et al., 2006), Iceland (Buchardt and Símónarson, 2003),
2517 and the North Pacific (Heusser and Morley, 1996). A global summary of mid-Pliocene biomes
2518 by Salzmán et al. (2008) concluded that Arctic mean-annual-temperature anomalies were in
2519 excess of 10°C ; some sites indicate temperature anomalies of as much as 15°C . Estimates of
2520 global sea-surface temperature anomalies are from Dowsett (2007).

2521 Global reconstructions of mid-Pliocene temperature anomalies from proxy data and
2522 general circulation models show modest warming (average, $4^{\circ} \pm 1^{\circ}\text{C}$) across low to middle
2523 latitudes (Dowsett et al., 1999; Raymo et al., 1996; Sloan et al., 1996, Budyko et al., 1985;
2524 Haywood and Valdes, 2004; Jiang et al., 2005; Haywood and Valdes, 2006; Salzmán et al.,
2525 2008).

2526

2527

2527 **Chapter 4 References**

2528

2529 **Abbott, M.B., B.P. Finney, M.E. Edwards, and K.R. Kelts, 2000:** Lake-level reconstructions and
2530 paleohydrology of Birch Lake, central Alaska, based on seismic reflection profiles
2531 and core transects. *Quaternary Research*, **53**, 154-166.

2532

2533 **ACIA, 2005:** *Arctic Climate Impact Assessment*. Cambridge University Press, Cambridge, U.K.,
2534 1042 pp.

2535

2536 **Adkins, J.F., E.A. Boyle, L.D. Keigwin, E. Cortijio, 1997.:** Variability of the North Atlantic
2537 thermohaline circulation during the last interglacial period. *Nature*, **390**, 154-156.

2538

2539 **Ager, T.A. and L.B. Brubaker, 1985:** Quaternary palynology and vegetation history of Alaska.
2540 In: *Pollen Records of Late-Quaternary North American Sediments*, [Bryant, V.M.,
2541 Jr. and R.G. Holloway, (eds.)]. American Association of Stratigraphic
2542 Palynologists, Dallas, pp. 353-384.

2543

2544 **Aksu, A.E., 1985:** Planktonic foraminiferal and oxygen isotope stratigraphy of CESAR cores
2545 102 and 103—Preliminary results. In: *Initial geological report on CESAR—The*
2546 *Canadian Expedition to Study the Alpha Ridge, Arctic Ocean* [Jackson, H.R., P.J.
2547 Mudie, and S.M. Blasco (eds.)]. Geological Survey of Canada Paper 84-22, pp. 115-
2548 124.

2549

2550 **Alfimov, A.V., D.I. Berman, and A.V. Sher, 2003:** Tundra **Tundra**-steppe insect assemblages
2551 and the reconstruction of the Late Pleistocene climate in the lower reaches of the
2552 Kolyma River. *Zoologicheskii Zhurnal*, **82**, 281-300 (In Russian).

2553

2554 **Alley, R.B., 1991:** Deforming-bed origin for southern Laurentide till sheets? *Journal of*
2555 *Glaciology*, **37(125)**, 67-76.

2556

- 2557 **Alley, R.B.**, 2003: Paleoclimatic insights into future climate challenges. *Philosophical*
2558 *Transactions of the Royal Society of London, Series A*, **361(1810)**, 1831-1849.
2559
- 2560 **Alley, R.B.**, 2007: Wally was right: Predictive ability of the North Atlantic “conveyor belt”
2561 hypothesis for abrupt climate change. *Annual Review of Earth and Planetary*
2562 *Sciences*, **35**, 241-272.
2563
- 2564 **Alley, R.B.** and S. Anandakrishnan, 1995: Variations in melt-layer frequency in the GISP2 ice
2565 core: implications for Holocene summer temperatures in central Greenland. *Annals*
2566 *of Glaciology*, **21**, 64-70.
2567
- 2568 **Alley, R.B.** and A.M. Ágústsdóttir, 2005: The 8k event: Cause and consequences of a major
2569 Holocene abrupt climate change. *Quaternary Science Reviews*, **24**, 1123 -1149.
2570
- 2571 **Alley, R.B.**, E.J. Brook and S. Anandakrishnan, 2002: A northern lead in the orbital band:
2572 North-south phasing of ice-age events. *Quaternary Science Reviews*, **21(1-3)**, 431-
2573 441.
2574
- 2575 **Alley, R.B.** and K.M. Cuffey, 2001: Oxygen- and hydrogen-isotopic ratios of water in
2576 precipitation: Beyond paleothermometry. In: *Stable Isotope Geochemistry*, [Valley,
2577 J.W. and D. Cole (eds.)]. Mineralogical Society of America Reviews in Mineralogy
2578 and Geochemistry, **43**, , p. 527-553
2579
- 2580 **Alley, R.B.**, D.A. Meese, C.A. Shuman, A.J. Gow, K.C. Taylor, P.M. Grootes, J.W.C. White, M.
2581 Ram, E.D. Waddington, P.A. Mayewski, and G.A. Zielinski, 1993: Abrupt increase in
2582 snow accumulation at the end of the Younger Dryas event. *Nature*, **362**, 527-529.
2583
- 2584 **Alley, R.B.**, C.A. Shuman, D.A. Meese, A.J. Gow, K.C. Taylor, K.M. Cuffey, J.J. Fitzpatrick,
2585 P.M. Grootes, G.A. Zielinski, M. Ram, G. Spinelli, and B. Elder, 1997: Visual-
2586 stratigraphic dating of the GISP2 ice core—Basis, reproducibility, and application.
2587 *Journal of Geophysical Research*, **102**, 26,367-26,381.

- 2588
- 2589 **Ammann, C.M., F.Joos, D.S. Schimel, B.L. Otto-Bliesner, and .R.A. Tomas, 2007:** Solar
2590 influence on climate during the past millennium—Results from transient simulations
2591 with the NCAR Climate System Model. *Proceedings of the National Academy of*
2592 *Sciences, U.S.A.*, www.pnas.org/cgi/doi/10.1073/pnas.0605064103
- 2593
- 2594 **Andersen, K.K., A. Svensson, S. Johnsen, S.O. Rasmussen, M. Bigler, R. Rothlisberger, U.**
2595 **Ruth, M.L. Siggaard-Andersen, J.P. Steffensen, D. Dahl-Jensen, B.M. Vinther, and**
2596 **H.B. Clausen, 2006:** The Greenland Ice Core Chronology 2005, 15–42 kyr. Part I—
2597 Constructing the time scale. *Quaternary Science Reviews*, **25**, 3246-3257.
- 2598
- 2599 **Anderson, N.J. and M.J. Leng, 2004:** Increased aridity during the early Holocene in West
2600 Greenland inferred from stable isotopes in laminated-lake sediments. *Quaternary*
2601 *Science Reviews*, **23**, 841-849.
- 2602
- 2603 **Anderson, L., M.B. Abbott, and B.P. Finney, 2001:** Holocene climate inferred from oxygen
2604 isotope ratios in lake sediments, central Brooks Range, Alaska. *Quaternary Research*,
2605 **55**, 313-321.
- 2606
- 2607 **Anderson, L., M.B. Abbott, B.P. Finney, and S.J. Burns, 2005:** Regional atmospheric circulation
2608 change in the North Pacific during the Holocene inferred from lacustrine carbonate
2609 oxygen isotopes, Yukon Territory, Canada. *Quaternary Research*, **64**, 1-35.
- 2610
- 2611 **Anderson, P.M. and A.V. Lozhkin, 2001:** The stage 3 interstadial complex (Karginiskii/middle
2612 Wisconsinan interval) of Beringia: variations in paleoenvironments and implications
2613 for paleoclimatic interpretations. *Quaternary Science Reviews*, **20**, 93-125.
- 2614
- 2615 **Anderson, P.M., P.J. Bartlein, L.B. Brubaker, K. Gajewski, and J.C. Ritchie, 1989:** Modern
2616 analogues of late Quaternary pollen spectra from the western interior of North
2617 America. *Journal of Biogeography*, **16**, 573-596.
- 2618

- 2619 **Anderson, P.M., P.J. Bartlein, L.B. Brubaker, K. Gajewski, and J.C. Ritchie, 1991:** Vegetation-
2620 pollen-climate relationships for the arcto-borealboreal region of North America and
2621 Greenland. *Journal of Biogeography*, **18**, 565-582.
2622
- 2623 **Anderson, R.K., G.H. Miller, J.P. Briner, N.A. Lifton, and S.B. DeVogel, 2008:** A millennial
2624 perspective on Arctic warming from 14C in quartz and plants emerging from beneath
2625 ice caps. *Geophysical Research Letters*, **35**, L01502, doi:10.1029/2007GL032057.
2626
- 2627 **Andreev, A.A., D.M. Peteet, P.E. Tarasov, F.A. Romanenko, L.V. Filimonova, and L.D.**
2628 **Sulerzhitsky, 2001:** Late pleistocene interstadial environment on Faddeyevskiy
2629 Island, East-Siberian Sea, Russia. *Arctic, Antarctic, and Alpine Research*, **33**, 28-35.
2630
- 2631 **Andrews, J.T., L.M. Smith, R. Preston, T. Cooper, and A.E. Jennings, 1997:** Spatial and
2632 temporal patterns of iceberg rafting (IRD) along the East Greenland margin, ca. 68 N,
2633 over the last 14 cal ka. *Journal of Quaternary Science*, **12**, 1-13.
2634
- 2635 **Archer, D., 2007:** Methane hydrate stability and anthropogenicanthropogenic climate change.
2636 *Biogeosciences*, **4**,521-544
2637
- 2638 **Arctic Climate Impact Assessment (ACIA), 2004:** *Impacts of a Warming Arctic—Arctic*
2639 *Climate Impact Assessment*. Cambridge University Press, Cambridge, U.K., 1042 pp.
2640
- 2641 **Arctic Monitoring and Assessment Programme (AMAP), 1998:** *AMAP Assessment Report*
2642 *Arctic Pollution Issues*. AMAP, Oslo, Norway, 871 pp.
2643
- 2644 **Astakhov, V.I., 1995:** The mode of degradation of Pleistocene permafrost in West Siberia.
2645 *Quaternary International*, **28**, 119-121.
2646
- 2647 **Backman, J., M. Jakobsson, R. Løvlie, L. Polyak, and L.A. Febo, 2004:** Is the central Arctic
2648 Ocean a sediment starved basin? *Quaternary Science Reviews*, **23**, 1435-1454.
2649

- 2650 **Backman, J.**, K. Moran, D.B. McInroy, L.A. Mayer, and the Expedition 302 scientists, 2006:
2651 *Proceedings of IODP, 302*. Edinburgh (Integrated Ocean Drilling Program
2652 Management International, Inc.). doi:10.2204/iodp.proc.302.2006.
2653
- 2654 **Balco, G.**, C.W. Rovey, and O.H. Stone, 2005a: The First Glacial Maximum in North America.
2655 *Science*, **307**, 222.
2656
- 2657 **Balco, G.**, O.H. Stone, and C. Jennings, 2005b: Dating Plio-Pleistocene glacial sediments using
2658 the cosmic-ray-produced radionuclides ^{10}Be and ^{26}Al . *American Journal of Science*,
2659 **305**, 1-41.
2660
- 2661 **Ballantyne, A.P.**, N.L. Rybczynski, P.A. Baker, C.R. Harington, and D. White, 2006: Pliocene
2662 Arctic temperature constraints from the growth rings and isotopic composition of
2663 fossil larch. *Palaeogeography, Palaeoclimatology, Palaeoecology*, **242**, 188-200
2664
- 2665 **Barber, V.A.** and B.P. Finney, 2000: Lake Quaternary paleoclimatic reconstructions for interior
2666 Alaska based on paleolake-level data and hydrologic models. *Journal of*
2667 *Paleolimnology*, **24**, 29-41.
2668
- 2669 **Bard, E.**, 2002: Climate shocks—Abrupt changes over millennial time scales. *Physics Today*,
2670 **December**, 32-38.
2671
- 2672 **Barley, E.M.**, I.R. Walker, and J. Kurek, L.C. Cwynar, R.W. Mathewes, K. Gajewski, and B.P.
2673 Finney, 2006: A northwest North American training set—Distribution of freshwater
2674 midges in relation to air temperature and lake depth. *Journal of Paleolimnology*, **36**,
2675 295-314.
2676
- 2677 **Barnekow, L.** and P. Sandgren, 2001: Palaeoclimate and tree-line changes during the Holocene
2678 based on pollen and plant macrofossil records from six lakes at different altitudes in
2679 northern Sweden. *Review of Palaeobotany and Palynology*, **117**, 109-118.
2680

- 2681 **Barron, E.J., P.J. Fawcett, D. Pollard, and S. Thompson, 1993:** Model simulations of cretaceous
2682 climates - the role of geography and carbon-dioxide. *Philosophical Transactions of*
2683 *the Royal Society of London Series B-Biological Sciences*, **341(1297)**, 307-315.
2684
- 2685 **Barron, E.J., P.J. Fawcett, W.H. Peterson, D. Pollard, and S.L. Thompson, 1995:** A
2686 “simulation” of mid-Cretaceous climate. *Paleoceanography*, **8**, 785-798.
2687
- 2688 **Barry, R.G., M.C. Serreze, J.A. Maslanik, and R.H. Preller, 1993:** The arctic sea-ice climate
2689 system — observations and modeling. *Reviews of Geophysics*, **31(4)**, 397-422.
2690
- 2691 **Bartlein, P.J., K.H. Anderson, P.M. Anderson, M.E. Edwards, C.J. Mock, R.S. Thompson, R.S.**
2692 **Webb, T. Webb, III, and C. Whitlock, 1998:** Paleoclimate simulations for North
2693 America over the past 21,000 years: features of the simulated climate and
2694 comparisons with paleoenvironmental data. *Quaternary Science Reviews*, **17**, 549–
2695 585.
2696
- 2697 **Bauch, D., J. Carstens, and G. Wefer, 1997:** Oxygen isotope composition of living
2698 *Neogloboquadrina pachyderma* (sin.) in the Arctic Ocean. *Earth and Planetary*
2699 *Science Letters*, **146**, 47-58.
2700
- 2701 **Bauch, D., P. Schlosser, and R.G. Fairbanks, 1995:** Freshwater balance and the sources of deep
2702 and bottom waters in the Arctic Ocean inferred from the distribution of H₂¹⁸O.
2703 *Progress in Oceanography*, **35**, 53-80.
2704
- 2705 **Bauch, H.A., H. Erlenkeuser, K. Fahl, R.F. Spielhagen, M.S. Weinelt, H. Andruleit, and R.**
2706 **Henrich, 1999:** Evidence for a steeper Eemian than Holocene sea surface temperature
2707 gradient between Arctic and sub-Arctic regions. *Palaeogeography,*
2708 *Palaeoclimatology, Palaeoecology*, **145**, 95-117.
2709

- 2710 **Bauch, H.A., H. Erlenkeuser, J.P. Helmke, and U. Struck, 2000:** A paleoclimatic evaluation of
2711 marine oxygen isotope stage 11 in the high-northern Atlantic (Nordic seas). *Global*
2712 *and Planetary Change*, **24**, 27-39.
- 2713
- 2714 **Bauch, H.A. and H. Erlenkeuser, 2003:** Interpreting Glacial-Interglacial Changes in Ice Volume
2715 and Climate From Subarctic Deep Water Foraminiferal $\delta^{18}O$. In: *Earth's Climate and*
2716 *Orbital Eccentricity: The Marine Isotope Stage 11 Question*. [Droxler, A.W., R.Z.
2717 Poore, and L.H. Burckle (eds.)]. Geophysical Monograph Series, **137**.
- 2718
- 2719 **Bauch, H.A. and E.S. Kandiano, 2007:** Evidence for early warming and cooling in North
2720 Atlantic surface waters during the last interglacial. *Paleoceanography*, **22**, PA1201,
2721 doi:10.1029/2005PA001252.
- 2722
- 2723 **Beget, J.E., 2001:** Continuous Late Quaternary proxy climate records from loess in Beringia.
2724 *Quaternary Science Reviews* 20, 499-507.
- 2725
- 2726 **Behl, R.J., and J.P. Kennett, 1996:** Brief interstadial events in the Santa Barbara Basin, NE
2727 Pacific, during the past 60 kyr. *Nature*, **379**, 243-246.
- 2728
- 2729 **Bennike, O., K.P. Brodersen, E. Jeppesen, and I.R. Walker, 2004:** Aquatic invertebrates and
2730 high latitude paleolimnology. In: *Long-Term Environmental Change in Arctic and*
2731 *Antarctic Lakes* [Pienitz, R., M.S.V. Douglas, and J.P. Smol (eds.)]. Springer,
2732 Dordrecht, pp. 159-186.
- 2733
- 2734 **Berger, A. and M.F. Loutre, 1991:** Insolation values for the climate of the last million years.
2735 *Quaternary Sciences Review*, **10(4)**, 297-317.
- 2736 **Berger, A. and M.F. Loutre, 2002:** An Exceptionally long Interglacial Ahead? *Science*, **297**,
2737 1287-1288.
- 2738
- 2739 **Berger, A., M.F. Loutre, and J. Laskar, 1992:** Stability of the Astronomical Frequencies Over
2740 the Earth's History for Paleoclimate Studies. *Science*, **255(5044)**, 560-566.

2741

2742 **Berner, R.A.**, and Z. Kothavala, 2001: GEOCARB III: A revised model of atmospheric CO₂
 2743 over Phanerozoic time. *American Journal of Science*, **301(2)**, 182-204.

2744

2745 **Bice, K.L.**, D. Birgel, P.A. Meyers, K.A. Dahl, K.U. Hinrichs, and R.D. Norris, 2006: A
 2746 multiple proxy and model study of Cretaceous upper ocean temperatures and
 2747 atmospheric CO₂ concentrations. *Paleoceanography*, **21(2)**, PA2002.

2748

2749 **Bigelow, N.**, L.B. Brubaker, M.E. Edwards, S.P. Harrison, I.C. Prentice, P.M. Anderson, A.A.
 2750 Andreev, P.J. Bartlein, T.R. Christensen, W. Cramer, J.O. Kaplan, A.V. Lozhkin,
 2751 N.V. Matveyeva, D.F. Murrery, A.D. McGuire, V.Y. Razzhivin, J.C. Ritchie, B.
 2752 Smith, D.A. Walker, K. Gajewski, V. Wolf, B.H. Holmqvist, Y. Igarashi, K.
 2753 Kremenetskii, A. Paus, M.F.J. Pisaric, and V.S. Volkova, 2003: Climate change and
 2754 Arctic ecosystems—1. Vegetation changes north of 55°N between the last glacial
 2755 maximum, mid-Holocene, and present. *Journal of Geophysical Research*, **108**,
 2756 doi:10.1029/2002JD002558.

2757

2758 **Bigler, C.** and R.I. Hall, 2003: Diatoms as quantitative indicators of July temperature—A
 2759 validation attempt at century-scale with meteorological data from northern Sweden.
 2760 *Palaeogeography, Palaeoclimatology, Palaeoecology*, **189**, 147-160.

2761

2762 **Bintanja, R.** and R.S.W. van de Wal, 2008: North American ice-sheet dynamics and the onset
 2763 of 100,000-year glacial cycles. *Nature*, **454**, 869-872. doi:10.1038/nature07158

2764

2765 **Birks, H.H.**, 1991: Holocene vegetational history and climatic change in west Spitzbergen—
 2766 Plant macrofossils from Skardtjorna, an arctic lake. *The Holocene*, **1**, 209–218.

2767

2768 **Birks, H.J.B.**, 1998: Numerical tools in palaeolimnology—Progress, potentialities, and
 2769 problems. *Journal of Paleolimnology*, **20**, 307-332.

2770

- 2771 **Björk, G., J. Soöderkvist, P. Winsor, A. Nikolopoulos, and M. Steele, 2002:** Return of the cold
2772 halocline layer to the Amundsen Basin of the Arctic Ocean—Implications for the sea
2773 ice mass balance. *Geophysical Research Letters*, **29(11)**, 1513,
2774 doi:10.1029/2001GL014157.
2775
- 2776 **Boellstorff, J., 1987:** North American Pleistocene stages reconsidered in light of probably
2777 Pliocene-Pleistocene continental glaciation. *Science*, **202(2004365)**, 305-307.
2778
- 2779 **Bonan, G.B., D. Pollard, and S.L. Thompson, 1992:** Effects of boreal**boreal** forest vegetation on
2780 global climate. *Nature*, **359(6397)**, 716-718.
2781
- 2782 **Boyd, T.J., M. Steel, R.D. Muench, and J.T. Gunn, 2002:** Partial recovery of the Arctic Ocean
2783 halocline. *Geophysical Research Letters*, **29(14)**, 1657, doi:10.1029/2001GL014047
2784
- 2785 **Box, J.E., D.H. Bromwich, B.A. Veenhuis, L.S. Bai, J.C. Stroeve, J.C. Rogers, K. Steffen, T.**
2786 **Haran, and S.H. Wang, 2006:** Greenland ice sheet surface mass balance variability
2787 (1988-2004) from calibrated polar MM5 output. *Journal of Climate*, **19(12)**, 2783-
2788 2800
2789
- 2790 **Braconnot, P., B. Otto-Bliesner, S. Harrison, F.S. Jousaume, J.-Y. Peterchmitt, A. Abe-Ouchi,**
2791 **M. Crucifix, E. Driesschaert, T. Fichefet, C.D. Hewitt, M. Kageyama, A. Kitoh, A.**
2792 **Laine, M.-F. Loutre, O. Marti, U. Merkel, G. Ramstein, P. Valdes, S.L. Weber, Y.**
2793 **Yu, and Y. Zhao, 2007:** Results of PMIP2 coupled simulations of the Mid-
2794 Holocene and Last Glacial Maximum – Part 1: experiments and large-scale features.
2795 *Climates of the Past*, **3**, 261– 277.
2796
- 2797 **Bradley, R.S., 1990:** Holocene paleoclimatology of the Queen Elizabeth Islands, Canadian high
2798 Arctic. *Quaternary Science Reviews*, **9**, 365-384.
2799
- 2800 **Bradley, R.S., 1999:** *Paleoclimatology: reconstructing climates of the Quaternary* (second
2801 edition), Academic Press, New York, 613 pp.

2802

2803 **Bradley, R. S.**, 2000: Past global changes and their significance for the future. *Quaternary*
2804 *Science Reviews*, **19**, 391-402.

2805

2806 **Bradley, R.S., K.R. Briffa, J. Cole, and T.J. Osborn**, 2003a: The climate of the last millennium.
2807 In: *Paleoclimate, Global Change and the Future*, [Alverson, K.D., R.S. Bradley, and
2808 T.F. Pedersen (eds.)]. Springer, Berlin, pp. 105-141.

2809

2810 **Bradley, R.S., Hughes, M.K., and Diaz, H.F.**, 2003b: Climate in Medieval Time. *Science*, **302**,
2811 404-405, doi: 10.1126/science.1090372.

2812

2813 **Bradley, R.S. and P.D. Jones (eds.)**, 1992: *Climate Since AD 1500*. Routledge, London. 677 pp.

2814

2815 **Brassell, S.C., G. Eglinton, I.T. Marlowe, U. Pflaumann, and M. Sarnthein**, 1986: Molecular
2816 stratigraphy—A new tool for climatic assessment. *Nature*, **320**, 129-133.

2817

2818 **Bray, P.J., S.P.E. Blockey, G.R. Coope, L.F. Dadswell, S.A. Elias, J.J. Lowe, and A.M. Pollard**,
2819 2006: Refining mutual climatic range (MCR) quantitative estimates of
2820 paleotemperature using ubiquity analysis. *Quaternary Science Reviews*, **25(15-16)**,
2821 1865-1876.

2822

2823 **Brewer, S., J. Guiot, and F. Torre**, 2007: Mid-Holocene climate change in Europe: a data-
2824 model comparison. *Climate of the Past*, **3**, 499-512.

2825

2826 **Briffa, K. and E. Cook**, 1990: Methods of response function analysis In: *Methods of*
2827 *Dendrochronology* [Cook, E.R. and L.A. Kairiukstis (eds.)], sect. 5.6.

2828

2829 **Briffa, K.R., T.J. Osborn, F.H. Schweingruber, I.C. Harris, P.D. Jones, S.G. Shiyatov, and E.A.**
2830 **Vaganov**, 2001: Low-frequency temperature variations from a northern tree ring
2831 density network. *Journal of Geophysical Research*, **106**, 2929-2941.

2832

- 2833 **Brigham, J.K.**, 1985: *Marine stratigraphy and amino acid geochronology of the Gubik*
2834 *Formation, western Arctic Coastal Plain, Alaska*. Doctoral dissertation, University of
2835 Colorado, Boulder; U.S. Geological Survey Open-File Report 85-381, 21pp.
2836
- 2837 **Brigham-Grette, J.** and L.D. Carter, 1992: Pliocene marine transgressions of northern Alaska—
2838 Circumarctic correlations and paleoclimate. *Arctic*, **43(4)**, 74-89.
2839
- 2840 **Brigham-Grette, J.** and D.M. Hopkins, 1995: Emergent-marine record and paleoclimate of the
2841 last interglaciation along the northwest Alaskan coast. *Quaternary Research*, **43**, 154-
2842 173.
2843
- 2844 **Brigham-Grette, J.**, A.V. Lozhkin, P.M. Anderson, and O.Y. Glushkova, 2004:
2845 Paleoenvironmental conditions in western Beringia before and during the Last Glacial
2846 Maximum. In: *Entering America: Northeast Asia and Beringia Before the Last*
2847 *Glacial Maximum*,.[Madsen, D.B. (ed.)]. University of Utah Press, Chapter 2, pp. 29-
2848 61.
2849
- 2850 **Briner, J.P.**, N. Michelutti, D.R. Francis, G.H. Miller, Y. Axford, M.J. Wooller, and A.P. Wolfe,
2851 2006: A multi-proxy lacustrine record of Holocene climate change on northeastern
2852 Baffin Island. *Quaternary Research*, **65**, 431-442.
2853
- 2854 **Brinkhuis, H.**, S. Schouten, M.E. Collinson, A. Sluijs, J.S.S. Damsfte, G.R. Dickens, M. Huber,
2855 T.M. Cronin, J. Onodera, K. Takahashi, J.P. Bujak, R. Stein, J. van der Burgh, J.S.
2856 Eldrett, I.C. Harding, A.F. Lotter, F. Sangiorgi, H.V.V. Cittert, J.W. de Leeuw, J.
2857 Matthiessen, J. Backman, and K. Moran, (Expedition 302 Scientists), 2006: Episodic
2858 fresh surface waters in the Eocene Arctic Ocean. *Nature*, **441(7093)**, 606-609.
2859
- 2860 **Broecker, W.S.**, 2001: Was the Medieval Warm Period Global? *Science*, **291** (5508) 1497-
2861 1499, doi:10.1126/science.291.5508.1497
2862

- 2863 **Broecker**, W.S. and S. Hemming, 2001: Climate swings come into focus. *Nature*, **294:5550**
2864 2308-2309.
2865
- 2866 **Broecker**, W.S., D.M. Peteet, D. Rind, 1985: Does the ocean-atmosphere system have more than
2867 one stable mode of operation. *Nature*, **315(6014)**, 21-26.
2868
- 2869 **Brouwers**, E.M., 1987: On *Prerygocythereis vunnieuwenhusei* Brouwers sp.nov. In: *A stereo-*
2870 *atlas of ostracode shells*, [Bate, R.H., D.J. Home, J.W. Neale, and D.J. Siveter,
2871 [eds.]]. British Micropaleontological Society, London 14, Part **1**,17-20.
2872
- 2873 **Brown**, J. and V. Romanovsky, 2008: Report from the International Permafrost Association:
2874 State of Permafrost in the First Decade of the 21st Century. Permafrost and
2875 Periglacial Processes. *Permafrost and Periglacial Processes*, **19(2)**, 255-260.
2876
- 2877 **Buchardt**, B. and L.A. Símónarson, 2003: Isotope palaeotemperatures from the Tjörnes beds in
2878 Iceland: evidence of Pliocene cooling. *Palaeogeography, Palaeoclimatology,*
2879 *Palaeoecology* ,**189**, 71-95.
2880
- 2881 **Budyko**, M.I., A.B. Ronov, and A.L. Yanshin, 1985: *The History of the Earth's Atmosphere.*
2882 Leningrad, Gidrometeoirdat, 209 pp. (In Russian; English translation: Springer,
2883 Berlin, 1987, 139 pp.
2884
- 2885 **Calkin**, P.E., 1988: Holocene glaciation of Alaska (and adjoining Yukon Territory, Canada).
2886 *Quaternary Science Reviews*, **7**, 159-184.
2887
- 2888 **CAPE Project Members**, 2001: Holocene paleoclimate data from the Arctic: testing models of
2889 global climate change. *Quaternary Science Reviews*, **20**, 1275-1287.
2890
- 2891 **CAPE–Last Interglacial Project Members**, 2006: Last Interglacial Arctic warmth confirms
2892 polar amplification of climate change. *Quaternary Science Reviews*, **25**, 1383-1400.
2893

- 2894 **Carter**, L.D., 1981: A Pleistocene sand sea on the Alaskan Arctic Coastal Plain. *Science*,
2895 **211(4480)**, 381-383.
2896
- 2897 **Carter**, L.D., J. Brigham-Grette, L. Marincovich, Jr., V.L. Pease, and U.S. Hillhouse, 1986: Late
2898 Cenozoic Arctic Ocean sea ice and terrestrial paleoclimate. *Geology*, **14**, 675-678.
2899
- 2900 **Chapin**, F.S. III, M. Sturm, M.C. Serreze, J.P. Mcfadden, J.R. Key, A.H. Lloyd, T.S. Rupp, A.H.
2901 Lynch, J.P. Schimel, J. Beringer, W.L. Chapman, H.E. Epstein, E.S. Euskirchen, L.D.
2902 Hinzman, G. Jia, C.L. Ping, K.D. Tape, C.D.C. Thompson, D.A. Walker, and J.M.
2903 Welker, 2005: Role of land-surface changes in Arctic summer warming. *Science*, **310**,
2904 657-660.
2905
- 2906 **Chapman**, M.R., N.J. Shackleton, and J.-C. Duplessy, 2000: Sea surface temperature variability
2907 during the last glacial-interglacial cycle—Assessing the magnitude and pattern of
2908 climate change in the North Atlantic. *Palaeogeography, Palaeoclimatology,*
2909 *Palaeoecology*, **157**, 1-25.
2910
- 2911 **Chapman**, W.L. and J.E. Walsh, 2007: Simulations of Arctic temperature and pressure by global
2912 coupled models. *Journal of Climate*, **20(4)**, 609-632.
2913
- 2914 **Clark**, P.U. and D. Pollard, 1998: Origin of the Middle Pleistocene transition by ice sheet
2915 erosion of regolith. *Paleoceanography*, **13**, 1-9.
2916
- 2917 **Clark**, P.U., D. Archer, D. Pollard, J.D. Blum, J.A. Rial, V. Brovkin, A.C. Mix, N.G. Pisias, and
2918 M. Roy, 2006: The middle Pleistocene transition: characteristics, mechanisms, and
2919 implications for long-term changes in atmospheric pCO₂. *Quaternary Science*
2920 *Reviews*, **25**, 3150-3184.
2921
- 2922 **Clayden**, S.L., L.C. Cwynar, G.M. MacDonald, and A.A. Velichko, 1997: Holocene pollen and
2923 stomates from a forest-tundra site on the Taimyr Peninsula, Siberia. *Arctic and*
2924 *Alpine Research*, **29**, 327-333.

- 2925
- 2926 Climate Long-Range Investigation Mapping and Prediction (**CLIMAP**) Project Members, 1981:
2927 Seasonal reconstructions of the Earth's surface at the last glacial maximum.
2928 *Geological Society of America Map and Chart Series MC-36*, p. 1-18
2929
- 2930 Climate Long-Range Investigation Mapping and Prediction (**CLIMAP**) Project Members, 1984:
2931 The last interglacial ocean. *Quaternary Research*, **21**, 123-224.
2932
- 2933 **Cockford**, S.J. and S.G. Frederick, 2007: Sea ice expansion in the Bering Sea during the
2934 Neoglacial—Evidence from archeozoology. *The Holocene*, **17**, 699-706.
2935
- 2936 **Cohen**, A.S., 2003: *Paleolimnology—The history and evolution of lake systems*. Oxford
2937 University Press, Oxford, U.K., 528 pp.
2938
- 2939 **Colinvaux**, P.A., 1964: The environment of the Bering Land Bridge. *Ecological Monographs*,
2940 **34**, 297-329.
2941
- 2942 **Conte**, M.H., M. Sicre, C. Rühlemann, J.C. Weber, S. Schulte, D. Schulz-Bull, and T. Blanz,
2943 2006: Global temperature calibration of the alkenone unsaturation index (UK'₃₇) in
2944 surface waters and comparison with surface sediments. *Geochemistry, Geophysics,*
2945 *Geosystems*, **7**, Q02005, doi:10.1029/2005GC001054.
2946
- 2947 **Cronin**, T.M, G.S. Dwyer, T. Kamiyac, S. Schwedea, and D.A. Willarda, 2003: Medieval
2948 Warm Period, Little Ice Age and 20th century temperature variability from
2949 Chesapeake Bay. *Global and Planetary Change*, **36**, 17-29
2950
- 2951 **Crowley**, T.J., 1998: Significance of tectonic boundary conditions for paleoclimate simulations.
2952 In: *Tectonic Boundary Conditions for Climate Reconstructions* [Crowley, T.J., and
2953 K.C. Burke (eds.)]. Oxford University Press, New York, pp. 3-17.
2954

- 2955 **Crowley, T.J.**, 1990: Are there any satisfactory geologic analogs for a future greenhouse
2956 warming? *Journal of Climatology*, **3**, 1282-1492.
2957
- 2958 **Crowley, T.J.**, 2000: Causes of climate change over the past 1000 years. *Science*, **289**, 270-277.
2959
- 2960 **Crowley, T.J.**, S.K. Baum, K.Y. Kim, G.C. Hegerl, and W.T. Hyde, 2003: Modeling ocean heat
2961 content changes during the last millennium. *Geophysical Research Letters*, **30**, 1932,
2962 doi:10.1029/2003GL017801.
2963
- 2964 **Crowley, T.J.** and T. Lowery, 2000: How warm was the Medieval warm period? *Ambio*, **29**, 51-
2965 54.
2966
- 2967 **Cuffey, K.M.** and G.D. Clow, 1997: Temperature, accumulation, and ice sheet elevation in
2968 central Greenland through the last deglacial transition. *Journal of Geophysical*
2969 *Research*, **102(C12)**, 26,383-26,396.
2970
- 2971 **Cuffey, K.M.**, G.D. Clow, R.B. Alley, M. Stuiver, E.D. Waddington, and R.W. Saltus, 1995:
2972 Large Arctic temperature change at the Wisconsin-Holocene glacial transition.
2973 *Science*, **270**, 455-458.
2974
- 2975 **D'Arrigo, R.**, Wilson, R., Jacoby, G., 2006: On the long-term context for late twentieth century
2976 warming. *Journal of Geophysical Research*, **111**, D03103,
2977 doi:10.1029/2005JD006352.
2978
- 2979 **Dahe, Q.**, J.R. Petit, J. Jouzel, and M. Stievenard, 1994: Distribution of stable isotopes in surface
2980 snow along the route of the 1990 International Trans-Antarctic Expedition. *Journal of*
2981 *Glaciology*, **40**, 107-118.
2982
- 2983 **Dahl, S.O.** and A. Nesje, 1996: A new approach to calculating Holocene winter precipitation by
2984 combining glacier equilibrium-line altitudes and pine-tree limits: a case stud from

- 2985 Hardangerjokulen, central southern Norway. *The Holocene*, **6(4)**, 381-398,
2986 doi:10.1177/095968369600600401
2987
- 2988 **Dahl-Jensen**, D., K. Mosegaard, N. Gundestrup, G.D. Clow, S.J. Johnsen, A.W. Hansen, and N.
2989 Balling, 1998: Past temperature directly from the Greenland Ice Sheet. *Science*, **282**,
2990 268-271.
2991
- 2992 **Dansgaard**, W., 1964: Stable isotopes in precipitation. *Tellus*, **16**, 436-468.
2993
- 2994 **Dansgaard**, W., J.W.C. White, and S.J. Johnsen, 1989: The abrupt termination of the Younger
2995 Dryas climate event. *Nature*, **339(6225)**, 532-534.
2996
- 2997 **Delworth**, T.L., and T.R. Knutson, 2000: Simulation of early 20th century global warming.
2998 *Science*, **287(5461)**, 2246-225.
2999
- 3000 **de Vernal**, A., C. Hillaire-Marcel, and D.A. Darby, 2005: Variability of sea ice cover in the
3001 Chukchi Sea (western Arctic Ocean) during the Holocene. *Paleoceanography*, **20**,
3002 PA4018, doi:10.1029/2005PA001157.
3003
- 3004 **Denton**, G.H., R.B. Alley, G.C. Comer and W.S. Broecker, 2005: The role of seasonality in
3005 abrupt climate change. *Quaternary Science Reviews*, **24(10-11)**, 1159-1182.
3006
- 3007 **Digerfeldt**, G., 1988: Reconstruction and regional correlation of Holocene lake-level
3008 fluctuations in Lake Bysjön, South Sweden. *Boreas*, **17**, 237-263.
3009
- 3010 **Donnadieu**, Y., R. Pierrehumbert, R. Jacob, and F. Fluteau, 2006: Modeling the primary control
3011 of paleogeography on Cretaceous climate. *Earth and Planetary Science Letters*, **248**,
3012 426-437.
3013

- 3014 **Douglas, M.S.V.**, 2007: Environmental change at high latitudes. In: *Geological and*
3015 *Environmental Applications of the Diatom—Pond Scum to Carbon Sink* [Starratt,
3016 S.W. (ed.)]. The Paleontological Society Papers, **13**, 169-179.
3017
- 3018 **Douglas, M.S.V.** and J.P. Smol, 1994: Limnology of high arctic ponds (Cape Herschel,
3019 Ellesmere Island, N.W.T.). *Archiv für Hydrobiologie*, **131**, 401-434.
3020
- 3021 **Douglas, M.S.V.** and J.P. Smol, 1999: Freshwater diatoms as indicators of environmental change
3022 in the High Arctic. In: *The Diatoms—Applications for the Environment and Earth*
3023 *Sciences*, [Stoermer, E. and J.P. Smol (eds.)]. Cambridge University Press,
3024 Cambridge, U.K., 488 pp.
3025
- 3026 **Douglas, M.S.V.**, J.P. Smol, and W. Blake, Jr., 1994: Marked post-18th century environmental
3027 change in high Arctic ecosystems. *Science*, **266**, 416-419.
3028
- 3029 **Douglas, M.S.V.**, J.P. Smol, R. Pienitz, and P. Hamilton, 2004: Algal indicators of
3030 environmental change in arctic and antarctic lakes and ponds. In: *Long-Term*
3031 *Environmental Change in Arctic and Antarctic Lakes*, [Pienitz, R., M.S.V. Douglas,
3032 and J.P. Smol (eds.)]. Springer, Dordrecht. pp. 117-157.
3033
- 3034 **Dowdeswell, J.A.**, J.O. Hagen, H. Björnsson, A.F. Glazovsky, W.D. Harrison, P. Holmlund, J.
3035 Jania, R.M. Koerner, B. Lefauconnier, C.S.L. Ommanney, and R.H. Thomas, 1997:
3036 The mass balance of circum-Arctic glaciers and recent climate change. *Quaternary*
3037 *Research*, **48**, 1-14.
3038
- 3039 **Dowsett, H.J.**, 2007: The PRISM Palaeoclimate Reconstruction and Pliocene Sea-Surface
3040 Temperature. In: *Deep-time perspectives on climate change: marrying the signal*
3041 *from computer models and biological proxies*, [Williams, M., A.M. Haywood, F.J.
3042 Gregory, and D.N. Schmidt (eds.)] The Micropalaeontological Society, Special
3043 Publication, The Geological Society, London, pp. 459-480.
3044

- 3045 **Dowsett, H.J.** , J.A. Barron, R.Z. Poore, R.S. Thompson, T.M. Cronin, S.E. Ishman, S.E., D.A.
3046 Willard, 1999: Middle Pliocene paleoenvironmental reconstruction: PRISM2, U.S.
3047 Geological Survey Open File Report 99-535.
3048
- 3049 **Dowsett, H.J.**, and eight others, 1994: Joint investigations of the middle Pliocene climate I—
3050 PRISM paleoenvironmental reconstructions. *Global and Planetary Change*, **9**, 169-
3051 195
3052
- 3053 **Droxler, A.W.** and J.W. Farrell, 2000: Marine Isotope Stage 11 (MIS11): New insights for a
3054 warm future. *Global and Planetary Change*, **24(1)**, 1-5
3055
- 3056 **Droxler, A.W.**, R.B. Alley, W.R. Howard, R.Z. Poore and L.H. Burckle. 2003: Unique and
3057 exceptionally long interglacial marine isotope stage 11: Window into Earth future
3058 climate. In: *Earth's Climate and Orbital Eccentricity: The Marine Isotope Stage 11*
3059 *Question*, [Droxler, A.W., R.Z. Poore and L.H. Burckle (eds.)]. Geophysical
3060 Monograph, **137**, American Geophysical Union, pp. 1-14.
3061
- 3062 **Duk-Rodkin, A.**, R.W. Barendregt, D.G. Froese, F. Weber, R.J. Enkin, I.R. Smith, Grant D.
3063 Zazula, P. Waters, and R. Klassen, 2004: Timing and Extent of Plio-Pleistocene
3064 glaciations in North-Western Canada and East-Central Alaska. In: *Quaternary*
3065 *Glaciations-Extent and Chronology, Part II, North America*, [Ehlers, J. and P.L.
3066 Gibbard (eds.)]. Elsevier, New York, pp. 313-345.
3067
- 3068 **Dyke, A.S.** and J.M. Savelle, 2001: Holocene history of the Bering Sea bowhead whale (*Balaena*
3069 *mysticetus*) in its Beaufort Sea summer grounds off southwestern Victoria Island,
3070 western Canadian Arctic. *Quaternary Research*, **55**, 371-379.
3071
- 3072 **Dykoski, C.A.**, R.L. Edwards, H. Cheng, D. Yuan, Y. Cai, M. Zhang, Y. Lin, J. Qing, Z. An,
3073 and J. Revenaugh, 2005: A high-resolution, absolute-dated Holocene and deglacial
3074 Asian monsoon record from Dongge Cave, China. *Earth and Planetary Science*
3075 *Letters*, **233**, 71-86.

3076

3077 **Edwards, M.E., N.H. Bigelow, B.P. Finney, and W.R. Eisner, 2000:** Records of aquatic pollen
3078 and sediment properties as indicators of late-Quaternary Alaskan lake levels. *Journal*
3079 *of Paleolimnology*, **24**, 55-68.

3080

3081 **Elias, S.A., 2007:** Beetle records—Late Pleistocene North America. In: *Encyclopedia of*
3082 *Quaternary Science* [Elias, S.A. (ed.)]. Elsevier, Amsterdam, pp. 222-236.

3083

3084 **Elias, S.A., K. Anderson, and J.T. Andrews, 1996:** Late Wisconsin climate in the northeastern
3085 United States and southeastern Canada, reconstructed from fossil

3086

3087 **Elias, S.A., J.T. Andrews, and K.H. Anderson, 1999:** New insights on the climatic constraints on
3088 the beetle fauna of coastal Alaska derived from the mutual climatic range method of
3089 paleoclimate reconstruction. *Arctic, Antarctic, and Alpine Research*, **31**, 94-98.

3090

3091 **Elias, S.A. and J.V. Matthews, Jr., 2002:** Arctic North American seasonal temperatures in the
3092 Pliocene and Early Pleistocene, based on mutual climatic range analysis of fossil
3093 beetle assemblages. *Canadian Journal of Earth Sciences*, **39**, 911-920.

3094 beetle assemblages. *Journal of Quaternary Science*, **11**, 417-421.

3095

3096 **Ellis, J.M., and P.E. Calkin, 1984:** Chronology of Holocene glaciation, central Brooks Range,
3097 Alaska. *Geological Society of America Bulletin*, **95**, 897-912.

3098

3099 **Epstein, S., H. Buchsbaum, H. Lowenstam, and H.C. Urey, 1953:** Revised carbonate-water
3100 isotopic temperature scale. *Geological Society of America Bulletin*, **64**, 1315-1325.

3101

3102 **Erez, J. and B. Luz, 1982:** Temperature control of oxygen-isotope fractionation of cultured
3103 planktonic foraminifera. *Nature*, **297**, 220-222.

3104

- 3105 **Eronen, M., P. Zetterberg, K.R. Briffa, M. Lindholm, J. Meriläinen, and M. Timonen, 2002:**
3106 The supra-long Scots pine tree-ring record for Finnish Lapland: Part 1, chronology
3107 construction and initial inferences. *The Holocene*, **12(6)**, 673-680.
3108
- 3109 **Esper, J., E.R. Cook, and F.H. Schweingruber, 2002: Low-frequency signals in long tree-ring**
3110 chronologies for reconstructing past temperature variability. *Science*, **295**, 2250-
3111 2253.
3112
- 3113 **Esper, J. and F.H. Schweingruber, 2004: Large-scale treeline changes recorded in Siberia.**
3114 *Geophysical Research Letters*, **31**, L06202, doi:10.1029/2003GL019178.
3115
- 3116 **Fairbanks, R.G., 1989: A 17,000-year glacio-eustatic sea level record—Influence of glacial**
3117 melting rates on the Younger Dryas event and deep-ocean circulation. *Nature*, **343**,
3118 612-616.
3119
- 3120 **Farrera, I., S.P. Harrison, I.C. Prentice, G. Ramstein, J. Guiot, P.J. Bartlein, R. Bonnelle, M.**
3121 Bush, W. Cramer, U. von Grafenstein, K. Holmgren, H. Hooghiemstra, G. Hope, D.
3122 Jolly, S.-E. Lauritzen, Y. Ono, S. Pinot, M. Stute, and G. Yu, 1999: Tropical
3123 climates at the Last Glacial Maximum: a new synthesis of terrestrial palaeoclimate
3124 data. I. Vegetation, lake-levels and geochemistry. *Climate Dynamics*, **15**, 823-856.
3125
- 3126 **Finney, B., K. Rühland, J.P. Smol, and M.-A. Fallu, 2004: Paleolimnology of the North**
3127 American subarctic. In: *Long-Term Environmental Change in Arctic and Antarctic*
3128 *Lakes* [Pienitz, R., M.S.V. Douglas, and J.P. Smol (eds.)]. Springer, Dordrecht, pp.
3129 269-318.
3130
- 3131 **Fisher, D.A., 1979: Comparison of 100,000 years of oxygen isotope and insoluble impurity**
3132 profiles from the Devon Island and Camp Century ice cores. *Quaternary Research*,
3133 **11**, 299-304.
3134

- 3135 **Fisher, D.A.** and R.M. Koerner, 2003: Holocene ice core climate history, a multi-variable
 3136 approach. In: *Global Change in the Holocene*, [Mackay, A., R. Battarbee, J. Birks
 3137 and F. Oldfield, (eds.)] Arnold, London, pp. 281-293.
 3138
- 3139 **Fisher, D.A.,** R.M. Koerner, J.C. Bourgeois, G. Zielinski, C. Wake, C.U. Hammer, H.B.
 3140 Clausen, N. Gundestrup, S. Johnsen, K. Goto- Azuma, T. Hondoh, E. Blake, and M.
 3141 Gerasimoff, 1998: Penny Ice Cap cores, Baffin Island, Canada, and the Wisconsinan
 3142 Foxe Dome connection—Two states of Hudson Bay ice cover. *Science*, **279**, 692-695.
 3143
- 3144 **Fisher, D.A.,** C. Wake, K. Kreutz, K. Yalcin, E. Steig, P. Mayewski, L. Anderson, J. Aheng, S.
 3145 Rupper, C. Zdanowicz, M. Demuth, M. Waskiewicz, D. Dahl-Jensen, K. Goto-
 3146 Azuma, J.B. Bourgeois, R.M. Koerner, J. Sekerka, E. Osterberg, M.B. Abbott, B.P.
 3147 Finney, and S.J. Burns, 2004: Stable isotope records from Mount Logan, Eclipse ice
 3148 cores and nearby Jellybean Lake. Water cycle of the North Pacific over 2000 years
 3149 and over five vertical kilometres—Sudden shift and tropical connections. *Geographie*
 3150 *physique et Quaternaire*, **58**, 9033-9048.
 3151
- 3152 **Flowers, G.E.,** H. Björnsson, Á. Geirsdóttir, G.H. Miller, J.L. Black, and G.K.C. Clarke, 2008:
 3153 Holocene climate conditions and glacier variation in central Iceland from physical
 3154 modelling and empirical evidence. *Quaternary Science Reviews*, **27**, 797-813.
 3155
- 3156 **Francis, J.E.,** 1988: A 50-million-year-old fossil forest from Strathcona Fiord, Ellesmere Island,
 3157 Arctic Canada—Evidence for a warm polar climate. *Arctic*, **41(4)**, 314-318.
 3158
- 3159 **Fricke, H.C.** and J.R. O’Neil, 1999: The correlation between $^{18}\text{O}/^{16}\text{O}$ ratios of meteoric water
 3160 and surface temperature: its use in investigating terrestrial climate change over
 3161 geologic time. *Earth and Planetary Science Letters*, **170**, 181-196.
 3162
- 3163 **Fritts, H.C.,** 1976: *Tree Rings and Climate*. London Academic Press
 3164

3165 **Fronval**, T. and E. Jansen, 1997: Eemian and early Weichselian (140- 60 ka) paleoceanography
3166 and paleoclimate in the Nordic seas with comparisons to Holocene conditions.
3167 *Paleoceanography*, **12**, 443-462.

3168

3169 **Funder**, S., 1989: Quaternary geology of East Greenland. In: *Quaternary Geology of Canada*
3170 *and Greenland*, [Fulton, R.J. (ed.)]. Geological Society of America Decade of North
3171 American Geology, vol. **K1**, pp. 756-763.

3172

3173 **Funder**, S., O. Bennike, J. Böcher, C. Israelson, K.S. Petersen, and L.A. Simonarson, 2001: Late
3174 Pliocene Greenland—The Kap Kobenhavn Formation in North Greenland. *Bulletin of*
3175 *the Geological Society of Denmark*, **48**, 117-134.

3176

3177 **Funder**, S., I. Demidov, and Y. Yelovicheva, 2002: Hydrography and mollusc faunas of the
3178 Baltic and the White Sea-North Sea seaway in the Eemian. *Palaeogeography,*
3179 *Palaeoclimatology, Palaeoecology*, **184**, 275-304.

3180

3181 **Fyles**, J.G., L. Marinovich, Jr., J.V. Mathews, Jr., and R. Barendregt, 1991: Unique mollusc
3182 find in the Beaufort Formation (Pliocene) Meighen Island, Arctic Canada. In: *Current*
3183 *Research, Part B, Geological Survey of Canada, Paper 91-1B*, pp. 461-468.

3184

3185 **Gajewski**, K. and G.M. MacDonald, 2004: Palynology of North American Arctic Lakes. In:
3186 *Long Term Environmental Change in Arctic and Antarctic Lakes* [R. Pienitz, M.S.V.
3187 Douglas and J.P. Smol (eds.)]. Springer, Netherlands, pp. 89-116.

3188

3189 **Gard**, G., 1986: Calcareous nannofossil biostratigraphy north of 80° latitude in the eastern
3190 Arctic Ocean. *Boreas*, **15**, 217-229.

3191

3192 **Gard**, G., 1987: Late Quaternary calcareous nannofossil biostratigraphy and sedimentation
3193 patterns—Fram Strait, Arctica. *Paleoceanography*, **2**, 219-229.

3194

3195 **Gard**, G., 1993: Late Quaternary coccoliths at the North Pole—Evidence of ice-free conditions

- 3196 and rapid sedimentation in the central Arctic Ocean. *Geology*, **21**, 227-230.
- 3197
- 3198 **Geirsdottir**, A., Miller, G.H., Axford, Y. and Olafsdottir, S., in press, Holocene and latest
3199 Pleistocene climate and glacier fluctuations in Iceland. *Quaternary Science Reviews*.
3200
- 3201 **Gervais**, B.R., G.M. MacDonald, J.A. Snyder, and C.V. Kremenetski, 2002: *Pinus sylvestris*
3202 treeline development and movement on the Kola Peninsula of Russia—Pollen and
3203 stomate evidence. *Journal of Ecology*, **90**, 627-638.
3204
- 3205 **Goetcheus**, V.G., and H.H. Birks, 2001: Full-glacial upland tundra vegetation preserved
3206 under tephra in the Beringia National Park, Seward Peninsula, Alaska. *Quaternary*
3207 *Science Reviews*, **20(1-3)**, 135-147.
3208
- 3209 **Goetz**, S.J., M.C. Mack, K.R. Gurney, J.T. Randerson, and R.A. Houghton, 2007: Ecosystem
3210 responses to recent climate change and fire disturbance at northern high latitudes—
3211 Observations and model results contrasting northern Eurasia and North America.
3212 *Environmental Research Letters*, **2**, 045031, doi:10.1088/1748-9326/2/4/045031
3213
- 3214 **Goodfriend**, G.A., J. Brigham-Grette, G.H. Miller, 1996: Enhanced age resolution of the
3215 marine quaternary record in the Arctic using aspartic acid racemization dating of
3216 bivalve shells. *Quaternary Research*, **45**, 176-187
3217
- 3218 **Goosse**, H., H. Renssen, A. Timmermann, and R.A. Bradley, 2005: Internal and forced climate
3219 variability during the last millennium—A model-data comparison using ensemble
3220 simulations. *Quaternary Science Reviews*, **24**, 1345-1360.
3221
- 3222 **Gradstein**, F.M., J.G. Ogg, and A.G. Smith (eds.), 2004: *A Geologic Time Scale*. Cambridge
3223 University Press, Cambridge, 589 pp.
3224

- 3225 **Grice, K.**, W.C.M. Klein Breteler, S. Schoten, V. Grossi, J.W. de Leeuw, and J.S. Sinninge
3226 Damste, 1998: Effects of zooplankton herbivory on biomarker proxy records.
3227 *Paleoceanography*, **13**, 686-693.
3228
- 3229 **Grootes, P.M.**, M. Stuiver, J.W.C. White, S. Johnsen, and J. Jouzel, 1993: Comparison of
3230 oxygen isotope records from the GISP2 and GRIP Greenland Ice cores. *Nature*, **366**,
3231 522-555.
3232
- 3233 **Grove, J.M.**, 1988: *The Little Ice Age*. Methuen, London, 498 pp.
3234
- 3235 **Grudd, H.**, K.R. Briffa, W. Karlén, T.S. Bartholin, P.D. Jones, and B. Kromer, 2002: A 7400-
3236 year tree-ring chronology in northern Swedish Lapland—Natural climatic variability
3237 expressed on annual to millennial timescales. *The Holocene*, **12**, 657-666.
3238
- 3239 **Gudina, V.D.** Kryukov, L.K. Levchuk and L.A. Sudkov, 1983: Upper-Pleistocene sediments in
3240 north-eastern Taimyr. *Bulletin of Commission on Quaternary Researches*, **52**, 90-97
3241 (in Russian).
3242
- 3243 **Haerberli, W.**, G.D. Cheng, A.P. Gorbunov, and S.A. Harris, 1993: Mountain permafrost and
3244 climatic change. *Permafrost and Periglacial Processes*, **4(2)**, 165-174.
3245
- 3246 **Hammarlund, D.**, L. Barnekow, H.J.B. Birks, B. Buchardt, and T.W.D. Edwards, 2002:
3247 Holocene changes in atmospheric circulation recorded in the oxygen-isotope
3248 stratigraphy of lacustrine carbonates from northern Sweden. *The Holocene*, **12**, 339-
3249 351.
3250
- 3251 **Hannon, G.E.** and M.J. Gaillard, 1997: The plant-macrofossil record of past lake-level changes.
3252 *Journal of Paleolimnology*, **18**, 15-28.
3253
- 3254 **Hantemirov, R.M.** and S.G. Shiyatov, 2002: A continuous multi-millennial ring-width
3255 chronology in Yamal, northwestern Siberia. *The Holocene*, **12(6)**, 717-726.

3256

3257 **Harrison, S., P. Braconnot, C. Hewitt, and R.J. Stouffer, 2002:** Fourth International Workshop
3258 of the Palaeoclimate Modelling Inter- comparison Project (PMIP): Launching PMIP
3259 Phase Ii. *EOS*, **83**, 447-447.

3260

3261 **Harrison, S.P., D. Jolly, F. Laarif, A. Abe-Ouchi, B. Dong, K. Herterich, C. Hewitt, S.**
3262 **Joussaume, J.E. Kutzbach, J. Mitchell, N. de Noblet, and P. Valdes, 1998:**
3263 **Intercomparison of simulated global vegetation distributions in response to 6 kyr BP**
3264 **orbital forcing. *Journal of Climate*, **11**, 2721-2742.**

3265

3266 **Harrison, S.P., J.E. Kutzbach, I.C. Prentice, P.J. Behling, and M.T. Sykes, 1995:** The response
3267 of northern hemisphere extratropical climate and vegetation to orbitally induced
3268 changes in insolation during the last interglaciation. *Quaternary Research*, **43(2)**,
3269 174-184.

3270

3271 **Haywood, A.M., P. Dekens, A.C. Ravelo, and M. Williams, 2005:** Warmer tropics during the
3272 mid-Pliocene? Evidence from alkenone paleothermometry and a fully coupled
3273 ocean-atmosphere GCM. *Geochemistry, Geophysics, Geosystems*, **6**, Q03010,
3274 doi:10.1029/2004GC000799.

3275

3276 **Haywood, A.M. and P.J. Valdes, 2004:** Modeling Pliocene warmth: contribution of
3277 atmosphere, oceans and cryosphere. *Earth and Planetary Science Letters*, **218**, 363-
3278 377.

3279

3280 **Haywood, A.M. and P.J. Valdes, 2006:** Vegetation cover in a warmer world simulated using a
3281 dynamic global vegetation model for the Mid-Pliocene. *Palaeogeography,*
3282 *Palaeoclimatology, Palaeoecology*, **237**, 412-427.

3283

3284 **Helmke, J.P. and H.A. Bauch, 2003:** Comparison of glacial and interglacial conditions between
3285 the polar and subpolar North Atlantic region over the last five climatic cycles.
3286 *Paleoceanograph*, **18(2)**, 1036, doi:10.1029/2002PA000794

- 3287
- 3288 **Henrich** R. and K.-H. Baumann, 1994: Evolution of the Norwegian current and the
3289 Scandinavian ice sheets during the past 2.6 m.y.: evidence from ODP Leg 104
3290 biogenic carbonate and terrigenous records. *Palaeogeography, Palaeoclimatology,*
3291 *Palaeoecology*, **108**, 75-94.
- 3292
- 3293 **Herbert**, T.D., 2003: *Alkenone paleotemperature determinations*. In: *Treatise in Marine*
3294 *Geochemistry*, [Elderfield, H. and K.K. Turekian (eds.)]. Elsevier, Amsterdam, pp.
3295 391-432.
- 3296
- 3297 **Heusser**, L. and J. Morley, 1996: Pliocene climate of Japan and environs between 4.8 and 2.8
3298 Ma: a joint pollen and marine faunal study. *Marine Micropaleontology*, **27**, 85-106.
- 3299
- 3300 **Hewitt**, C.D. and J.F.B. Mitchell, 1998: A Fully Coupled GCM Simulation of the Climate of the
3301 Mid-Holocene. *Geophysical Research Letters*, **25**, 361-364.
- 3302
- 3303 **Hoffmann**, G., M. Werner, and M. Heimann, 1998: Water isotope module of the ECHAM
3304 atmospheric general circulation model—A study on timescales from days to several
3305 years. *Journal of Geophysical Research*, **103**, 16,871-16,896.
- 3306
- 3307 **Holland**, M.M. and C.M. Bitz, 2003: Polar amplification of climate change in coupled models.
3308 *Climate Dynamics*, **21**, 221-232.
- 3309
- 3310 **Holland**, M.H., C.M., Bitz, and B. Tremblay, 2006: Future abrupt reductions in the summer
3311 Arctic sea ice. *Geophysical Research Letters*, **33**, L23503,
3312 doi:10.1029/2006GL028024.
- 3313
- 3314 **Huber**, C., M. Leuenberger, R. Spahni, J. Flückiger, J. Schwander, T. F. Stocker, S. Johnsen, A.
3315 Landals, and J. Jouzel, 2006: Isotope calibrated Greenland temperature record over
3316 Marine Isotope Stage 3 and its relation to CH₄. *Earth and Planetary Science Letters*,
3317 **243**, 504-519.

3318

3319 **Hughen, K., J.Overpeck, R.F. Anderson, K.M. and Williams, 1996:** The potential for
3320 palaeoclimate records from varved Arctic lake sediments: Baffin Island, Eastern
3321 Canadian Arctic. In: *Lacustrine Environments. Palaeoclimatology and*
3322 *Palaeoceanography from Laminated Sediments* [Kemp, A.E.S. (ed.)]. Geological
3323 Society, London, Special Publications 116, pp. 57-71.

3324

3325 **Hughes, M.K. and H.F. Diaz, 1994:** Was there a ‘Medieval Warm Period’ and if so, where and
3326 when? *Journal of Climatic Change*, **265**, 109-142.

3327

3328 **Huybers, P., 2006:** Early Pleistocene glacial cycles and the integrated summer insolation
3329 forcing. *Science*, *313*, 508-511.

3330

3331 **Huybers, P. 2007:** Glacial variability over the last two million years: an extended depth-derived
3332 agetmodel, continuous obliquity pacing, and the Pleistocene progression. *Quaternary*
3333 *Science Reviews*, **26**, 37-55. doi:10.1016/j.quascirev.2006.07.005.

3334

3335 **Hyvärinen, H., 1976:** Flandrian pollen deposition rates and tree-line history in northern
3336 Fennoscandia. *Boreas*, **5(3)**, 163-175.

3337

3338 **Ilyashuk, E.A, B.P. Ilyashuk, D. Hammarlund, and I. Larocque, 2005:** Holocene climatic and
3339 environmental changes inferred from midge records (Diptera: Chironomidae,
3340 Chaoboridae, Ceratopogonidae) at Lake Berkut, southern Kola Peninsula, Russia.
3341 *Holocene*, **15**, 897-914.

3342

3343 **Imbrie, J. and N.G. Kipp, 1971:** A new micropaleontological method for Quantitative
3344 Paleoclimatology: Application to a late Pleistocene Caribbean Core. In: *The Late*
3345 *Cenozoic Glacial Age*,. [Turekian, K.K. (ed.)]. Yale Univeristy Press, New Haven,
3346 CT, pp. 71-181.

3347

- 3348 **Imbrie, J.,** A. Berger, E.A. Boyle, S.C. Clemens, A. Duffy, W.R. Howard, G. Kukla, J.
3349 Kutzbach, D.G. Martinson, A. McIntyre, A.C. Mix, B. Molino, J.J. Morley, L.C.
3350 Peterson, N.G. Pisias, W.L. Prell, M.E. Raymo, N.J. Shackleton, and J.R. Toggweiler,
3351 1993: On the structure and origin of major glaciation cycles. 2. The 100,000-year
3352 cycle. *Paleoceanography*, **8**, 699-735.
3353
- 3354 **IPCC, 1990:** *Climate Change: The IPCC scientific assessment*, [Houghton, J.T., G.J. Jenkins,
3355 and J.J. Ephraums, (eds.)]. Cambridge University Press, Cambridge.
3356
- 3357 **IPCC, 2007:** Summary for Policymakers. In: *Climate Change 2007: The Physical Science Basis*
3358 — Contribution of Working Group I to the Fourth Assessment Report of the
3359 Intergovernmental Panel on Climate Change, [Solomon, S., D. Qin, M. Manning, Z.
3360 Chen, M. Marquis, K.B. Averyt, M. Tignor and H.L. Miller (eds.)]. Cambridge
3361 University Press, Cambridge, United Kingdom and New York, 996 pp.
3362
- 3363 **Iversen, J., 1944:** *Viscum, Hedera and Ilex* as climatic indicators. A contribution to the study of
3364 past-glacial temperature climate. *Geologiska Foreningens Forhandlingar*, **66**, 463-
3365 483.
3366
- 3367 **Jacoby, G.C. and R.D. D'Arrigo, 1995:** Tree ring width and density evidence of climatic and
3368 potential forest change in Alaska. *Global Biogeochemical Cycles*, **9(2)**, 227-234.
3369
- 3370 **Jakobsson, M., and R. Macnab, 2006:** A comparison between GEBCO sheet 5.17 and the
3371 International Bathymetric Chart of the Arctic Ocean (IBCAO) version 1.0. *Marine*
3372 *Geophysical Researches*, **27(1)**, 35-48.
3373
- 3374 **Jakobsson, M., R. Løvlie, H. Al-Hanbali, E. Arnold, J. Backman, and M. Mörth, 2000:**
3375 Manganese color cycles in Arctic Ocean sediments constrain Pleistocene chronology.
3376 *Geology*, **28**, 23-26.
3377

- 3378 **Jansen, E., E. Bleil, R. Henrich, L. Kringstad, and B. Slettemark, B., 1988:** Paleoenvironmental
3379 changes in the Norwegian Sea and the northeast atlantic during the last 2.8 m.y.: deep
3380 sea drilling project/ocean drilling program sites 610, 642, 643 and 644.
3381 *Paleoceanography*, **3**, 563-581.
3382
- 3383 **Jansen, E., J. Overpeck, K.R. Briffa, J.-C. Duplessy, F. Joos, V. Masson-Delmotte, D. Olago, B.**
3384 **Otto-Bliesner, W.R. Peltier, S. Rahmstorf, R. Ramesh, D. Raynaud, D. Rind, O.**
3385 **Solomina, R. Villalba, and D. Zhang, 2007:** Palaeoclimate. In: *Climate Change*
3386 *2007—The Physical Science Basis. Contribution of Working Group I to the Fourth*
3387 *Assessment Report of the Intergovernmental Panel on Climate Change*, [Solomon, S.,
3388 D. Qin, M. Manning, Z. Chen, M. Marquis, K.B. Averyt, M. Tignor, and H.L. Miller
3389 (eds.)]. Cambridge University Press, Cambridge, U.K., and New York.
3390
- 3391 **Jenkyns, H.C., A. Forster, S. Schouten, and J.S. Sinninghe Damsté, 2004:** High temperatures in
3392 the Late Cretaceous Arctic Ocean. *Nature*, **432(7019)**, 888-892.
3393
- 3394 **Jennings, A., K. Knudsen, M. Hald, C. Hansen, and J. Andrews, 2002:** A mid-Holocene shift in
3395 Arctic sea-ice variability on the East Greenland Shelf. *The Holocene*, **12**, 49-58.
3396
- 3397 **Jiang D., H. Wang, Z. Ding, X. Lang, H. Drange, 2005:** Modeling the middle Pliocene climate
3398 with a global atmospheric general circulation model. *Journal of Geophysical*
3399 *Research*, **110**, D14107, doi:10.1029/2004JD005639.
3400
- 3401 **Johnsen, S., H. Clausen, W. Dansgaard, K. Fuhrer, N. Gundestrup, C. Hammer, P. Iversen, J.**
3402 **Jouzel, B. Stauffer, and J. Steffensen, 1992:** Irregular glacial interstadials recorded in
3403 a new Greenland ice core. *Nature*, **359**, 311-313.
3404
- 3405 **Johnsen, S.J., D. Dahl-Jensen, W. Dansgaard, and N. Gundestrup, 1995:** Greenland
3406 palaeotemperatures derived from GRIP bore hole temperature and ice core isotope
3407 profiles. *Tellus*, **47B**, 624-629.
3408

- 3409 **Johnsen, S.J.**, W. Dansgaard, and J.W.C. White, 1989: The origin of Arctic precipitation under
3410 present and glacial conditions. *Tellus*, **41B**, 452-468.
3411
- 3412 **Jones, P.D.**, K.R. Briffa, T.P. Barnett, and S.F.B. Tett, 1998: High-resolution palaeoclimatic
3413 records for the last millennium: interpretation, integration and comparison with
3414 General Circulation Model control-run temperatures. *Holocene*, **8**, 455-471.
3415
- 3416 **Jouzel, J.**, V. Masson-Delmotte, O. Cattani, G. Dreyfus, S. Falourd, G. Hoffmann, B. Minster, J.
3417 Nouet, J. M. Barnola, J. Chappellaz, H. Fischer, J.C. Gallet, S. Johnsen, M.
3418 Leuenberger, L. Loulergue, D. Luethi, H. Oerter, F. Parrenin, G. Raisbeck, D.
3419 Raynaud, A. Schilt, J. Schwander, E. Selmo, R. Souchez, R. Spahni, B. Stauffer, J.P.
3420 Steffensen, B. Stenni, T.F. Stocker, J.L. Tison, M. Werner, and E.W. Wolff, 2007:
3421 Orbital and Millennial Antarctic Climate Variability over the Past 800,000 Years.
3422 *Science*, **317**, 793-796, doi:10.1126/science.1141038.
3423
- 3424 **Jouzel, J.**, R.B. Alley, K.M. Cuffey, W. Dansgaard, P. Grootes, G. Hoffmann, S.J. Johnsen, R.D.
3425 Koster, D. Peel, C.A. Shuman, M. Stievenard, M. Stuiver, and J. White, 1997:
3426 Validity of the temperature reconstruction from water isotopes in ice cores. *Journal of*
3427 *Geophysical Research*, **102**, 26471-26487.
3428
- 3429 **Joynt, E.H.**, III and A.P. Wolfe, 2001: Paleoenvironmental inference models from sediment
3430 diatom assemblages in Baffin Island lakes (Nunavut, Canada) and reconstruction of
3431 summer water temperature. *Canadian Journal of Fisheries and Aquatic Sciences*, **58**,
3432 1222-1243.
3433
- 3434 **Kaakinen, A.** and M. Eronen, 2000: Holocene pollen stratigraphy indicating climatic and tree-
3435 line changes derived from a peat section at Ortino, in the Pechora lowland, northern
3436 Russia. *The Holocene*, **10**, 611-620.
3437

- 3438 **Kageyama, M., O. Peyron, S. Pinot, P. Tarasov, J. Guiot, S. Joussaume, and G. Ramstein, 2001:**
3439 The Last Glacial Maximum climate over Europe and western Siberia: a PMIP
3440 comparison between models and data. *Climate Dynamics*, **17**, 23-43.
3441
- 3442 **Kandiano, E.S. and H.A. Bauch, 2007:** Phase relationship and surface water mass change in
3443 the Northeast Atlantic during Marine Isotope Stage 11 (MIS11). *Quaternary*
3444 *Research*, **68(3)**, 445-455
3445
- 3446 **Kaplan, J.O., N.H. Bigelow, P.J. Bartlein, T.R. Christiansen, W. Cramer, S.P. Harrison, N.V.**
3447 **Matveyeva, A.D. McGuire, D.F. Murray, I.C. Prentice, V.Y. Razzhivin, B. Smith,**
3448 **D.A. Walker, P.M. Anderson, A.A. Andreev, L.B. Brubaker, M.E. Edwards, A.V.**
3449 **Lozhkin, and J.C. Ritchie, 2003:** Climate change and arctic ecosystems II—Modeling
3450 paleodata-model comparisons, and future projections. *Journal of Geophysical*
3451 *Research*, **108(D19)**, 8171, doi:10.1029/2002JD002559.
3452
- 3453 **Kaplan, M.R. and A.P. Wolfe, 2006:** Spatial and temporal variability of Holocene temperature
3454 trends in the North Atlantic sector. *Quaternary Research*, **65**, 223-231.
3455
- 3456 **Kapsner, W.R., R.B. Alley, C.A. Shuman, S. Anandakrishnan, and P.M. Grootes, 1995:**
3457 Dominant influence of atmospheric circulation on snow accumulation in Greenland
3458 over the past 18,000 years. *Nature*, **373**, 52-54.
3459
- 3460 **Karlén, W., 1988:** Scandinavian glacial and climate fluctuations during the Holocene.
3461 *Quaternary Science Reviews*, **7**, 199-209.
3462
- 3463 **Kaspar, F., N. Kühl, U. Cubasch, and T. Litt, 2005:** A model-data-comparison of European
3464 temperatures in the Eemian interglacial, *Geophysical Research Letters*, **32**, L11703,
3465 doi:10.1029/2005GL022456.
3466
- 3467 **Kaufman, D.S., T.A. Ager, N.J. Anderson, P.M. Anderson, J.T. Andrew, P.J. Bartlein, L.B.**
3468 **Brubaker, L.L. Coats, L.C. Cwynar, M.L. Duvall, A.S. Dyke, M.E. Edwards, W.R.**

- 3469 Eisner, K. Gajewski, A. Geirsdóttir, F.S. Hu, A.E. Jennings, M.R. Kaplan, M.W.
3470 Kerwin, A.V. Lozhkin, G.M. MacDonald, G.H. Miller, C.J. Mock, W.W. Oswald,
3471 B.L. Otto-Bliesver, D.F. Porinchu, K. Ruüland, J.P. Smol, E.J. Steig, and B.B. Wolfe,
3472 2004: Holocene thermal maximum in the western Arctic (0–180°W). *Quaternary*
3473 *Science Reviews*, **23**, 529-560.
- 3474
- 3475 **Kaufman**, D.S. and J. Brigham-Grette, 1993: Aminostratigraphic correlations and
3476 paleotemperature implications, Pliocene-Pleistocene high sea level deposits,
3477 northwestern Alaska. *Quaternary Science Reviews*, **12**, 21-33.
- 3478
- 3479 **Kellogg**, T.B., 1977: Paleoclimatology and paleo-oceanography of the Norwegian and
3480 Greenland seas: the last 450,000 years. *Marine Micropaleontology*, **2**, 235-249.
- 3481
- 3482 **Kerwin**, M., J.T. Overpeck, R.S. Webb, A. DeVernal, D.H. Rind and R.J. Healy, 1999: The role
3483 of oceanic forcing in mid-Holocene northern hemisphere climatic change.
3484 *Paleoceanography* **14**, 200-210.
- 3485
- 3486 **Kirk-Davidov**, D.B., D.P. Schrag, and J.G. Anderson, 2002: On the feedback of stratospheric
3487 clouds on polar climate. *Geophysical Research Letters*, **29(11)**, 1556.
- 3488
- 3489 **Kitoh**, A.. and S. Murakami, 2002: Tropical Pacific Climate at the mid-Holocene and the Last
3490 Glacial Maximum simulated by a coupled ocean-atmosphere general circulation
3491 model, *Paleoceanography*, **17**, 1-13
- 3492
- 3493 **Knutson**, T.R., T.L. Delworth, K.W. Dixon, I.M. Held, J. Lu, V. Ramaswamy, M.D.
3494 Schwarzkopf, G. Stenchikov, and R.J. Stouffer, 2006: Assessment of twentieth-
3495 century regional surface temperature trends using the GFDL CM2 coupled models.
3496 *Journal of Climate*, **19(9)**, 1624-1651.
- 3497
- 3498 **Koç**, N. and E. Jansen, 1994: Response of the high-latitude Northern Hemisphere to climate
3499 forcing—Evidence from the Nordic Seas. *Geology*, **22**, 523-526.

3500

3501 **Koç, N., E. Jansen, and H. Haflidason, 1993:** Paleoceanographic reconstruction of surface
3502 ocean conditions in the Greenland, Iceland and Norwegian Seas through the last 14 ka
3503 based on diatoms. *Quaternary Science Reviews*, **12**, 115-140.

3504

3505 **Koerner, R.M., 2005:** Mass Balance of glaciers in the Queen Elizabeth Islands, Nunavut,
3506 Canada. *Annals of Glaciology*, **42(1)**, 417-423.

3507

3508 **Koerner, R.M. and D.A. Fisher, 1990:** A record of Holocene summer climate from a Canadian
3509 high-Arctic ice core. *Nature*, **343**, 630-631.

3510

3511 **Korhola, A., H. Olander, and T. Blom, 2000:** Cladoceran and chironomid assemblages as
3512 quantitative indicators of water depth in sub-Arctic Fennoscandian lakes. *Journal of*
3513 *Paleolimnology*, **24**, 43-54.

3514

3515 **Korty, R.L., K.A. Emanuel, and J.R. Scott, 2008:** Tropical cyclone-induced upper-ocean
3516 mixing and climate: Application to equable climates. *Journal of Climate*, **21(4)**, 638-
3517 654.

3518

3519 **Kremenetski, C.V., L.D. Sulerzhitsky, and R. Hantemirov, 1998:** Holocene history of the
3520 northern range limits of some trees and shrubs in Russia. *Arctic and Alpine Research*,
3521 **30**, 317-333.

3522

3523 **Kukla, G.J., 2000:** The last interglacial. *Science*, **287**, 987-988.

3524

3525 **Kump, L.R. and D. Pollard, 2008:** Amplification of Cretaceous Warmth by Biological Cloud
3526 Feedbacks. *Science*, **11,(5873)**, 195, doi:10.1126/science.1153883.

3527

3528 **Kvenvolden, K.A., 1988:** Methane hydrate—a major reservoir of carbon in the shallow
3529 geosphere? *Chemical Geology*, **71**, 41-51.

3530

- 3531 **Kvenvolden, K.A.**, 1993: A primer on gas hydrates. In: *The Future of Energy Gases*, [Howel,
3532 D.G. (Ed)]. U.S. Geological Survey Professional Paper 1570, pp. 279-291.
3533
- 3534 **Lamb, H.H.**, 1977: *Climate History and the Future. Climate—Past, Present and Future.*
3535 Metheun, London, vol. 2, 835 pp.
3536
- 3537 **Lambeck, K.**, Y. Yokoyama, and T. Purcell, 2002: Into and out of the Last Glacial Maximum:
3538 sea-level change during oxygen isotope stages 3 and 2. *Quaternary Science Reviews*,
3539 **21**, 343-360.
3540
- 3541 **Larocque, I.** and R.I. Hall, 2004: Holocene temperature estimates and chironomid community
3542 composition in the Abisko Valley, northern Sweden. *Quaternary Science Reviews*,
3543 **23**, 2453-2465.
3544
- 3545 **Lauritzen, S.-E.**, 1996: Calibration of speleothem stable isotopes against historical records: a
3546 Holocene temperature curve for north Norway?. In: *Climatic Change: the Karst*
3547 *Record* [Lauritzen, S.-E. (Ed.)] Vol. 2 Karst Waters Institute Special Publication,
3548 Charles Town, West Virginia, pp. 78-80.
3549
- 3550 **Lauritzen, S.E.** and J. Lundberg, 1998: Rapid temperature variations and volcanic events during
3551 the Holocene from a Norwegian speleothem record. *Past Global Changes and their*
3552 *Significance for the Future. Volume of Abstracts, IGBP-PAGES, Bern 00*, p. 88.
3553
- 3554 **LeGrande, A.N.**, and G.A. Schmidt, 2006: Global gridded data set of the oxygen isotopic
3555 composition in seawater. *Geophysical. Research Letters*, **33**, L12604,
3556 doi:10.1029/2006GL026011.
3557
- 3558 **Lemke, P.**, J. Ren, R.B. Alley, I. Allison, J. Carrasco, G. Flato, Y. Fujii, G. Kaser, P. Mote, R.H.
3559 Thomas, and T. Zhang, 2007: Observations: Changes in Snow, Ice and Frozen
3560 Ground. In: *Climate Change 2007: The Physical Science Basis— Contribution of*
3561 *Working Group I to the Fourth Assessment Report of the Intergovernmental Panel on*

- 3562 *Climate Change*, [Solomon, S., D. Qin, M. Manning, Z. Chen, M. Marquis, K.B.
3563 Averyt, M. Tignor and H.L. Miller (eds.)]. Cambridge University Press, Cambridge
3564 and New York, 996 pp.
3565
- 3566 **Leng**, M.J. and J.D. Marshall, 2004: Palaeoclimate interpretation of stable isotope data from lake
3567 sediment archives. *Quaternary Science Reviews*, **23**, 811-831.
3568
- 3569 **Levac**, E., A. de Vernal, and W.J. Blake, 2001: Sea-surface conditions in northernmost Baffin
3570 Bay during the Holocene—Palynological evidence. *Journal of Quaternary Science*,
3571 **16**, 353-363.
3572
- 3573 **Levy**, L.B., D.S. Kaufman, and A. Werner, 2003: Holocene glacier fluctuations, Waskey Lake,
3574 northeastern Ahklun Mountains, southwestern Alaska. *Holocene*, **14**, 185-193.
3575
- 3576 **Ling**, F. and T.J. Zhang, 2007: Modeled impacts of changes in tundra snow thickness on
3577 ground thermal regime and heat flow to the atmosphere in Northernmost Alaska.
3578 *Global and Planetary Change* **57(3-4)**, 235-246.
3579
- 3580 **Lisiecki**, L.E. and M.E. Raymo, 2005: A Pliocene-Pleistocene stack of 57 globally distributed
3581 benthic $d^{18}O$ records. *Paleoceanography*, **20**, PA1003, doi:10.1029/2004PA001071.
3582
- 3583 **Lisiecki**, L.E. and M.E. Raymo, 2007: Plio-Pleistocene climate evolution—Trends and
3584 transitions in glacial cycle dynamics. *Quaternary Science Reviews*, **26**, 56-69.
3585
- 3586 **Loutre**, M.F., 2003: Clues from MIS 11 to predict the future climate – a modeling point of
3587 view. *Earth and Planetary Science Letters*, **212(1-2)**, 213-224
3588
- 3589 **Lozhkin**, A.V. and P.M. Anderson, 1995: The last interglaciation of northeast Siberia.
3590 *Quaternary Research*, **43**, 147-158.
3591

- 3592 **Lozhkin**, A.V. and P.M. Anderson, 1996: A late Quaternary pollen record from Elikchan 4
3593 Lake, northeast Siberia. *Geology of the Pacific Ocean*, **12**, 6-9-616.
3594
- 3595 **Lozhkin**, A.V., P.M. Anderson, W.R. Eisner, L.G. Ravako, D.M. Hopkins, L.B. Brubaker, P.A.
3596 Colinvaux, and M.C. Miller, 1993: Late Quaternary lacustrine pollen records from
3597 southwestern Beringia. *Quaternary Research*, **9**, 314-324.
3598
- 3599 **Lozhkin**, A.V., P.M. Anderson, T.V. Matrosova, and P.S. Minyuk, 2007: The pollen record from
3600 El'gygytgyn Lake: implications for vegetation and climate histories of northern
3601 Chukotka since the late middle Pleistocene. *Journal of Paleolimnology*, **37(1)**, 135-
3602 153.
3603
- 3604 **Lubinski**, D.J., S.L. Forman, and G.H. Miller, 1999: Holocene glacier and climate fluctuations
3605 on Franz Josef Land, Arctic Russia, 80°N. *Quaternary Science Reviews*, **18**, 85-108.
3606
- 3607 **Luckman**, B.H., 2007: Dendroclimatology. In: *Encyclopedia of Quaternary Science* [Elias, S.
3608 (ed.)] **1**, 465-475.
3609
- 3610 **MacDonald**, G.J., 1990: Role of methane clathrates in past and future climates. *Climatic*
3611 *Change*, **16(3)** 247-281.
3612
- 3613 **MacDonald**, G.M., T. Edwards, K. Moser, and R. Pienitz, 1993: Rapid response of treeline
3614 vegetation and lakes to past climate warming. *Nature*, **361**, 243-246.
3615
- 3616 **MacDonald**, G.M., B.R. Gervais, J.A. Snyder, G.A. Tarasov, and O.K. Borisova, 2000a:
3617 Radiocarbon dated *Pinus sylvestris* L. wood from beyond treeline on the Kola
3618 Peninsula, Russia. *The Holocene*, **10**, 143-147.
3619
- 3620 **MacDonald**, G.M., K.V. Kremenetski, and D.W. Beilman, D.W., 2007: Climate change and
3621 the northern Russian treeline zone. *Philosophical Transactions of the Royal Society*
3622 *B*, doi:10.1098/rstb.2007.2200.

- 3623
- 3624 **MacDonald, G.M., A.A. Velichko, C.V. Kremenetski, O.K. Borisova, A.A. Goleva, A.A.**
3625 **Andreev, L.C. Cwynar, R.T. Riding, S.L. Forman, T.W.D. Edwards, R. Aravena, D.**
3626 **Hammarlund, J.M. Szeicz, and V.N. Gattaulin, 2000b: Holocene treeline history and**
3627 **climate change across northern Eurasia. *Quaternary Research*, **53**, 302-311.**
- 3628
- 3629 **Macdonald, R.W. and J.M. Bowers, 1996: Contaminants in the arctic marine environment:**
3630 **priorities for protection. *ICES Journal of Marine Science*, **53**, 537-563.**
- 3631
- 3632 **Mahowald, N. M., D. R. Muhs, S. Levis, P. J Rasch, M. Yoshioka, C. S. Zender, and C. Luo,**
3633 **2006: Change in atmospheric mineral aerosols in response to climate: Last glacial**
3634 **period, preindustrial, modern, and doubled carbon dioxide climates, *ournal of***
3635 ***Geophysical Research*, **111**, D10202, doi:10.1029/2005JD006653**
- 3636
- 3637 **Manabe, S. and R.J. Stouffer, 1980: Sensitivity of a global climate model to an increase of CO₂**
3638 **in the atmosphere. *Journal of Geophysical Research*, **85(C10)**, 5529-5554.**
- 3639
- 3640 **Mann, M.E., R.S. Bradley, and M.K. Hughes, 1998: Global-scale temperature patterns and**
3641 **climate forcing over the past six centuries. *Nature*, **392**, 779-787.**
- 3642
- 3643 **Mann, D.H., D.M. Peteet, R.E. Reanier, and M.L. Kunz, 2002: Responses of an arctic landscape**
3644 **to Late glacial and early Holocene climatic changes: The importance of moisture:**
3645 ***Quaternary Science Reviews*, **21**, 997-1021, doi: 10.1016/S0277-3791(01)00116-0.**
- 3646
- 3647 **Mann, M.E., and P.D. Jones, 2003: Global surface temperatures over the past two millennia.**
3648 ***Geophysical Research Letters*, **30(15)**, 1820, doi:10.1029/2003GL017814**
- 3649
- 3650 **Mann, M.E., A. Zhang, M.K. Hughes, R.S. Bradley, S.K. Miller, S. Rutherford, and S. Ni, F., in**
3651 **press: Proxy-based Reconstructions of Hemispheric and Global Surface Temperature**
3652 **Variations over the past Two Millennia. *Proceedings of the National Academy of***
3653 ***Sciences*.**

3654

3655 **Marchant**, D.R., and G.H. Denton, 1996: Miocene and Pliocene paleoclimate of the Dry
3656 Valleys region, southern Victoria Land: A geomorphological approach. *Marine*
3657 *Micropaleontology*, **27**, 253-271.

3658

3659 **Marincovitch**, L., Jr. and A.Y. Gladenkov, 2000: New evidence for the age of Bering Strait.
3660 *Quaternary Science Reviews*, **20(1-3)**, 329-335.

3661

3662 **Marlowe** I.T., J.C. Green, A.C. Neal, S.C. Brassell, G. Eglinton, P.A. Course, 1984: Long-chain
3663 (N-C37-C39) alkenones in the prymnesiophyceae - distribution of alkenones and
3664 other lipids and their taxonomic significance. *British Phycological Journal*, **19(3)**,
3665 203-216.

3666

3667 **Marotzke**, J., 2000: Abrupt climate change and thermohaline circulation—Mechanisms and
3668 predictability. *Proceedings of the National Academy of Sciences, U.S.A.*, **97(4)**, 1347-
3669 1350.

3670

3671 **Marshall**, S.J. and P.U. Clark, 2002: Basal temperature evolution of North American ice sheets
3672 and implications for the 100-kyr cycle. *Geophysical Research Letters*, **29(24)**, 2214.

3673

3674 **Martinson**, D.G. and M. Steele, 2001: Future of the Arctic sea ice cover—Implications of an
3675 Antarctic analog. *Geophysical Research Letters*, **28**, 307-310.

3676

3677 **Masson-Delmotte**, V., J. Jouzel, A. Landais, M. Stievenard, S.J. Johnsen, J.W.C. White, M.A.
3678 Werner, A. Sveinbjornsdottir, and K. Fuhrer, 2005: GRIP deuterium excess reveals
3679 rapid and orbital-scale changes in Greenland moisture origin. *Science*, **309**, 118-121.

3680

3681 **Mathieu**, R., D. Pollard, J.E. Cole, J.W.C. White, R.S. Webb, and S.L. Thompson, 2002:
3682 Simulation of stable water isotope variations by the GENESIS GCM for modern
3683 conditions. *Journal of Geophysical Research*, **107**, doi:10.1029/2001JD900255.

3684

- 3685 **Matthews, J.V., Jr., C.E. Schweger, and J. Janssens, 1990:** The last (Koy-Yukon) interglaciation
3686 in the northern Yukon—Evidence from unit 4 at Chijee's Bluff, Bluefish Basin.
3687 *Geographie physique et Quaternaire*, **44**, 341-362.
- 3688
- 3689 **Mayewski, P.A., L.D. Meeker, M.S. Twickler, S.I. Whitlow, Q. Yang, W.B. Lyons, and M.**
3690 **Prentice, 1997:** Major features and forcing of high-latitude Northern Hemisphere
3691 atmospheric circulation using a 110,000-year-long glaciochemical series. *Journal of*
3692 *Geophysical Research*, **102**, 26,345-26,366.
- 3693
- 3694 **Maximova, L.N. and V.E. Romanovsky, 1988:** A hypothesis of the Holocene permafrost
3695 evolution. *Proceedings of the Fifth International Conference on Permafrost*,
3696 Norwegian Institute of Technology, Trondheim, Norway, 102-106.
- 3697
- 3698 **McGhee, R., 2004:** The last imaginary place; a human history of the Arctic world. Key Porter,
3699 Ontario, 296 pp.
- 3700
- 3701 **McKenna, M.C., 1980.** Eocene paleolatitude, climate and mammals of Ellesmere Island.
3702 *Paleogeography, Paleoclimatology and Paleoecology*, **30**, 349-362.
- 3703
- 3704 **McLaughlin, F., E. Carmack, R. Macdonald, A.J. Weaver, and J. Smith, 2002:** The Canada
3705 Basin, 1989–1995—Upstream events and far-field effects of the Barents Sea. *Journal*
3706 *of Geophysical Research*, **107(C7)**, 3082, doi:10.1029/2001JC000904.
- 3707
- 3708 **McManus, J.F., 2004:** A great grand-daddy of ice cores. *Nature*, **429**, 611-612.
- 3709
- 3710 **Meehl, G.A., T.F. Stocker, W.D. Collins, P. Friedlingstein, A.T. Gaye, J.M. Gregory, A. Kitoh,**
3711 **R. Knutti, J.M. Murphy, A. Noda, S.C.B. Raper, I.G. Watterson, A.J. Weaver and Z.-**
3712 **C. Zhao, 2007:** Global Climate Projections. In: *Climate Change 2007: The Physical*
3713 *Science Basis — Contribution of Working Group I to the Fourth Assessment Report*
3714 *of the Intergovernmental Panel on Climate Change*, [Solomon, S.,D. Qin, M.
3715 Manning, Z. Chen, M. Marquis, K.B. Averyt, M. Tignor and H.L. Miller (eds.)].

- 3716 Cambridge University Press, Cambridge, United Kingdom and New York, pp. 747-
3717 845.
3718
- 3719 **Meeker**, L.D. and P.A. Mayewski, 2002: A 1400-year high-resolution record of atmospheric
3720 circulation over the North Atlantic and Asia. *Holocene*, **12**, 257-266.
3721
- 3722 **Meier**, M.F., M.B. Dyurgerov, U.K. Rick, S. O'Neel, W.T. Pfeffer, R.S. Anderson, S.P.
3723 Anderson, and A.F. Glazovsky, 2007: Glaciers dominate eustatic sea-level rise in the
3724 21st Century. *Science*, **317(5841)**, 1064-1067 doi: 10.1126/science.1143906
3725
- 3726 **Miller**, G.H., A.P. Wolfe, J.P. Briner, P.E. Sauer, and A. Nesje, 2005: Holocene glaciation and
3727 climate evolution of Baffin Island, Arctic Canada. *Quaternary Science Reviews*, **24**,
3728 1703-1721.
3729
- 3730 **Moberg**, A., D.M. Sonechkin, K. Holmgren, N.M. Datsenko, and W. Karlen, 2005: Highly
3731 variable northern hemisphere temperatures reconstructed from low- and high-
3732 resolution proxy data. *Nature*, **433**, 613-617.
3733
- 3734 **Montoya**, M., H. von Storch, and T.J. Crowley, 2000: Climate Simulation for 125 kyr BP with
3735 a Coupled Ocean–Atmosphere General Circulation Model. *Journal of Climate*, **13**,
3736 1057-1072.
3737
- 3738 **Moran**, K., J. Backman, H. Brinkhuis, S.C. Clemens, T. Cronin, G.R. Dickens, F. Eynaud, J.
3739 Gattacceca, M. Jakobsson, R.W. Jordan, M. Kaminski, J. King, N. Koc, A. Krylov, N.
3740 Martinez, J. Matthiessen, D. McInroy, T.C. Moore, J. Onodera, M. O'Regan, H.
3741 Palike, B. Rea, D. Rio, T. Sakamoto, D.C. Smith, R. Stein, K. St. John, I. Suto, N.
3742 Suzuki, K. Takahashi, M. Watanabe, M. Yamamoto, J. Farrell, M. Frank, P. Kubik,
3743 W. Jokat, and Y. Kristoffersen, 2006: The Cenozoic palaeoenvironment of the Arctic
3744 Ocean. *Nature*, **441**, 601-605.
3745

- 3746 **Morison, J., K. Aagaard, and M. Steele, 2000:** Recent environmental changes in the arctic.
3747 *Arctic*, **53(4)**, 359-371.
3748
- 3749 **Muhs, D.R. and J.R. Budahn, 2006:** Geochemical evidence for the origin of late Quaternary
3750 loess in central Alaska. *Canadian Journal of Earth Science*, **43**, 323-337
3751
- 3752 **Muller, P.J., G. Kirst, G. Ruhland, I. von Storch, and A. Rossell-Mele, 1998:** Calibration of the
3753 alkenone paleotemperature index U_k37 based on core-tops from the eastern South
3754 Atlantic and the global ocean (60°N–60°S). *Geochimica et Cosmochimica Acta*, **62**,
3755 1757-1772.
3756
- 3757 **National Research Council, 2006:** *Surface temperature reconstructions for the last 2,000*
3758 *years*. National Academies Press, Washington, DC. 160pp.
3759
- 3760 **Naurzbaev, M.M., E.A. Vaganov, O.V. Sidorova, and F.H. Schweingruber, 2002:** Summer
3761 temperatures in eastern Taimyr inferred from a 2427-year late-Holocene tree-ring
3762 chronology and earlier floating series. *The Holocene*, **12**, 727-736.
3763
- 3764 **Nelson, R.E., and Carter, L.D. 1991.** Preliminary interpretation of vegetation and paleoclimate in
3765 northern Alaska during the late Pliocene Colvillian marine transgression. In: *Geologic*
3766 *studies in Alaska*, [Bradley, D.C. and A.B. Ford (eds.)]. U.S. Geological Survey
3767 Bulletin 1999, pp. 219-222.
3768
- 3769 **Nesje, A., J. Bakke, S.O. Dahl, O. Lie, and J.A. Matthews, 2008:** Norwegian mountain glaciers
3770 in the past, present and future. *Global and Planetary Change*, **60**, 10-27.
3771
- 3772 **Nesje, A., J.A. Matthews, S.O. Dahl, M.S. Berrisford, and C. Andersson, 2001:** Holocene
3773 glacier fluctuations of Flatebreen and winter precipitation changes in the
3774 Jostedalbreen region, western Norway, based on glaciolacustrine records. *The*
3775 *Holocene*, **11**, 267-280.
3776

- 3777 **Nørgaard-Pedersen, N., N. Mikkelsen, and Y. Kristoffersen, 2007a:** Arctic Ocean record of last
3778 two glacial-interglacial cycles off North Greenland/Ellesmere Island—Implications
3779 for glacial history. *Marine Geology*, **244(2007)**, 93-108.
3780
- 3781 **Nørgaard-Pedersen, N., N. Mikkelsen, S.J. Lassen, Y. Kristoffersen, and E. Sheldon, 2007b:**
3782 Reduced sea ice concentrations in the Arctic Ocean during the last interglacial period
3783 revealed by sediment cores off northern Greenland. *Paleoceanography*, **22**, PA1218,
3784 doi:10.1029/2006PA001283.
3785
- 3786 **Nørgaard-Pedersen, N., R.F. Spielhagen, H. Erlenkeuser, P.M. Grootes, J. Heinemeier, and J.**
3787 **Knies, 2003:** The Arctic Ocean during the Last Glacial Maximum—Atlantic and
3788 polar domains of surface water mass distribution and ice cover. *Paleoceanography*,
3789 **18**, 8-1 to 8-19.
3790
- 3791 **Nørgaard-Pedersen, N., R.F. Spielhagen, J. Thiede, and H. Kassens, 1998:** Central Arctic
3792 surface ocean environment during the past 80,000 years. *Paleoceanography*, **13**, 193-
3793 204.
3794
- 3795 **Nürnberg, D. and R. Tiedemann, 2004:** Environmental changes in the Sea of Okhotsk during
3796 the last 1.1 million years. *Paleoceanography*, **19**, PA4011.
3797
- 3798 **O'Brien, S.R., P.A. Mayewski, L.D. Meeker, D.A. Meese, M.S. Twickler, and S.I. Whitlow,**
3799 **1995:** Complexity of Holocene climate as reconstructed from a Greenland ice core.
3800 *Science*, **270**, 1962-1964.
3801
- 3802 **Obata, A., 2007:** Climate-carbon cycle model response to freshwater discharge into the North
3803 Atlantic. *Journal of Climate*, **20(24)** 5962-5976.
3804
- 3805 **Ogilvie, A.E.J. and T. Jónsson, 2001:** "Little Ice Age" Research: A Perspective from Iceland.
3806 *Climate Change*, **48**, 9-52.
3807

- 3808 **Ogilvie**, A.E.J. and I. Jónsdóttir, 2000. Sea ice, climate and Icelandic fisheries in historical times.
3809 *Arctic*, **53(4)**, 383-394.
3810
- 3811 **Ohkouchi**, N., T.I. Eglinton, L.D. Keigwin, and J.M. Hayes, 2002: Spatial and temporal offsets
3812 between proxy records in a sediment drift. *Science*, **298**, 1224-1227.
3813
- 3814 **Oswald**, W.W., L.B. Brubaker, and P.M. Anderson, 1999, Late Quaternary vegetational history
3815 of the Howard Pass area, northwestern Alaska. *Canadian Journal of Botany*, **77(4)**,
3816 570-581
3817
- 3818 **Oswald**, W.W., L.B. Brubaker, F.S. Hu, and G.W. Kling, 2003: Holocene pollen records from
3819 the central Arctic Foothills, northern Alaska—Testing the role of substrate in the
3820 response of tundra to climate change. *Journal of Ecology*, **91**, 1034-1048
3821
- 3822 **Otto-Bliesner**, B.L., C.D. Hewitt, T.M. Marchitto, E. Brady, A. Abe-Ouchi, M. Crucifix, S.
3823 Murakami, and S.L. Weber, 2007: Last Glacial Maximum ocean thermohaline
3824 circulation: PMIP2 model inter-comparisons and data constraints. *Geophysical*
3825 *Research Letters*, **34**, L12706, doi:10.1029/2007GL029475.
3826
- 3827 **Otto-Bliesner**, B.L., S.J. Marshall, J.T. Overpeck, G.H. Miller, A. Hu, and CAPE Last
3828 Interglacial Project members, 2006, Simulating Arctic climate warmth and icefield
3829 retreat in the Last Interglaciation. *Science*, **311**, 1751-1753,
3830 doi:10.1126/science.1120808
3831
- 3832 **Overpeck**, J., K. Hughen, D. Hardy, R. Bradley, R. Case, M. Douglas, B. Finney, K. Gajewski,
3833 C. Jacoby, A. Jennings, S. Lamoureux, A. Lasca, G. MacDonald, J. Moore, M.
3834 Retelle, S. Smith, A. Wolfe, and G. Zielinski, 1997: Arctic environmental change of
3835 the last four centuries. *Science*, **278**, 1251-1256.
3836

- 3837 **Overpeck**, Jonathan T., Bette L. Otto-Bliesner, Gifford H. Miller, Daniel R. Muhs, Richard B.
3838 Alley, Jeffrey T. Kiehl, 2006: Paleoclimatic Evidence for Future Ice-Sheet Instability
3839 and Rapid Sea-Level Rise. *Science*, **311**, 1747-1750. DOI: 10.1126/science.1115159
3840
- 3841 **Pagani**, M., K. Caldeira, D. Archer, and J.C. Zachos, 2006: An Ancient Carbon Mystery.
3842 *Science*, **314**, 1556 - 1557 doi: 10.1126/science.1136110
- 3843 **Pearson**, P.N., B.E. van Dongen, C.J. Nicholas, R.D. Pancost, S. Schouten, J.M. Singano, and
3844 B.S. Wade, 2007: Stable warm tropical climate through the Eocene Epoch. *Geology*,
3845 **35**, 211-214.
3846
- 3847 **Peterson**, B.J., R.M. Holmes, J.W. McClelland, C.J. Vorosmarty, R.B. Lammers, A.I.
3848 Shiklomanov, I.A. Shiklomanov, and S. Rahmstorf, 2002: Increasing river discharge
3849 to the Arctic Ocean. *Science*, **298**, 2171-2173.
3850
- 3851 **Peterson**, B.J., J. McClelland, R. Murry, R.M. Holmes, J.E. Walsh, and K. Aagaard, 2006:
3852 Trajectory shifts in the Arctic and subarctic freshwater cycle. *Science*, **313**, 1061-
3853 1066.
3854
- 3855 **Pienitz**, R., M.S.V. Douglas, and J.P. Smol (eds.), 2004: *Long-Term Environmental Change in*
3856 *Arctic and Antarctic Lakes*. Dordrecht, Germany: Springer, 579 pp.
3857
- 3858 **Pienitz**, R. and J.P. Smol, 1993: Diatom assemblages and their relationship to environmental
3859 variables in lakes from the boreal**boreal** forest-tundratundra ecotone near
3860 Yellowknife, Northwest-Territories, Canada. *Hydrobiologia*, **269**, 391-404.
3861
- 3862 **Pienitz**, R., J.P. Smol, W.M. Last, P.R. Leavitt, and B.F. Cumming, 2000: Multi-proxy
3863 Holocene palaeoclimatic record from a saline lake in the Canadian Subarctic. *The*
3864 *Holocene*, **10(6)**, 673-686 doi:10.1191/09596830094935
3865

- 3866 **Pierrehumbert**, R.T., H. Brogniez, and R. Roca, 2007: On the relative humidity of the
3867 atmosphere. In: *The Global Circulation of the Atmosphere* [Schneider, T. and A.
3868 Sobel (eds.)]. Princeton University Press, Princeton, New Jersey, pp.143-185.
3869
- 3870 **Peixoto**, J.P. and A.H. Oort, 1992: *Physics of Climate*. American Institute of Physics, New York,
3871 520 pp.
3872
- 3873 **Pinot**, S., G. Ramstein, S.P. Harrison, I.C. Prentice, J. Guiot, M. Stute. and S. Jousaume, 1999:
3874 Tropical paleoclimates of the Last Glacial Maximum: comparison of Paleoclimate
3875 Modelling Intercomparison Project (PMIP) simulations and paleodata. *Climate*
3876 *Dynamics*, **15**, 857-874.
3877
- 3878 **Pisaric**, M.F J., G.M. MacDonald, A.A Velichko, and L.C. Cwynar, 2001: The late-glacial and
3879 post-glacial vegetation history of the northwestern limits of Beringia, from pollen,
3880 stomates and tree stump evidence. *Quaternary Science Reviews*, **20**, 235-245.
3881
- 3882 **Pollard**, D. and S.L. Thompson, 1997: Climate and ice-sheet mass balance at the Last Glacial
3883 Maximum from the GENESIS Version 2 global climate model. *Quaternary Science*
3884 *Reviews*, **16**, 841-864
3885
- 3886 **Polyak**, L., W.B. Curry, D.A. Darby, J. Bischof, and T.M. Cronin, 2004: Contrasting
3887 glacial/interglacial regimes in the western Arctic Ocean as exemplified by a
3888 sedimentary record from the Mendeleev Ridge. *Palaeogeography,*
3889 *Palaeoclimatology, Palaeoecology*, **203**, 73-93.
3890
- 3891 **Porter**, S.C. and G.H. Denton, 1967: Chronology of neoglaciation. *American Journal of Science*,
3892 **165**, 177-210.
3893
- 3894 **Poulsen**, C.J., E.J. Barron, W.H. Peterson, and P.A. Wilson, 1999: A reinterpretation of mid-
3895 Cretaceous shallow marine temperatures through model-data comparison.
3896 *Paleoceanography*, **14(6)** 679-697.

- 3897
- 3898 **Prahl, F.G., G.J. de Lange, M. Lyle, and M.A. Sparrow, 1989: Post-depositional stability of**
3899 **long-chain alkenones under contrasting redox conditions. *Nature*, **341**, 434-437.**
3900
- 3901 **Prahl, F.G., L.A. Muelhausen, and D.L. Zahnle, 1988: Further evaluation of long-chain**
3902 **alkenones as indicators of paleoceanographic conditions. *Geochimica et***
3903 ***Cosmochimica Acta*, **52**, 2303-2310.**
3904
- 3905 **Prentice, I.C. and T. Webb III, 1998: BIOME 6000—Reconstructing global mid-Holocene**
3906 **vegetation patterns from palaeoecological records. *Journal of Biogeography*, **25**, 997-**
3907 **1005.**
3908
- 3909 **Rahmstorf, S., 1996: On the freshwater forcing and transport of the Atlantic thermohaline**
3910 **circulation. *Climate Dynamics*, **12**, 799-811.**
3911
- 3912 **Rahmstorf, S., 2002: Ocean circulation and climate during the past 120,000 years. *Nature*, **419**,**
3913 **207-214.**
3914
- 3915 **Rasmussen, S.O., K.K. Andersen, A.M. Svensson, J.P. Steffensen, B.M. Vinther, H.B. Clausen,**
3916 **M.L. Siggaard-Andersen, S.J. Johnsen, L.B. Larsen, D. Dahl-Jensen, M. Bigler, R.**
3917 **Rothlisberger, H. Fischer, K. Goto-Azuma, M.E. Hansson, and U. Ruth, 2006: A new**
3918 **Greenland ice core chronology for the last glacial termination. *Journal of***
3919 ***Geophysical Research*, **111**, D061202, doi:10.1029/2005JD006079.**
3920
- 3921 **Raymo, M.E., 1994: The initiation of northern hemisphere glaciation. *Annual Review of Earth***
3922 ***and Planetary Sciences*, **22**, 353-383, doi:10.1146/annurev.ea.22.050194.002033**
3923
- 3924 **Raymo, M. E., 1997: The timing of major climate terminations, *Paleoceanography*, **12**, 577-585.**
3925
- 3926 **Raymo, M.E., B. Grant, M. Horowitz, and G.H. Rau, 1996: Mid-Pliocene warmth—Stronger**
3927 **greenhouse and stronger conveyor. *Marine Micropaleontology*, **27**, 313-326.**

3928

3929 **Raymo, M.E., L.E. Lisiecki, and K.H. Nisancioglu, 2006:** Plio-Pleistocene ice volume,
3930 Antarctic climate, and the global $\delta^{18}\text{O}$ record. *Science*, **313**, 492-495.

3931

3932 **Raymo, M.E., D.W. Oppo, and W. Curry, 1997:** The mid-Pleistocene climate transition: A deep
3933 sea carbon isotopic perspective: *Paleoceanography*, **12**, 546-559.

3934

3935 **Renssen, H., E. Driesschaert, M.F. Loutre, and T. Fichefet, 2006:** On the importance of initial
3936 conditions for simulations of the Mid-Holocene climate. *Climate of the Past*, **2**, 91-
3937 97.

3938

3939 **Renssen, H., H. Goosse, T. Fichefet, V. Brovkin, E. Dresschaert, and F. Wolk, 2005:** Simulating
3940 the Holocene climate evolution at northern high latitudes using a coupled
3941 atmosphere–sea ice–ocean–vegetation model. *Climate Dynamics*, **24**, 23-43.

3942

3943 **Reyes, A.V., G.C. Wiles, D.J. Smith, D.J. Barclay, S. Allen, S. Jackson, S. Larocque, S. Laxton,**
3944 **D. Lewis, P.E. Calkin, and J.J. Clauge, 2006:** Expansion of alpine glaciers in Pacific
3945 North America in the first millennium A.D. *Geology*, **34**, 57-60.

3946

3947 **Rignot, E. and R.H. Thomas, 2002:** Mass balance of polar ice sheets. *Science* **297**, 1502-1506.

3948

3949 **Rigor, I.G. and J.M. Wallace, 2004:** Variations in the age of Arctic sea-ice and summer sea-ice
3950 extent. *Geophysical Research Letters*, **31**, L09401, doi:10.1029/2004GL019492.

3951

3952 **Rimbu, N., G. Lohmann, and K. Grosfeld, 2007:** Northern Hemisphere atmospheric blocking
3953 in ice core accumulation records from northern Greenland. *Geophysical Research*
3954 *Letters*, **34**, L09704, doi:10.1029/2006GL029175.

3955

3956 **Ritchie, J.C., 1984:** *Past and Present Vegetation of the Far Northwest of Canada*. University of
3957 Toronto Press, Toronto, 251 pp.

3958

- 3959 **Ritchie, J.C., L.C. Cwynar, and R.W. Spear, 1983:** Evidence from northwest Canada for an early
3960 Holocene Milankovitch thermal maximum. *Nature*, **305**, 126-128.
3961
- 3962 **Rivers, A.R., and A.H. Lynch, 2004:** On the influence of land cover on early Holocene climate
3963 in northern latitudes. *Journal of Geophysical Research-Atmospheres*, **109(D21)**,
3964 D21114.
3965
- 3966 **Roe, G.H. and M.R. Allen, 1999:** A comparison of competing explanations for the 100,000-yr
3967 ice age cycle. *Geophysical Research Letters*, **26(15)**, 2259-2262.
3968
- 3969 **Rosell-Mele, A. and P. Comes, 1999:** Evidence for a warm Last Glacial Maximum in the Nordic
3970 sea or an example of shortcomings in Uk37 δ and Uk37 to estimate low sea surface
3971 temperature? *Paleoceanography*, **14**, 770-776.
3972
- 3973 **Rosell-Mele, A., G. Eglinton, U. Pflaumann, and M. Sarnthein, 1995:** Atlantic core top
3974 calibration of the Uk37 index as a sea-surface temperature indicator. *Geochimica et*
3975 *Cosmochimica Acta*, **59**, 3099-3107.
3976
- 3977 **Royer, D.L., 2006:** CO₂-forced climate thresholds during the Phanerozoic. *Geochimica et*
3978 *Cosmochimica Acta*, **70(23)**, 5665-5675.
3979
- 3980 **Royer, D.L., R.A. Berner, and J. Park, 2007:** Climate sensitivity constrained by CO₂
3981 concentrations over the past 420 million years. *Nature*, **446**, 530-532.
3982
- 3983 **Ruddiman, W.F., 2003:** Insolation, Ice Sheets and Greenhouse Gases. *Quaternary Science*
3984 *Reviews*, **22**, 1597.
3985
- 3986 **Ruddiman, W.F., 2006:** Ice-driven CO₂ feedback on ice volume. *Climate of the Past*, **2**, 43-55.
3987
- 3988 **Ruddiman, W.F., N.J. Shackleton, and A. McIntyre, 1986:** North Atlantic sea-surface
3989 temperatures for the last 1.1 million years. In: *North Atlantic Paleoceanography*,

- 3990 [Summerhayes, C.P. and N.J. Shackleton, (eds.)]. Geological Society of London,
3991 Special Publication, **21**, 155-173.
3992
- 3993 **Rudels, B., L.G. Anderson, E.P. Jones, and G. Kattner, 1996:** Formation and evolution of the
3994 surface mixed layer and halocline of the Arctic Ocean. *Journal of Geophysical*
3995 *Research*, **101**, 8807-8821.
3996
- 3997 **Rühland, K., A. Priesnitz, and J.P. Smol, 2003:** Evidence for recent environmental changes in
3998 50 lakes the across Canadian Arctic treeline. *Arctic, Antarctic, and Alpine Research*,
3999 **35**, 110-23.
4000
- 4001 **Salvigsen, O., S.L. Forman, and G.H. Miller, 1992:** Thermophilous mollusks on Svalbard during
4002 the Holocene and their paleoclimatic implications. *Polar Research*, **11**, 1-10.
4003
- 4004 **Salzmann, U., A.M. Haywood, D.J. Lunt, P.J. Valdes, and D.J. Hill, 2008:** A new global biome
4005 reconstruction and data-model comparison for the Middle Pliocene. *Global Ecology*
4006 *and Biogeography*, **17**, 432-447.
4007
- 4008 **Sauer, P.E., G.H. Miller, and J.T. Overpeck, 2001:** Oxygen isotope ratios of organic matter in
4009 Arctic lakes as a paleoclimate proxy—Field and laboratory investigations. *Journal of*
4010 *Paleolimnology*, **25**, 43-64.
4011
- 4012 **Schauer, U., B. Rudels, E.P. Jones, L.G. Anderson, R.D. Muench, G. Björk, J.H. Swift, V.**
4013 **Ivanov, and A.-M. Larsson, 2002:** Confluence and redistribution of Atlantic water in
4014 the Nansen, Amundsen and Makarov basins. *Annals of Geophysics*, **20**, 257- 273.
4015
- 4016 **Schindler, D.W. and J.P. Smol, 2006:** Cumulative effects of climate warming and other human
4017 activities on freshwaters of Arctic and subarctic North America. *Ambio*, **35**, 160-68.
4018
- 4019 **Schlosser, P., B. Ekwurzel, S. Khatiwala, B. Newton, W. Maslowski, and S. Pfirman, 2000:**
4020 Tracer studies of the Arctic freshwater budget. In: *The Freshwater Budget of the*

- 4021 *Arctic Ocean* [Lewis, E.L. (ed.)]. Kluwer Academic Publishers, Norwell, Mass. pp.
4022 453- 478.
4023
- 4024 **Schlosser, P.**, R. Newton, B. Ekwurzel, S. Khatiwala, R. Mortlock, and R. Fairbanks, 2002:
4025 Decrease of river runoff in the upper waters of the Eurasian Basin, Arctic Ocean,
4026 between 1991 and 1996—Evidence from d¹⁸O data. *Geophysical Research Letters*,
4027 **29(9)**, 1289, doi:10.1029/ 2001GL013135.
4028
- 4029 **Schmidt, G.A.**, A.N. LeGrande, and G. Hoffman, 2007: Water isotope expressions of intrinsic
4030 and forced variability in a coupled ocean-atmosphere model. *Journal Geophysical*
4031 *Research*, **112**, D10103, doi:10.1029/2006JD007781.
4032
- 4033 **Schmittner, A.**, 2005: Decline of the marine ecosystem caused by a reduction in the Atlantic
4034 overturning circulation. *Nature*, **434**, 628-33.
4035
- 4036 **Schneider, K.B.** and B. Faro, 1975: Effects of sea ice on sea otters (*Enhydra lutris*). *Journal*
4037 *of Mammalogy*, **56**, 91-101.
4038
- 4039 **Schouten, S.**, E.C. Hopmans, and J.S.S. Damsté, 2004: The effect of maturity and depositional
4040 redox conditions on archaeal tetraether lipid palaeothermometry. *Organic*
4041 *Geochemistry*, **35(5)**, 567-571
4042
- 4043 **Schrag, D.P.**, J.F. Adkins, K. McIntyre, J.L. Alexander, D.A. Hodell, C.D. Charles, and J.F.
4044 McManus, 2002: The oxygen isotopic composition of seawater during the Last
4045 Glacial Maximum. *Quaternary Science Reviews*, **21(1-3)**, 331-342
- 4046 **Schulz, H.**, U. von Rad, and H. Erlenkeuser, 1998: Correlation between Arabian Sea and
4047 Greenland climate oscillations of the past 110,000 years: *Nature*, **393**, 54-57.
4048
- 4049 **Scott, D.B.**, P.J. Mudie, V. Baki, K.D. MacKinnon, and F.E. Cole, 1989: Biostratigraphy and
4050 late Cenozoic paleoceanography of the Arctic Ocean—Foraminiferal,

- 4051 lithostratigraphic, and isotopic evidence. *Geological Society of America Bulletin*, **101**,
4052 260-277.
- 4053
- 4054 **Seager**, R., D.S. Battisti, J. Yin. N. Gordon, N. Naik, A.C. Clement, and M.A. Cane, 2002: Is the
4055 Gulf Stream responsible for Europe's mild winters? *Quarterly Journal of the Royal*
4056 *Meteorological Society*, **128(586)**, 2563-2586.
- 4057
- 4058 **Seppä**, H., 1996: Post-glacial dynamics of vegetation and tree-lines in the far north of
4059 Fennoscandia. *Fennia*, **174**, 1-96.
- 4060
- 4061 **Seppä**, H. and H.J.B. Birks, 2001: July mean temperature and annual precipitation trends during
4062 the Holocene in the Fennoscandian tree-line area—Pollen-based climate
4063 reconstructions. *The Holocene*, **11**, 527-539.
- 4064
- 4065 **Seppä**, H. and H.J.B. Birks, 2002: Holocene climate reconstructions from the Fennoscandian
4066 tree-line area based on pollen data from Toskaljavri. *Quaternary Research*, **57**, 191-
4067 199.
- 4068
- 4069 **Seppä**, H. and D. Hammarlund, 2000: Pollen-stratigraphical evidence of Holocene hydrological
4070 change in northern Fennoscandia supported by independent isotopic data. *Journal of*
4071 *Paleolimnology*, **24(1)**, 69-79.
- 4072
- 4073 **Seppä**, H., H.J.B. Birks, A. Odland, A. Poska, and S. Veski, 2004: A modern pollen-climate
4074 calibration set from northern Europe—Developing and testing a tool for
4075 palaeoclimatological reconstructions. *Journal of Biogeography*, **31**, 251-267.
- 4076
- 4077 **Seppä**, H., L.C. Cwynar, and G.M. MacDonald, 2003: Post-glacial vegetation reconstruction and
4078 a possible 8200 cal. Yr BP event from the low arctic of continental Nunavut, Canada.
4079 *Journal of Quaternary Science*, **18**, 621-629.
- 4080
- 4081 **Serreze**, M.C. and J.A. Francis, 2006: The Arctic amplification debate. *Climatic Change*, **76**,

4082 241-264.

4083

4084 **Serreze, M.C., A.P. Barrett, A.G. Slater, M. Steele, J. Zhang, and K.E. Trenberth, 2007a:** The
4085 large-scale energy budget of the Arctic. *Journal of Geophysical Research*, **112**,
4086 D11122, doi:10.1029/2006JD008230.

4087

4088 **Serreze, M.C., A.P. Barrett, A.G. Slater, R.A. Woodgate, K. Aagaard, R.B. Lammers, M. Steele,**
4089 **R. Moritz, M. Meredith, and C.M. Lee, 2006:** The large-scale freshwater cycle of the
4090 Arctic, *Journal of Geophysical Research-Oceans*, **111(C11)**, C11010.

4091

4092 **Serreze, M.C., M.M. Holland, and J. Stroeve, 2007b:** Perspectives on the Arctic's shrinking sea
4093 ice cover. *Science*, **315**, 1533-1536.

4094

4095 **Severinghaus, J.P. and E.J. Brook, 1999:** Abrupt climate change at the end of the last glacial
4096 period inferred from trapped air in polar ice. *Science*, **286**, 930-934.

4097

4098 **Severinghaus, J.P., T. Sowers, E.J. Brook, R.B. Alley and M.L. Bender. 1998:** Timing of
4099 abrupt climate change at the end of the Younger Dryas interval from thermally
4100 fractionated gases in polar ice. *Nature*, **391(6663)**, 141-146.

4101

4102 **Sewall, J.O. and L.C. Sloan, 2004:** Disappearing Arctic sea ice reduces available water in the
4103 American west. *Geophysical Research Letters*, **31**, doi:10.1029/2003GL019133.

4104

4105 **Sewall, J.O. and L.C. Sloan, 2001:** Equable Paleogene climates: The result of a stable, positive
4106 Arctic Oscillation? *Geophysical Research Letters*, **28(19)**, 3693-3695.

4107

4108 **Shackleton, N.J., 1967:** Oxygen isotope analyses and paleotemperatures reassessed. *Nature*,
4109 **215**, 15-17.

4110

- 4111 **Shackleton**, N.J., 1974: Attainment of isotopic equilibrium between ocean water and the
4112 benthonic foraminifera genus *Uvigerina*—Isotopic changes in the ocean during the
4113 last glacial. *Coll. Int. du CNRS*, **219**, 203-209.
4114
- 4115 **Shellito**, C. J., L.C. Sloan, and M. Huber, 2003: Climate model sensitivity to atmospheric CO₂
4116 levels in the early-middle Paleogene. *Palaeogeography, Palaeoclimatology,*
4117 *Palaeoecology*, **193**, 113-123.
4118
- 4119 **Shindell**, D.T., G.A. Schmidt, M.E. Mann, D. Rind, and A. Waple, 2001: Solar forcing of
4120 regional climate change during the Maunder Minimum. *Science*, **294**, 2149-2152.
4121
- 4122 **Shuman**, C.A., R.B. Alley, S. Anandkrishnan, J.W.C. White, P.M. Grootes and C.R. Stearns,
4123 1995: Temperature and accumulation at the Greenland Summit: comparison of high-
4124 resolution isotope profiles and satellite passive microwave brightness temperature
4125 trends. *Journal of Geophysical Research*, **100(D5)**, 9165-9177.
4126
- 4127 **Siegenthaler**, U., T.F. Stocker, E. Monnin, E. Lüthi, J. Schwander, B. Stauffer, D. Raynaud,
4128 J.M. Barnola, H. Fischer, V. Masson-Delmotte, and J. Jouzel, 2005: Stable carbon
4129 cycle–climate relationship during the late Pleistocene. *Science*, **310**, 1313-1317,
4130 doi:10.1126/science.1120130
4131
- 4132 **Sloan**, L.C. and E.J. Barron, 1992: A comparison of eocene climate model results to quantified
4133 paleoclimatic interpretations. *Palaeogeography, Palaeoclimatology, Palaeoecology*,
4134 **93(3-4)**, 183-202
4135
- 4136 **Sloan**, L., T.J. Crowley, and D. Pollard, 1996: Modeling of middle Pliocene climate with the
4137 NCAR GENESIS general circulation model. *Marine Micropaleontology*, **27**, 51-61.
4138
- 4139 **Sloan**, L.C., and D. Pollard, 1998: Polar stratospheric clouds: A high latitude warming
4140 mechanism in an ancient greenhouse world. *Geophysical Research Letters*, **25(18)**,
4141 3517-3520.

4142

4143 **Sluijs, A., U. Rohl, S. Schouten, H.J. Brumsack, F. Sangiorgi, J.S.S. Damste, and H. Brinkhuis,**
4144 2008: Arctic late Paleocene-early Eocene paleoenvironments with special emphasis
4145 on the Paleocene-Eocene thermal maximum (Lomonosov Ridge, Integrated Ocean
4146 Drilling Program Expedition 302). *Paleoceanography*, **23(1)**, PA1S11.

4147

4148 **Sluijs, A., S. Schouten, M. Pagani, M. Woltering, H. Brinkhuis, J.S.S. Damste, G.R. Dickens, M.**
4149 **Huber, G.J. Reichart, R. Stein, J. Matthiessen, L.J. Lourens, N. Pedentchouk, J.**
4150 **Backman and K. Moran, 2006: Subtropical arctic ocean temperatures during the**
4151 **Palaeocene/Eocene thermal maximum. *Nature*, **441**, 610-613.**

4152

4153 **Smith, L.C., G.M. MacDonald, A.A. Velichko, D.W. Beilman, O.K. Borisova, K.E. Frey, K.V.**
4154 **Kremenetski, and Y. Sheng, 2004: Siberian peatlands a net carbon sink and global**
4155 **methane source since the early Holocene. *Science*, **303(5656)**, 353-356.**

4156

4157 **Smol, J.P., 1988: Paleoclimate proxy data from freshwater Arctic diatoms. *Internationale***
4158 ***Vereinigung für Limnologie*, **23**, 837-44.**

4159

4160 **Smol, J.P., 2008: *Pollution of lakes and rivers—A paleoenvironmental perspective*. Blackwell**
4161 **Publishing, Oxford, U.K., 2nd ed., 280 pp.**

4162

4163 **Smol, J.P. and B.F. Cumming, 2000: Tracking long-term changes in climate using algal**
4164 **indicators in lake sediments. *Journal of Phycology*, **36**, 986-1011.**

4165

4166 **Smol, J.P. and M.S.V. Douglas, 2007a: From controversy to consensus—Making the case for**
4167 **recent climatic change in the Arctic using lake sediments. *Frontiers in Ecology and***
4168 ***the Environment*, **5**, 466-474**

4169

4170 **Smol, J.P. and M.S.V. Douglas, 2007b: Crossing the final ecological threshold in high Arctic**
4171 **ponds. *Proceedings of the National Academy of Sciences, U.S.A.*, **104**, 12,395-12,397.**

4172

- 4173 **Solovieva, N., P.E. Tarasov, and G.M. MacDonald, 2005:** Quantitative reconstruction of
4174 Holocene climate from the Chuna Lake pollen record, Kola Peninsula, northwest
4175 Russia. *The Holocene*, **15**, 141-148.
4176
- 4177 **Sorvari, S. and A. Korhola, 1998:** Recent diatom assemblage changes in subarctic Lake
4178 Saanajarvi, NW Finnish Lapland, and their paleoenvironmental implications.
4179 *Journal of Paleolimnology*, **20(3)**, 205-215.
4180
- 4181 **Sorvari, S, A. Korhola, and R. Thompson, 2002:** Lake diatom response to recent Arctic warming
4182 in Finnish Lapland. *Global Change Biology*, **8**, 171-181.
4183
- 4184 **Sowers, T., Bender, M., Raynaud, D., 1989:** Elemental and isotopic composition of occluded O₂
4185 and N₂ in polar ice. *Journal of Geophysical Research-Atmospheres*, **94(D4)**, 5137-
4186 5150.
4187
- 4188 **Spencer, M.K., R.B. Alley and J.J. Fitzpatrick, 2006:** Developing a bubble number-density
4189 paleoclimatic indicator for glacier ice. *Journal of Glaciology*, **52(178)**, 358-364.
4190
- 4191 **Spielhagen, R.F., K-H Baumann, H. Erlenkeuser, N.R. Nowaczyk, N. Nørgaard-Pedersen, C.**
4192 **Vogt, and D. Weiel, 2004:** Arctic Ocean deep-sea record of northern Eurasian ice
4193 sheet history. *Quaternary Science Reviews*, **23(11-13)**, 1455-1483.
4194
- 4195 **Spielhagen, R.F., G. Bonani, A. Eisenhauer, M. Frank, T. Frederichs, H. Kassens, P.W. Kubik,**
4196 **N. Nørgaard-Pedersen, N. R. Nowaczyk, A. Mangini, S. Schäper, R. Stein, J. Thiede,**
4197 **R. Tiedemann, and M. Wahsner, 1997:** Arctic Ocean evidence for late Quaternary
4198 initiation of northern Eurasian ice sheets. *Geology*, **25(9)**, 783-786.
4199
- 4200 **Spielhagen, R.F. and H. Erlenkeuser, 1994:** Stable oxygen and carbon isotopes in planktic
4201 foraminifers from Arctic Ocean surface sediments—Reflection of the low salinity
4202 surface water layer. *Marine Geology*, **119(3/4)**, 227-250.
4203

- 4204 **Spielhagen, R.F.**, H. Erlenkeuser, and C. Siegert, 2005: History of freshwater runoff across the
4205 Laptev Sea (Arctic) during the last deglaciation. *Global and Planetary Change*, **48(1-**
4206 **3)**, 187-207.
- 4207
- 4208 **Stanton-Fraze**, C., D.A. Warnke, K. Venz, D.A. Hodell, 1999: The stage 11 problem as seen
4209 from ODP site 982, In: *Marine Oxygen Isotope Stage 11 and Associated Terrestrial*
4210 *Records*, [R.Z. Poore, L. Burckle, A. Droxler, W.E. McNulty (eds.)]. U.S. Geological
4211 Survey Open-file Report 99-312, 1999, pp.75.
- 4212
- 4213 **Steele, M.** and T. Boyd, 1998: Retreat of the cold halocline layer in the Arctic Ocean. *Journal of*
4214 *Geophysical Research*, **103**, 10,419-10,435.
- 4215
- 4216 **Stein, R.**, S.I. Nam, C. Schubert, C. Vogt, D. Fütterer, and J. Heinemeier, 1994: The last
4217 deglaciation event in the eastern central Arctic Ocean. *Science*, **264**, 692-696.
- 4218
- 4219 **Stötter, J.**, M. Wastl, C. Caseldine, and T. Häberle, 1999: Holocene palaeoclimatic
4220 reconstruction in Northern Iceland—Approaches and results. *Quaternary Science*
4221 *Reviews*, **18**, 457-474.
- 4222
- 4223 **Stroeve, J.**, M. Serreze, S. Drobot, S. Gearheard, M. Holland, J. Maslanik, W. Meier, and T.
4224 Scambos, 2008: Arctic Sea Ice Extent Plummets in 2007. *EOS, Transactions,*
4225 *American Geophysical Union*, **89(2)**, 13-14.
- 4226
- 4227 **Sturm, M.**, T. Douglas, C. Racine, and G.E. Liston, 2005: Changing Snow and shrub
4228 conditions affect albedo with global implications. *Journal of Geophysical Research*,
4229 **110**, G01004, doi:10.1029/2005JG000013.
- 4230
- 4231 **Svendsen, J.I.** and J. Mangerud, 1997: Holocene glacial and climatic variations on Spitsbergen,
4232 Svalbard. *The Holocene*, **7**, 45-57.
- 4233

- 4234 **Teece, M.A., J.M. Getliff, J.W. Leftley, R.J. Parkes, and J.R. Maxwell, 1998:** Microbial
 4235 degradation of the marine prymnesiophyte *Emiliana huxleyi* under oxic and anoxic
 4236 conditions as a model for early diagenesis—Long chain alkadienes, alkenones and
 4237 alkyl alkenoates. *Organic Geochemistry*, **29**, 863-880.
 4238
- 4239 **Thomas, D.J., J.C. Zachos, T.J. Bralower, E. Thomas, and S. Bohaty, 2002:** Warming the fuel
 4240 for the fire: Evidence for the thermal dissociation of methane hydrate during the
 4241 Paleocene-Eocene thermal maximum. *Geology*, **30(12)**, 1067-1070.
 4242
- 4243 **Thomsen, C., D.E. Schulz-Bull, G. Petrick, and J.C. Duinker, 1998:** Seasonal variability of the
 4244 long-chain alkenone flux and the effect on the Uk37 index in the Norwegian Sea.
 4245 *Organic Geochemistry*, **28**, 311-323.
 4246
- 4247 **Toggweiler, J. R., 2008:** Origin of the 100,000-year timescale in Antarctic temperatures and
 4248 atmospheric CO₂. *Paleoceanography*, **23**, PA2211, doi:10.1029/2006PA001405.
 4249
- 4250 **Troitsky, S.L., 1964:** Osnoviye zakonomernosti izmeneniya sostava fauny po razrezam morskikh
 4251 meshmorenykh sloev ust-eniseyskoy vpadiny i nishne-pechorskoy depressii.
 4252 *Akademia NAUK SSSR, Trudy instituta geologii i geofiziki*, **9**, 48-65 (in Russian).
 4253
- 4254 **Vassiljev, J., 1998:** The simulated response of lakes to changes in annual and seasonal
 4255 precipitation—Implication for Holocene lake-level changes in northern Europe.
 4256 *Climate Dynamics*, **14**, 791-801.
 4257
- 4258 **Vassiljev, J., S.P. Harrison, and J. Guiot, 1998:** Simulating the Holocene lake-level record of
 4259 Lake Bysjon, southern Sweden. *Quaternary Research*, **49**, 62-71.
 4260
- 4261 **Velichko, A.A., A.A. Andreev, and V.A. Klimanov, 1997:** Climate and vegetation dynamics in
 4262 the tundra and forest zone during the Late Glacial and Holocene. *Quaternary*
 4263 *International*, **41/42**, 71-96.
 4264

- 4265 **Velichko**, A.A., and V.P. Nechaev (eds), 2005: *Cenozoic climatic and environmental changes in*
4266 *Russia*. [H.E. Wright, Jr., T.A. Blyakharchuk, A.A. Velichko and Olga Borisova (eds.
4267 of English version)]. The Geological Society of America Special Paper, **382**, 226 pp.
4268
- 4269 **Vinther**, B.M., H.B. Clausen, S.J. Johnsen, S.O. Rasmussen, K.K. Andersen, S.L. Buchardt, D.
4270 Dahl-Jensen, I.K. Seierstad, M.L. Siggaard-Andersen, J.P. Steffensen, A. Svensson, J.
4271 Olsen, and J. Heinemeier, 2006: A synchronized dating of three Greenland ice cores
4272 throughout the Holocene. *Journal of Geophysical Research*, **111**, D13102,
4273 doi:13110.11029/12005JD006921.
4274
- 4275 **Vörösmarty**, C.J., L.D. Hinzman, B.J. Peterson, D.H. Bromwich, L.C. Hamilton, J. Morison,
4276 V.E. Romanovsky, M. Sturm, and R.S. Webb. 2001: The Hydrologic Cycle and its
4277 Role in Arctic and Global Environmental Change: A Rationale and Strategy for
4278 Synthesis Study. Fairbanks, Alaska: Arctic Research Consortium of the U.S., 84 pp.
4279
- 4280 **Vörösmarty**, C., L. Hinzman, and J. Pundsack, 2008: Introduction to special section on Changes
4281 in the Arctic Freshwater System: Identification, Attribution, and Impacts at Local and
4282 Global Scales. *Journal of Geophysical Research-Biogeosciences*, **113(G1)**, G01S91.
4283
- 4284 **Walter**, K.M., S.A. Zimov, J.P. Chanton, D. Verbyla, and F. S. Chapin, III, 2006: Methane
4285 Bubbling from Siberian Thaw Lakes as a Positive Feedback to Climate Warming.
4286 *Nature*, **443**, 71-75.
4287
- 4288 **Walter** K.M., M. Edwards S.A. Zimov G. Grosse F.S. Chapin, III, 2007: Thermokarst lakes as a
4289 source of atmospheric CH₄ during the last deglaciation. *Science*, **318,(5850)**, 633-
4290 636.
4291
- 4292 **Wang**, Y.J., H. Cheng, R. L. Edwards, Z. S. An, J. Y. Wu, C.-C. Shen, J. A. Dorale' 2001: A
4293 high-resolution absolute-dated late Pleistocene monsoon record from Hulu Cave,
4294 China. *Science*, **294**, 2345-2348.
4295

- 4296 **Weaver, A.J., C.M. Bitz, A.F. Fanning, and M.M. Holland, 1999:** Thermohaline circulation—
4297 High latitude phenomena and the difference between the Pacific and Atlantic. *Annual*
4298 *Review of Earth and Planetary Sciences*, **27**, 231-285.
- 4299
- 4300 **Weckström, J., A. Korhola, P. Erästö, and L. Holmström, 2006:** Temperature patterns over the
4301 past eight centuries in northern Fennoscandia inferred from sedimentary diatoms.
4302 *Quaternary Research*, **66**, 78-86.
- 4303
- 4304 **Weijers, J.W.H., S. Schouten, O.C. Spaargaren, and J.S.S. Damsté, 2006:** Occurrence and
4305 distribution of tetraether membrane lipids in solid—Implications for the use of the
4306 TEX₈₆ proxy and the BIT index. *Organic Geochemistry*, **37(12)**, 1680-1693.
- 4307
- 4308 **Weijers, J.W.H., S. Schouten, A. Sluijs, H. Brinkhuis, and J.S.S. Damsté, 2007:** Warm arctic
4309 continents during the Palaeocene-Eocene thermal maximum. *Earth and Planetary*
4310 *Science Letters*, **261(1-2)**, 230-238.
- 4311
- 4312 **Werner, M., U. Mikolajewicz, M. Heimann, and G. Hoffmann, 2000:** Borehole versus isotope
4313 temperatures on Greenland—Seasonality does matter. *Geophysical Research Letters*,
4314 **27**, 723-726.
- 4315
- 4316 **Whitlock, C. and M.R. Dawson, 1990:** Pollen and vertebrates of the early Neogene Haughton
4317 Formation, Devon Island, Arctic Canada. *Arctic*, **43(4)**, 324-330.
- 4318
- 4319 **Wiles, G.C., D.J. Barclay, P.E. Calkin, and T.V. Lowell, 2008:** Century to millennial-scale
4320 temperature variations for the last two thousand years indicated from glacial geologic
4321 records of Southern Alaska. *Global and Planetary Change*, **60**, 15-125.
- 4322
- 4323 **Williams, C.J., A.H. Johnson, B.A. LePage, D.R. Vann and T. Sweda, 2003:** Reconstruction of
4324 Tertiary Metasequoia Forests II. Structure, Biomass and Productivity of Eocene
4325 Floodplain Forests in the Canadian Arctic, *Paleobiology*, **29**, 271-292.
- 4326

- 4327 **Wohlfahrt, J.**, S.P. Harrison, and P. Braconnot, 2004: Synergistic feedbacks between ocean and
4328 vegetation on mid- and high-latitude climates during the Holocene. *Climate*
4329 *Dynamics*, **22**, 223-238.
- 4330
- 4331 **Wohlfarth, B.**, G. Lemdahl, S. Olsson, T. Persson, I. Snowball, J. Ising, and V. Jones, 1995:
4332 Early Holocene environment on Bjornoya (Svalbard) inferred from multidisciplinary
4333 lake sediment studies. *Polar Research*, **14**, 253-275.
- 4334 **A** **B**
- 4335 **Wooller, M.J.**, D. Francis, M.L. Fogel, G.H. Miller, I.R. Walker, and A.P. Wolfe, 2004:
4336 Quantitative paleotemperature estimates from delta O-18 of chironomid head
4337 capsules preserved in arctic lake sediments. *Journal of Paleolimnology*, **31(3)**, 267-
4338 274.
- 4339
- 4340 **Wuchter, C.**, S. Schouten, M.J.L. Coolen, and J.S.S. Damsté, 2004: Temperature-dependent
4341 variation in the distribution of tetraether membrane lipids of marine Crenarchaeota—
4342 Implications for TEX86 paleothermometry. *Paleoceanography*, **19(4)**, PA4028
- 4343
- 4344 **Zachos, J.C.**, Dickens, G.R., Zeebe, R.E., 2008: An early Cenozoic perspective on greenhouse
4345 warming and carbon-cycle dynamics. *Nature*, **451** (7176), 279-283.
- 4346
- 4347 **Zachos, Z.**, P. Pagani, L. Sloan, E. Thomas, and K. Billups, 2001: Trends, rhythms, and
4348 aberrations in global climate 65 Ma to present. *Science*, **292**, 686-693.
- 4349
- 4350 **Zazula G.D.**, D.G. Froese, C.E. Schweger, R.W. Mathewes, A.B. Beaudoin, A.M. Telka, C.R.
4351 Harington, and J.A. Westgate, 2003: Ice-age steppe vegetation in east Beringia -
4352 tiny plant fossils indicate how this frozen region once sustained huge herds of
4353 mammals. *Nature*, **423**, 603-603.
- 4354